The Role of Mechanosensitive Calcium Signaling in Remodeling of Epithelial Cell-Cell Junctions

by

Saranyaraajan Varadarajan

A dissertation submitted in partial fulfillment
of the requirements for the degree of
Doctor of Philosophy
(Molecular, Cellular, and Developmental Biology)
in the University of Michigan
2021

Doctoral Committee:

Associate Professor Ann L. Miller, Chair
Associate Professor Laura Buttitta
Professor Gyorgyi Csankovszki
Associate Professor Allen Liu
Professor Asma Nusrat

Saranyaraajan Varadarajan

varadars@umich.edu

ORCID iD: 0000-0002-4473-9435

Dedication

To Hari and my parents

Acknowledgements

I would like to acknowledge everyone who was critical to the completion of my dissertation. First, I want to thank my advisor, Dr. Ann Miller, for being an outstanding mentor and for always believing in me. I am very lucky to be mentored by Ann who leads by example and encourages me to aim high, work hard, think critically and methodically, communicate efficiently, and importantly have fun while doing good science. Thank you, Ann, for giving me the freedom to explore different research ideas, providing me the opportunities to present at scientific meetings, and to participate in science and career development courses. Ann's passion and commitment for research, teaching, and mentoring, has been a true inspiration for someone I hope to become one day, and pay it forward.

Next, I want to thank members of the Miller lab, both present and past, for making the lab an intellectually stimulating place and my graduate school journey a pleasant experience. A big shoutout to former postdoc, Tomohito Higashi, for taking me under your wing as a rotation student and training me on all the essential techniques where it never fails when done "The Tomo Way". I would also like to thank a former graduate student, Torey Arnold, for being a great desk-neighbor and a good friend who is always open to talk science, yoga, or nature. Special thanks to Rachel Stephenson, former graduate student, and a current research scientist in Miller lab, for laying a strong foundation on Rho flare project, being open to brainstorming new ideas, showing me the ropes of multiple techniques without which this document would be half empty, and providing constructive feedback on my manuscript and dissertation. Thanks to Ann, Rachel, Jen Landino, and my fellow graduate students, Shahana Chumki, Lotte van den Goor, and Suzie Craig, for being my wolfpack who is friendly, caring, and genuinely interested in the wellbeing of each other. You are the best! Thanks to the undergrads of Miller lab, who always keep the lab atmosphere positive and a happy place. Finally, a

special thanks to three very talented, smart, hardworking undergrads that I had a chance to mentor and supervise- Lauren Smith, Jessica Wu and Eillen Misterovich. Lauren and Jessica, you amaze me with your ability to get learn quicky and work independently. Jessica and Eileen, without your hard work and perseverance, Chapter 3 of my dissertation wouldn't have been possible.

Special thanks to my thesis committee members, Dr. Laura Buttitta, Dr. Gyorgyi Csankovszki, Dr. Allen Liu, and Dr. Asma Nusrat, for your valuable feedback on various aspects of my project, your genuine interest in my career development and your unwavering support for my stream of fellowship applications. I would also like to thank Laura Buttitta and Gyorgyi Csankovszki, for giving me an opportunity to rotate in their labs, and made MCDB feel like home right from the beginning. Thanks to Asma Nusrat, also my future postdoc advisor, for spreading your enthusiasm for science and teaching me all about Claudins during our collaboration project meetings.

I am also grateful to have a great support system outside of Miller lab in MCDB. Thanks to the fellow graduate student in my cohorts, especially Ajai Pulianmackhal, Zhangyuan Yin (Justin), and Sujeet Bhoite, for being friendly and compassionate through the ups and downs of graduate school. A huge thanks to Ajai, my graduate school twin, in addition to being my 3pm coffee buddy, you have been an optimistic, patient, and supportive friend for the past 6 years. Shyama Nandhakumar, thanks for being my well-wisher right from the day I interviewed at MCDB.

I am very lucky to have a loving and caring family and network of friends, who have been an immense source of encouragement to achieve my dreams, and supportive of my choices. I would like to thank my friends- Shirlee, Shreya and Janani, for being a part of my sisterhood and friends for life. Shreya, thanks for constantly encouraging me to apply for graduate school and for being my protective big sister. Shirlee and Janani, thanks for always having my back right from our undergrad days.

Thanks, Amma and Appa, for teaching me the value of education, hard work and determination from a young age. I must also thank my brother, Anush, my sister-in-law, Tuhina, and my husband's family for their love and constant encouragement through the challenging times of graduate school.

Finally, I want to thank my husband, Hari Kalluri. By far, you are my greatest strength and rock-solid support. I can’t thank you enough for being an amazingly supportive and understanding spouse, who finds pleasure in my success.

Table of Contents

List of Figures

Abstract

Epithelial cells line most of our body cavities, separating different compartments in our bodies, creating selective barriers, and protecting us from external pathogens. In epithelial tissues, cells experience a range of mechanical forces like fluid flow, tissue distention, and tissue compression or contraction, which occur both during development and normal organ function. All of these events require cells to sense the mechanical force and remodel their cell-cell junctions accordingly in order to maintain barrier function and structural integrity of the tissue. However, the precise mechanism by which epithelial barrier function is regulated in response to mechanical stimuli is unknown.

In the vertebrate epithelium, the most apically localized cell-cell junctions, called tight junctions (TJs), regulate barrier function by selectively allowing solutes and ions to pass through the space between cells, while the more basally localized adherens junctions (AJs) mechanically couple the cells together to maintain the structural integrity of the tissue. Using gastrula-stage *Xenopus laevis* embryos as a model for the vertebrate epithelium, previous work from our lab identified local, short-lived leaks in the epithelial TJ barrier, which occur in response to elongating cell-cell junctions. These leaks were rapidly repaired by reinforcement of TJ proteins, mediated by localized, transient activation of the small GTPase RhoA – termed “Rho flares”. But the mechanism by which cells sense the leak in the barrier and activate Rho flares locally at the site of the barrier leak remained unclear.

In this dissertation, I investigate how a mechanical cue is converted into biochemical signals to regulate barrier function in the vertebrate epithelium. Here, I found that a local calcium increase occurs at the site of barrier leaks in response to loss of the TJ protein ZO-1. Using intracellular calcium chelation and a mechanosensitive calcium channel (MSC) blocker, I show that a local calcium increase is required for robust activation of Rho flares to efficiently reinforce TJs at sites of local barrier breaches. Further, I show that MSC-dependent calcium influx is required to maintain global barrier function by regulating efficient repair of local barrier leaks through robust contraction of junctions. Thus, we propose that MSC-mediated calcium influx is a mechanism by which epithelial cells detect local leaks and regulate barrier function by activating Rho flares. Additionally, I explored the localization and function of a eukaryotic MSC, Piezo1, at cell-cell junctions. I found that Piezo1 localizes to AJs and regulates TJ barrier function during cell-generated tensile stress, possibly by strengthening cell-cell adhesion. Together, my work reveals MSC-mediated calcium signaling as part of a mechanotransduction pathway working at apical cell-cell junctions to regulate barrier function. In addition to revealing a novel role for intracellular calcium signaling in regulating TJ barrier function in a mature epithelium, application of my research could help identify new targets to treat chronic inflammation associated with impaired cell-cell junctions in response to aberrant mechanotransduction.

Chapter 1 Introduction

This chapter contains some text and figures that were originally published in *Journal of Cell Science*.

*Varadarajan S, *Stephenson RE, Miller AL. Multiscale dynamics of tight junction remodeling. J Cell Sci. 2019 Nov 21;132(22):jcs229286. doi: 10.1242/jcs.229286. PMID: 31754042; PMCID: PMC6899008

*these authors contributed equally to this work

1.1 Cell-cell junctions are essential for tissue architecture and generating barriers

A conserved feature of metazoans is the ability to form compartments with distinct environments in order to perform specialized functions (Tyler, 2003). The existence of separate compartments is essential for development and maintenance of functional organs. Compartmentalization is achieved by sheets of polarized, tightly packed individual epithelial or endothelial cells connected to their neighbors through cell-cell junctions. Epithelial sheets cover the external surface of our body (e.g. skin) and internal surfaces of our organs (e.g. lungs, liver, stomach, and intestine), acting as a barrier to toxic pathogens and to preserve the structural integrity of the tissue during physical and chemical stress. However, epithelial barriers are selectively permeable to ions and solutes to enable specialized tissue specific functions like absorption in the intestine, secretion in the stomach and liver, and sensation in the ear (Tsukita et al., 2001, Farquhar and Palade, 1963). Molecules on either side of the epithelium can cross the barrier via two pathways: through the cytoplasm of the cells (transcellular

permeability) or through the space between the cells (paracellular permeability), with paracellular permeability being the major route of transepithelial transport (Boulpaep and Seely, 1971, Fromter and Diamond, 1972). Dysfunction of the epithelial barrier can cause inflammatory diseases like inflammatory bowel disease (IBD), Crohn's disease, and asthma, and can contribute to metabolic disorders (Garcia-Hernandez et al., 2017, Luissint et al., 2016).

Epithelial cell-cell junctions of a vertebrate consist of three components: tight junctions (TJs), adherens junctions (AJs) and desmosomes (Farquhar and Palade, 1963). TJs are the most apically localized cell-cell junction, characterized by a continuous circumferential belt-like structure and close apposition of plasma membranes from adjacent cells, to regulate paracellular transport (Farquhar and Palade, 1963). TJs function as a barrier by regulating selective permeability of small solutes, such as ions, water, and small uncharged molecules, while generally restricting the passage of larger molecules and microorganisms (Marchiando et al., 2010) **(Figure 1.1)**. In addition to serving as a selective barrier, TJs also function as a fence in the apical plasma membrane to create distinct apical and basolateral membrane domains, by limiting the free diffusion of proteins and lipids in the membrane (Gumbiner, 1987). Together, TJs are critical for the development and maintenance of organ function, by establishing a polarized epithelium and creating specialized environments (Moriwaki et al., 2007, Navis and Bagnat, 2015, Baumholtz et al., 2017).

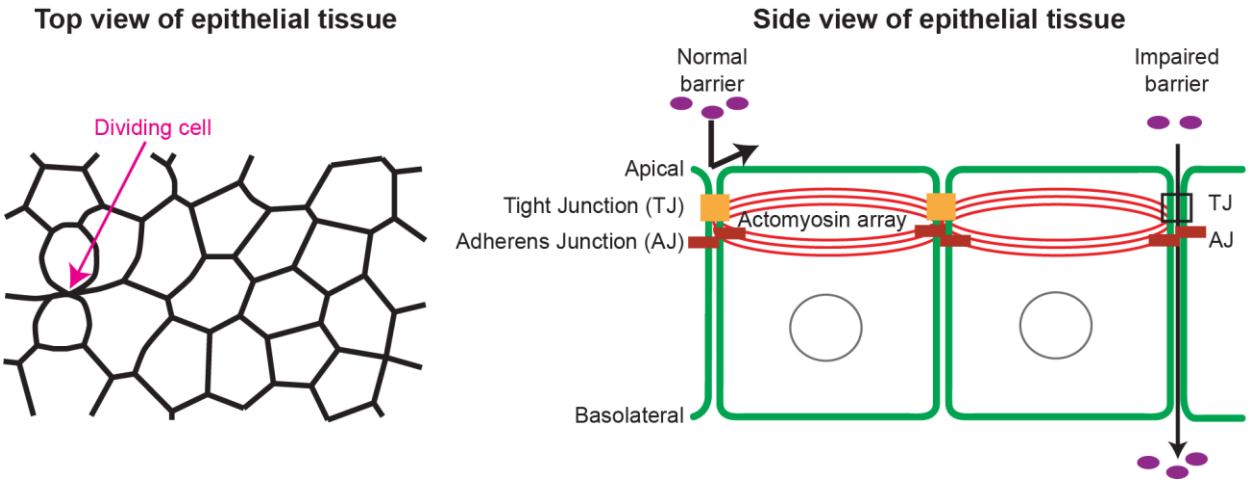

Figure 1.1: Epithelial cell-cell junctions

(Left) Epithelial cells exhibit different shapes during morphogenetic events. As cells divide (marked by arrow), both the dividing cell and its neighbors undergo cell shape changes. (Right) Schematic of key players that regulate paracellular permeability in a vertebrate epithelium. Polarized epithelial cells are connected by apical cell-cell junctions, including tight junctions (TJs) and adherens junctions (AJs). Both TJs and AJs are linked to the apical actomyosin array. Upon loss of TJ (shown by black box), paracellular permeability to molecules increases, thereby compromising barrier function.

1.2 Adherens junctions are sites of cell-cell adhesion

Basal to the TJs are the cadherin-based AJs and desmosomes where the apposing membranes are separated by an intercellular space of 15-20 nm at AJ and 20-35 nm at desmosomes (Farquhar and Palade, 1963). Cell-cell adhesion at the AJ is mediated by homophilic interaction of transmembrane E-Cadherins between adjacent cells, which is dependent on the presence of extracellular calcium (Takeichi, 1991). Following trans-dimerization of E-Cadherin, the cytoplasmic tail of E-Cadherin is coupled to the actin cytoskeleton through the catenin complex (α-, β-, and p120-Catenin) (Takeichi, 2014). β-Catenin binds the cytoplasmic tail of E-Cadherin and recruits α-Catenin to the junction (Peifer et al., 1992). The C-terminal domain of α-Catenin binds F-actin and thereby links the cadherin-catenin complex to the actomyosin array (Abe and Takeichi, 2008). The

mechanical coupling of the AJ to the apical actomyosin array is critical for epithelial cells to withstand tissue extrinsic and cell-mediated forces (Arnold et al., 2017).

1.3 Tight junctions are dynamic barriers

TJs are multi-protein complexes that are composed of transmembrane proteins and cytoplasmic scaffolding proteins. In this section I will discuss the structure and composition of TJ strands, cytoplasmic scaffolding proteins mediated linking of TJ strands to the perijunctional actomyosin, and the function of perijunctional actomyosin in regulating the barrier function.

TJ transmembrane proteins:

The three main TJ transmembrane protein classes that mediate cell adhesion are Claudins, Junctional Adhesion Molecules (JAMs), and TJ Associated Marvel Proteins (TAMPs, including Occludin and Tricellulin) **(Figure 1.2)** (Van Itallie and Anderson, 2014). Claudins and Occludin constitute the branched belt-like structure, called TJ strands, which encircle the apical surface of epithelial cells (Furuse et al., 1998). In humans, claudins comprise a family of 26 members, which are differentially expressed based on the function of the epithelium (Gunzel and Yu, 2013, Turksen and Troy, 2004, Garcia-Hernandez et al., 2017). Overexpression of claudins in fibroblasts, which do not normally make TJs, revealed that claudins form the backbone of the TJ strands by interacting with their counterparts on the neighboring cells and polymerizing within the membrane, to form a network of TJ strands similar to those seen by freeze fracture electron microscopy (FFEM) in epithelial cells (Claude and Goodenough, 1973, Furuse et al., 1998, Staehelin et al., 1969). Subsequently, quintuple knockdown of claudins in

an epithelial cell line, showed that claudins are required for formation of TJ strands, but dispensable for the formation of membrane apposition at the TJ (Otani et al., 2019). Additionally, a recent study showed that presence of occludin increased and stabilized the branching points in TJ-strands, thereby contributing to the anatomizing TJ-strand network (Saito et al., 2021).

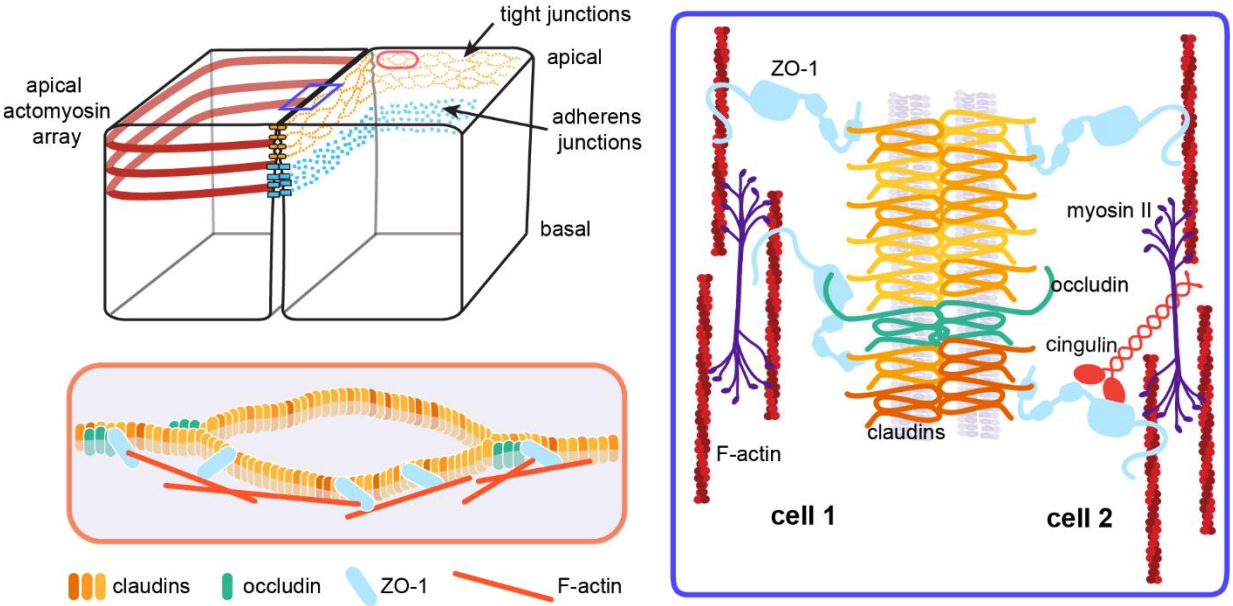

Figure 1.2: Composition and organization of tight junctions.

TJs seal the paracellular space with a family of transmembrane proteins called claudins, which oligomerize into strands and interlock with their counterparts on neighboring cells. Claudins are connected to the actin cytoskeleton through direct and indirect interactions with other TJ proteins, including Occludin, ZO family proteins, and Cingulin. Figure originally published in (Varadarajan et al., 2019).

Based on the composition of the claudins (pore-forming vs. barrier-forming) within the TJ strands, different epithelia can regulate the conductance of ions and small molecules through a charge selective pore pathway (Gunzel, 2017). In addition to the pore pathway, claudin strands are hypothesized to mediate flux of large molecules via a size selective leak pathway. This hypothesis was based on observations in fibroblasts expressing claudins that claudin strands can be remarkably dynamic within the

membrane, capable of breaking and annealing (Sasaki et al., 2003, Van Itallie et al., 2017). Together with claudin strands, other transmembrane proteins, Occludin, Tricellulin, Angulin and JAMs, help limit the paracellular flux of larger molecules (Saito et al., 2021, Raleigh et al., 2011, Otani et al., 2019). For instance, while JAM-A dependent membrane apposition at the TJ limits the paracellular flux of larger molecules (Otani et al., 2019), Occludin and Tricellulin increases the complexity of TJ-strands (more crosslinking between parallel strands) to limits the paracellular flux of larger molecules (Saito et al., 2021).

TJ scaffolding proteins:

The cytoplasmic domains of transmembrane TJ proteins (claudins, Occludin and JAM) are connected to the apical actomyosin array via ZO proteins (ZO-1, -2 and -3) (Fanning and Anderson, 2009, Itoh et al., 1999). Epithelial cells deficient in both ZO-1 and ZO-2, fail to form TJ strands and exhibit increased flux of large molecules through the paracellular space, indicating that ZO-1 and ZO-2 are essential for the structure and function of TJs (Otani et al., 2019, Umeda et al., 2006).

The highly conserved ZO-1 protein contains three PDZ domains, a SH3 domain, and a GUK domain at the N-terminus, which is required for homo- and hetero-dimerization of ZO- proteins and to bind transmembrane TJ proteins (Fanning and Anderson, 2009). The C-terminal region of ZO-1 links transmembrane TJ proteins to the apical actomyosin array by binding directly to F-actin via an actin-binding region (ABR) and indirectly through actin binding proteins (Itoh et al., 1999, Van Itallie et al., 2017, Furuse et al., 1998, Fanning et al., 1998). Fluorescence recovery after photobleaching

(FRAP) studies have shown that the linking of ZO-1 to the actin cytoskeleton through ZO-1's ABR is required for the stabilization of ZO-1 at the TJ (Shen et al., 2008a, Yu et al., 2010). Disruption of ZO proteins correlated with abnormally robust accumulation of F-actin and Myosin II at AJs, increased junctional tension, and increased paracellular permeability through the leak pathway (Van Itallie et al., 2009, Fanning et al., 2012, Umeda et al., 2006, Choi et al., 2016).

Dynamic linking of TJs to perijunctional actomyosin:

Early electron microscopy (EM) studies in epithelial chick hair cells identified two distinct yet interconnected actin populations at junctions: (i) bundles of actin filaments that run parallel to the membrane at the AJ, and (ii) a meshwork of filaments that lies just beneath the TJ (Hirokawa, 1982, Hirokawa et al., 1983). Later in 1987, Madara et al. identified an additional actin population that associated with TJ specifically at sites of membrane apposition (kissing points) using EM in guinea pig ileal epithelium (Madara, 1987). In support of actin connection to TJs, work from our lab has shown a strong F-actin enrichment at the level of the TJ in the epithelium of *Xenopus laevis* embryos (Higashi et al., 2019). Together, these data suggest that TJs are linked to perijunctional actomyosin and may feel the force from actomyosin-mediated cell shape changes.

Several studies have shown that contractility of the perijunctional actomyosin bundle regulates the structure and function of TJs. Acute treatments that either inhibited actin polymerization or inhibited Rho/ROCK-mediated Myosin II activation lead to increased paracellular permeability through the leak pathway (Van Itallie et al., 2009, Fanning et al., 2012, Van Itallie et al., 2015, Madara et al., 1986, Walsh et al., 2001).

Notably, activation of Myosin II activity mediated by myosin light chain kinase (MLCK), also increased paracellular permeability through leak pathway (Shen et al., 2006, Shen et al., 2011). Thus, both high and low levels of actomyosin contractility disrupt TJ barrier function. These findings emphasize the need for mechanisms that fine-tune the level of actomyosin contractility to maintain intact barrier function.

In order to better understand how the connection of TJs to the actin cytoskeleton influences the morphology and dynamics of TJ strands, ZO-1 and Occludin were introduced into fibroblasts expressing Claudin-2 (Van Itallie et al., 2017). The reconstituted claudin strands aligned with actin filaments in the presence of ZO-1. however, claudin strands were coupled to actin filaments only at sites of ZO-1 binding, thus for the first time directly showing the linking of claudin stands to actin via scaffolding protein, ZO-1 (Van Itallie et al., 2017). Further, introduction of ZO-1 stabilized the dynamics of claudin strands without altering the ability of strands to realign by breaking and joining. Thus, indicating that the linking of TJ strands to actin via ZO-1 is an important mechanism by which TJ strands are stabilized to maintain paracellular permeability, yet allow the TJ strands to remodel in response to cell shape changes (Van Itallie et al., 2017). In support of this idea, a recent study suggests that weak linking of ZO-1 to F-actin is an essential feature for TJ strands to be plastic enough to remodel without breaking (Belardi et al., 2020). This study showed that when the actin-binding site (ABS, 28aa region in the ABR) of ZO-1 was swapped with ABS from other proteins that exhibit higher affinity for F-actin (α-Catenin, Lifeact or Utrophin), this led to reduced barrier function. Further, a mathematical model predicts that the weak coupling of TJ strands to the actin cytoskeleton through ZO-1, is required for

dynamic rearrangement of TJ strands so that an optimal alignment of TJ strands and actin for robust barrier function can be achieved (Belardi et al., 2020). Together, these studies suggest that dynamic linking of ZO-1 to apical actomyosin enables the TJ strands to remodel without compromising barrier integrity as the junctions elongate and contract during cell shape changes.

Additionally, recent evidence from two independent groups, showed that linking of ZO protein to the actin cytoskeleton, is required for ZO-1 in phase separated condensates to form a continuous TJ strand in epithelial cells (Schwayer et al., 2019, Beutel et al., 2019), and for retrograde flow of non-junctional ZO biomolecular condensates towards the junction in developing zebrafish embryos. This suggests that, linking of ZO-1 to the actin cytoskeleton is also required for formation of TJ strands during TJ biogenesis, in addition to maintenance of a mature junction.

1.4 Tissue intrinsic and extrinsic forces regulate tight junction structure and function

During physiological process, epithelial tissues are exposed to both tissue extrinsic forces including tensile stress, shear stress, compressive stress or osmotic stress, and tissue intrinsic forces like actomyosin tension, cell-cell junctions, and cell-matrix adhesion. These processes involve actomyosin-mediated cell shape changes, which require that cell-cell boundaries expand and contract, thus posing challenges to the continuity of TJs around the perimeter of epithelial cells. For example, cells change shape during physiological events including cell division, cell extrusion, and cell migration, and pathophysiological events including wound healing and cancer cell

metastasis (Harris and Tepass, 2010). Other mechanical challenges arise from organ-specific function, including bladder expansion and gut peristalsis. All of these events require dynamic reorganization of perijunctional actomyosin. Given that TJ barrier function is tightly coupled to the actomyosin contractility, it is unclear how such dynamic tissues act as stable barriers. Because proper regulation of barrier function is essential for development and optimal organ function (Marchiando et al., 2010, Odenwald et al., 2017), epithelial cells must possess robust mechanisms for maintaining barrier function while remaining plastic enough to adapt to a tissue intrinsic and extrinsic forces.

TJ remodeling at the tissue scale:

Mechanical changes in junctional or tissue tension can alter the strand network morphology by reorienting the strand network or inducing strand breaks (Hull and Staehelin, 1976, Pitelka and Taggart, 1983). In tissues that have been experimentally stretched, TJ strands align with the axis of tension; they appear highly taut and are reduced in number (Pitelka and Taggart, 1983, Hull and Staehelin, 1976). However, radial tension generated by contraction of the apical actomyosin array resulted in networks with more vertically-oriented strands (Pitelka and Taggart, 1983). This indicates that tissue mechanics may influence strand network morphology, in turn impacting barrier function.

In addition to changes in strand morphology, mechanical changes in tissue tension can alter TJ structure and function by altering cytoskeletal-mediated tension (DiPaolo and Margulies, 2012, Samak et al., 2014, Acharya et al., 2018) and post translational modification of TJ proteins (Hashimoto et al., 2019, Samak et al., 2014).

For instance, when alveolar epithelial cells are stretched biaxially in a cyclic manner, they exhibit an increase in paracellular permeability and a decrease in perijunctional actomyosin (Cavanaugh et al., 2001, DiPaolo and Margulies, 2012). Additionally, upon biaxial stretch, the overall levels of ZO-1 and Occludin localization at TJs are reduced, with alternating regions of high and low intensity of TJ proteins visible along the junction (Cavanaugh et al., 2001). A similar phenotype was observed in Caco-2 cells when stretched biaxially for 6 hours; stretch induced loss of perijunctional actomyosin, and loss of ZO-1 and Occludin at TJs (Samak et al., 2014). Additionally, biochemical studies show that stretching of epithelial cells increased tyrosine phosphorylation of ZO-1 and Occludin, possibly leading to loss from TJs (Samak et al., 2014). Together, these studies suggest that epithelial cells modulate TJ structure and thereby paracellular permeability by altering both actomyosin cytoskeleton and post-translation modification of TJ in response to tensile forces. However, one should note that cells were exposed to an experimental stretch for 1-6 hours, which is not physiologically relevant to the dynamic movements experienced by epithelial tissue. In contrast to tensile stress, compression of epithelial cells increased ZO-1 recruitment to TJs, and phosphoproteome analysis showed an increase in ZO-1 phosphorylation at multiple sites (Hashimoto et al., 2019). Thus, showing that epithelial cells respond differently based on the mechanical stimuli- tensile or compressive forces. However, further studies are needed to understand the primary effects of physiological mechanical stimuli on remodeling of TJs and the effects on paracellular permeability.

TJ remodeling at the cell scale:

It is less clear how TJs respond to cell shape changes and how barrier function changes at the cell scale, particularly when existing cell-cell interfaces are elongated, or new cell-cell junctions are established, such as during cell division or cell extrusion. During cell division and cell extrusion, major shape changes occur not only in those cell interfaces that are directly involved in the process, but also in neighboring cells, which must change their shape in order to accommodate the movements of the dividing or extruding cells.

In a dividing cell, a relatively small portion of the cell-cell junction experiences direct pulling force from the contractile ring in the dividing cell. In *Xenopus laevis* embryos, FRAP of AJ proteins showed that they are stabilized at the cleavage furrow; however, there was no detectable change to FRAP of TJ proteins, indicating that AJs are mechanically coupled to the forces that are transmitted during cytokinesis (Higashi et al., 2016). Interestingly, ZO-1 intensity does increase at the furrow relative to the poles, indicating that there is some TJ remodeling during cytokinesis (Higashi et al., 2016). Indeed, FFEM showed that TJs in mitotic cells are more disorganized, with a higher number of free strand ends than in non-mitotic cells (Tice et al., 1979).

Cell extrusion presents another potential challenge to epithelial barrier integrity. During extrusion, dying or over-crowded cells are squeezed out of epithelial tissues by their neighbors (Gudipaty and Rosenblatt, 2017). During this process, TJs extend basally to maintain contact between neighboring cells and the extruded cell (Madara,

1990, Guan et al., 2011, Marchiando et al., 2011). Following extrusion, new cell-cell interfaces must be formed in the absence of the extruded cell.

Remarkably, during both cytokinesis and extrusion, the epithelial barrier is largely maintained (Higashi et al., 2016, Rosenblatt et al., 2001, Madara, 1990, Guan et al., 2011, Marchiando et al., 2011). However, we don't currently have a good understanding of the mechanisms that allow TJs to expand and contract, while simultaneously restricting ion and macromolecule flux; this is an important goal for the field.

1.5 Rho GTPase regulates the formation and function of tight junctions by modulating perijunctional actomyosin

The Rho family of small GTPases function as molecular switches that cycle between an active, GTP-bound state and an inactive, GDP-bound state **(Figure 1.3)**. RhoA is turned on by guanine nucleotide exchange factors (GEFs) that promote the exchange of GDP for GTP and turned off by GTPases activating proteins (GAPs) that accelerate the hydrolysis of GTP, converting it to GDP. Additionally, guanosine nucleotide dissociation inhibitor (GDI) sequesters inactive RhoA in the cytoplasm to prevent re-activation (Bishop and Hall, 2000). Thus, net activity of RhoA is the sum of the activity of the GEFs, GAPs, and GDI. In its active state, RhoA associates with the plasma membrane and activates its downstream effector proteins to regulate cytoskeletal organization during cellular events including cell-cell adhesion, cell migration, cell division, morphogenesis, and vesicle trafficking (Bishop and Hall, 2000, Miller and Bement, 2009, Bement et al., 2006).

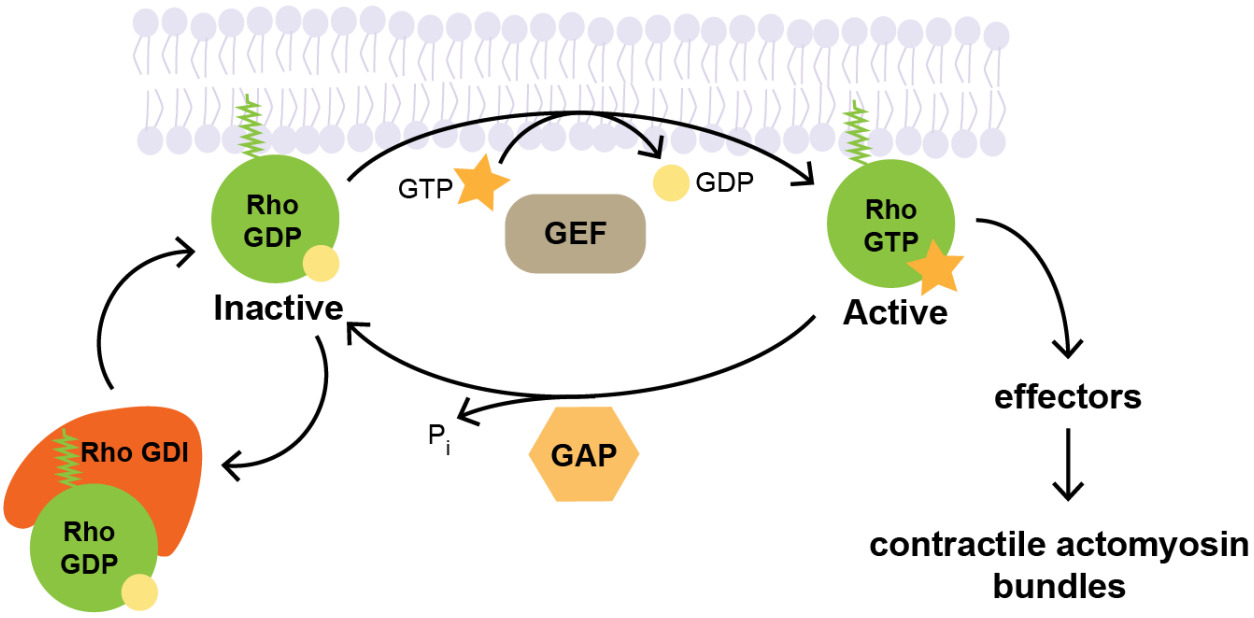

Figure 1.3: Regulation of Rho GTPase.

The small GTPase RhoA cycles between an active form (RhoA-GTP) and an inactive form (RhoA-GDP). The activity of RhoA is regulated by GEFs, GAPs and GDI. In its active form, RhoA promotes actin polymerization through its effector formin (Watanabe et al., 1999), and increases the activity of Myosin II through its effector ROCK by simultaneously phosphorylating myosin light chain (MLC) and inactivating MLC phosphatase (Kimura et al., 1996, Amano et al., 1996). For RhoA to mediate downstream actomyosin contractility, a sustained population of active RhoA is required to be anchored to the plasma membrane and be available to interact with its downstream effectors (Ratheesh et al., 2012). Figure adapted from (Arnold et al., 2017).

In epithelia, assembly, disassembly, remodeling, and contractility of the perijunctional actomyosin is tightly regulated by the Rho family of small GTPases: RhoA, Rac1, and Cdc42 (Quiros and Nusrat, 2014, Arnold et al., 2017). The function of small GTPases in regulation of TJs was first identified in 1995 by inhibiting the activity of RhoA using C3 transferase. Inhibition of Rho led to reorganization of perijunctional actomyosin and TJ barrier dysfunction (Nusrat et al., 1995a). Interestingly, additional studies found similar effects when either constitutively active or dominant negative mutant versions of RhoA were expressed (Jou et al., 1998, Quiros and Nusrat, 2014, Bruewer et al., 2004). These results indicate that RhoA activity must be tightly controlled in space and time, as both too much and too little are detrimental to the integrity of TJ structure and barrier function.

Though it was known that RhoA activity is required for formation and maintenance of cell-cell junctions, it was not until a almost decade ago that endogenous active RhoA was detected at the epithelial cell-cell junctions by microscopy (Ratheesh et al., 2012, Reyes et al., 2014, Breznau et al., 2015, Priya et al., 2015). A stable population of endogenous RhoA activity was detected using probes that specifically binds to the active form of RhoA (RhoA-GTP), including a RhoA-FRET biosensor (Ratheesh et al., 2012), the RhoA binding domain of rhotekin (rGBD) (Reyes et al., 2014), the Rho binding region plus PH domain of Anillin (AHPH) (Priya et al., 2015) . In addition to the stable baseline population of active Rho, our lab identified dynamic, local accumulations of active RhoA at apical cell-cell junctions, which we termed “Rho flares”, (Reyes et al., 2014, Stephenson et al., 2019).

1.6 Rho flares regulate the leak pathway of permeability on the subcellular scale

We recently demonstrated that when cell-cell junctions elongate in the *Xenopus laevis* embryonic epithelium, local discontinuities in ZO-1 and Occludin often occur along the expanding junction (Stephenson et al., 2019). Using a highly sensitive barrier assay (Zinc-based Ultrasensitive Microscopic Barrier Assay [ZnUMBA]), we identified that the local losses of ZO-1 and Occludin correspond to sites of leak pathway flux (Stephenson et al., 2019). Importantly, these leaks were quickly followed by “Rho flares”, local activations of RhoA at the site of ZO-1 discontinuities. Robust and sustained activation of Rho flares promotes local F-actin accumulation and Myosin II-mediated junction contraction, which concentrates TJ proteins to reinforce the barrier at sites of local leaks **(Figure 1.4)**. Additionally, AJ proteins (E-Cadherin and α-catenin) were reinforced

following the Rho flares, suggesting a role for AJs in the stabilization of TJs during repair.

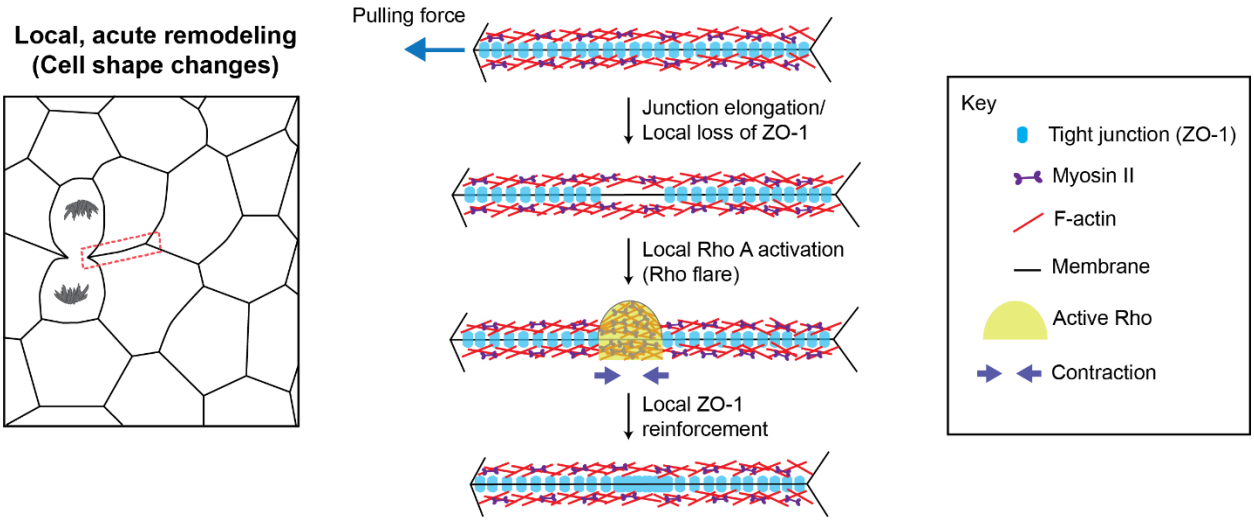

Figure 1.4: Rho flare mediated local remodeling of TJ

Elongation of a junction near a dividing cell (boxed area, magnification shown on the right) causes local loss of ZO-1 and a breach in barrier function (not shown). Activation of RhoA (green dome) at the site of ZO-1 loss promotes actomyosin mediated contraction of junctions (blue arrows), which concentrates TJ proteins to repair the barrier leak. Figure originally published in (Varadarajan et al., 2019).

Interestingly, Rho flares are associated with bleb-like membrane protrusions **(Figure 1.4,** green**),** displaying a change in membrane curvature and thereby a possible change in membrane tension, (Stephenson et al., 2019). Blebs in living cells are formed when the connection of the plasma membrane to the underlying actin-based cortex is weakened (Charras, 2008). Blebs have long been thought to be areas of increased membrane tension, which was confirmed by a recent study using a membrane tension probe, FlipTR (Colom et al., 2018). Together, these findings suggest a role for mechanosensitive signaling pathways in the local regulation of Rho flares specifically at the site of TJ discontinuities. In support of our hypothesis, a recent study showed that

junctional RhoA is activated at the AJ in response to tissue level mechanical stretch, in order to strengthen E-Cadherin-based cell-cell adhesion (Acharya et al., 2018).

Notably, not every instance of junction elongation causes a leak or is followed by subsequent contraction. Thus, Rho flares may be an emergency repair mechanism that initiates when a TJ is severely damaged in response to a mechanical stimulus. This raises the question: how do cells detect the TJ leak in response to a mechanical stimulus and activate RhoA to reinforce the barrier?

1.7 A case for intracellular calcium signaling in mechanosensitive regulation of tight junctions

In addition to RhoA, epithelial barrier function and the contractility of the perijunctional actomyosin is regulated by calcium signaling (Denker and Nigam, 1998). The first evidence to show that calcium is required for the formation of barrier function was established when epithelial cells lost their ability to establish transepithelial resistance (TER) in the absence of extracellular calcium (Gonzalez-Mariscal et al., 1985). However, when cells were switched from low calcium to normal calcium containing media, a technique commonly referred to as a calcium-switch assay, cell-cell contacts with TJ strands begin forming in as little as 15 minutes (Gonzalez-Mariscal et al., 1985), indicating that extracellular calcium is required for establishing a functional barrier.

As *extracellular* calcium is required for formation of AJs through homotypic E-Cadherin interactions between cells, the function of *intracellular* calcium in the formation of cell-cell junctions was still not clear. However, when intracellular calcium level was monitored using spectrofluorometric measurements in cells loaded with a calcium dye

(Fura 2-AM), a significant increase in cytosolic calcium was observed following the calcium-switch. Specifically, cytosolic calcium increase was observed both globally throughout the cell, and locally at sites of TJ formation, suggesting a role for intracellular calcium in the formation of TJs (Gonzalez-Mariscal et al., 1990, Nigam et al., 1992). Further, when intracellular calcium was chelated, epithelial cells failed to form TJs and establish a functional barrier, thereby confirming that intracellular calcium is indeed required for the formation of TJs (Stuart et al., 1994). But, it is important to note that in calcium-switch assay AJs are disrupted as well, thus it is difficult to isolate the precise role of intracellular calcium in regulation of TJ organization and function. Therefore, it is important to investigate the spatiotemporal dynamics of intracellular calcium in an intact epithelium that is subjected to physiological cell- and tissue-generated mechanical forces.

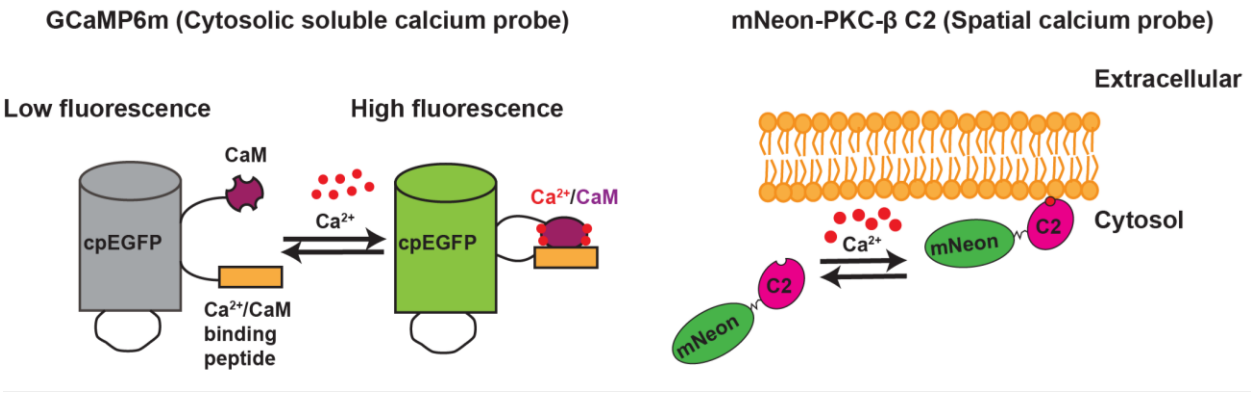

Figure 1.5: Genetically encoded calcium probes

(Left) GCaMP6m, a cytosolic soluble calcium probe contains circularly permuted GFP (cpGFP) with Calmodulin (CaM) at C-terminus and myosin light chain kinase fragment (M13) at N-terminus. In the presence of calcium (Ca^{2+}), M13 binds to CaM, causes conformational change resulting in spontaneous and reversible increase in fluorescence (Chen et al., 2013). (Right) mNeon-C2, C2 domain of PKC-β tagged to C2 is recruited to the plasma membrane from the cytoplasm when bound to calcium to detect calcium microdomains near plasma membrane (Yu and Bement, 2007).

Over the past decade, calcium signaling research has evolved significantly through the development of genetically encoded calcium indicators (GECIs) **(Figure 1.5)**, and live imaging with high spatiotemporal resolution (Chen et al., 2013, Akerboom et al., 2013, Yu and Bement, 2007). These advances have enabled the identification of various intracellular calcium transients that span a distance of few microns to 100s of microns and last anywhere between nanoseconds to hours in non-excitable cells like epithelial cells (Brodskiy and Zartman, 2018). The diversity in the frequency, amplitude, spatiotemporal pattern of calcium oscillations enables calcium signaling to have local or tissue-level effects via activating calcium-sensitive processes such as cytoskeletal assembly and contractility (Balaji et al., 2017, Clark et al., 2009, Soto et al., 2013).

In epithelial cells, a range of spatiotemporal calcium transients have been observed including: calcium waves, calcium flashes, calcium flickers, and calcium puffs, all of which regulate actomyosin contractility at different scales (Brodskiy and Zartman, 2018). For instance, long range calcium waves induced by cell wounding or tissue folding propagate across multiple cells and last on the order of minutes to mediate a tissue level contraction (Herrgen et al., 2014). In contrast, short lived calcium flashes contained in a single cell regulate apical constriction of the cell during *Xenopus* neurulation (Christodoulou and Skourides, 2015).

Elevation of intracellular calcium is largely mediated by influx of extracellular calcium through calcium channels in the plasma membrane or calcium release from the endoplasmic reticulum (ER) (Shao et al., 2015). The long- and short-range calcium waves are primarily mediated by IP_3-dependent release of calcium from the ER (Webb and Miller, 2006, Jaffe, 2008, Balaji et al., 2017, Wallingford et al., 2001, Soto et al.,

2013). In contrast, the localized calcium transients are generally mediated by plasma membrane-localized calcium channels, thereby creating a local microdomain of calcium near the opening of the channel (Berridge, 2006, Wei et al., 2009, Tsai et al., 2015).

1.8 Mechanosensitive calcium channels in the epithelium

Mechanosensitive calcium channels (MSCs) are a class of plasma membrane-localized calcium channels that are capable of sensing changes in the mechanical forces applied on the plasma membrane and eliciting a calcium influx into the cell **(Figure 1.6)** (Sachs, 2017). In eukaryotes, Piezo1, Piezo2 and members of the Transient Receptor Potential (TRP) family have been shown to sense mechanical tension and undergo conformational change to allow calcium ions into the cell (Martinac, 2004, Coste et al., 2010). MSCs can detect a wide range of mechanical stimuli generated by tissue extrinsic forces including tensile stress, shear stress or osmotic stress, and tissue intrinsic forces like actomyosin tension, force from cell-cell junctions, and cell-matrix adhesion (Nourse and Pathak, 2017, Ellefsen et al., 2019, Canales Coutino and Mayor, 2021, Luo et al., 2019). Several of the MSCs (Piezo1, TRPC1, TRPC5, TRPC6, TRPV2 and TRPV4) are expressed in epithelial tissues that undergo drastic changes in cell shape during physiological functions including lungs, kidney, intestine, urinary bladder and skin (Coste et al., 2010, Tiruppathi et al., 2006, Akazawa et al., 2013, Miyamoto et al., 2014, Weber and Muller, 2017). Impaired function of MSCs has been linked to developmental abnormalities, barrier defects, inflammation, and cancer (Zhong et al., 2020, Gudipaty and Rosenblatt, 2017, Ranade et al., 2014, Canales et al., 2019, Weber and Muller, 2017, Weber et al., 2015).

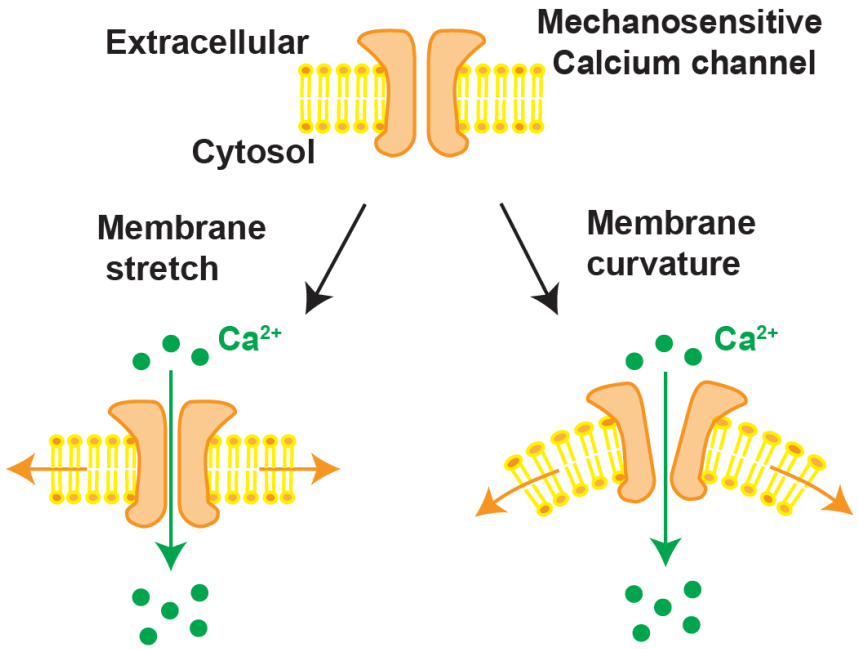

Figure 1.6: Mechanosensitive calcium channels

Plasma membrane localized MSCs sense changes in membrane tension caused by membrane stretching, and/or changes in membrane curvature, and respond by allowing calcium ions to pass through the channel into the cytoplasm.

Piezo1 senses membrane tension caused by stretch or curvature of the membrane to allow calcium ions to pass through the membrane (Zhao et al., 2018, Syeda et al., 2015, Coste et al., 2010). In epithelia, Piezo1, is implicated in maintaining barrier integrity by regulating both cell division and cell extrusion depending on the density of the cells in the tissue (Eisenhoffer et al., 2012, Gudipaty et al., 2017). In a crowded tissue, calcium influx through Piezo1 activates ROCK-mediated actomyosin around the extruding cell for successful cell extrusion (Eisenhoffer et al., 2012). On the other hand, calcium influx through Piezo1 drives cell division in areas of low cell density (Gudipaty et al., 2017). Given that both cell extrusion and cell division require rapid remodeling of cell-cell junctions, it is of interest to understand whether Piezo1 regulates epithelial adhesion and barrier function in response to local and/or global mechanical

stimuli. Additionally, activation of Piezo1, TRPV4 and TRPC6 mediates stress fiber formation by activation of RhoA in migrating cells, suggesting a potential role for MSCs in regulation of active RhoA at apical cell-cell junctions (Canales Coutino and Mayor, 2021). Future studies are required to better understand whether MSCs function as mechanotransducers in epithelial tissue during cell- and tissue-scale physiological movements.

1.9 *Xenopus laevis* embryos are an ideal system for studying mechanosensitive tight junction remodeling

Gastrula-stage *Xenopus laevis* embryos are an ideal system for studying dynamic remodeling of cell-cell junctions in response to mechanical stimuli because: 1. they have functional, polarized cell-cell junctions (Stephenson and Miller, 2017); 2. the embryonic epithelium mimics the mechanical forces cells experience in intact tissues (Stooke-Vaughan et al., 2017); 3. the junctional proteins and MSCs including Piezo1 are highly conserved between human and *Xenopus* (Coste et al., 2010); 4. the blastocoel (cavity) in the gastrula-stage embryos enables the use of ZnUMBA to identify dynamic breaks that correspond to sites of leak pathway flux (Stephenson et al., 2019); and 5. our lab is equipped to measure dynamic changes in RhoA activity in living tissue using fluorescent probes (GFP-rGBD or mCherry-2xrGBD) that binds specifically to the active (GTP-bound) state of RhoA (Benink and Bement, 2005, Davenport et al., 2016). Taken together, the intact epithelium of *Xenopus laevis* embryos is an ideal system for studying mechanosensitive regulation of epithelial barrier function.

1.10 Dissertation overview

In this dissertation, I investigate how a mechanical cue is converted into biochemical signals to regulate barrier function in the vertebrate epithelium. In Chapter 2, I explore the role of intracellular calcium in regulation of barrier function during cell shape changes. I demonstrate that following a local leak in the barrier, calcium increase mediated by MSC regulates the sustained activation of Rho flare repair pathway. The sustained activation of Rho flares is required to effectively repair local TJ leaks in order to maintain the tissue-level integrity of the barrier. This work reveals a new mechanism by which epithelial cells can sense and convert a local mechanical stimulus into biochemical signal. In Chapter 3, I characterize the role of Piezo1 in regulating barrier function. I show that Piezo1 localizes to AJs and partially overlaps with the zonula adherens (ZA). Further, I explore the function of Piezo1 in maintaining barrier function in response to mechanical forces. In Chapter 4, I discuss the implications of my finding in the context of mechanobiology during physiological and pathophysiological conditions, address possible calcium-mediated modulation of RhoA activity, speculate how calcium/calmodulin regulates TJ reinforcement in a Rho-independent manner, discuss mechanical tension that activates the potential MSC at Rho flares, and present future directions based on my findings.

1.11 References

ABE, K. & TAKEICHI, M. 2008. EPLIN mediates linkage of the cadherin catenin complex to F-actin and stabilizes the circumferential actin belt. *Proc Natl Acad Sci U S A,* 105**,** 13-9.

ACHARYA, B. R., NESTOR-BERGMANN, A., LIANG, X., GUPTA, S., DUSZYC, K., GAUQUELIN, E., GOMEZ, G. A., BUDNAR, S., MARCQ, P., JENSEN, O. E., BRYANT, Z. & YAP, A. S. 2018. A Mechanosensitive RhoA Pathway that Protects Epithelia against Acute Tensile Stress. *Dev Cell,* 47**,** 439-452 e6.

AKAZAWA, Y., YUKI, T., YOSHIDA, H., SUGIYAMA, Y. & INOUE, S. 2013. Activation of TRPV4 strengthens the tight-junction barrier in human epidermal keratinocytes. *Skin Pharmacol Physiol,* 26**,** 15-21.

AKERBOOM, J., CARRERAS CALDERÓN, N., TIAN, L., WABNIG, S., PRIGGE, M., TOLÖ, J., GORDUS, A., ORGER, M. B., SEVERI, K. E., MACKLIN, J. J., PATEL, R., PULVER, S. R., WARDILL, T. J., FISCHER, E., SCHÜLER, C., CHEN, T.-W., SARKISYAN, K. S., MARVIN, J. S., BARGMANN, C. I., KIM, D. S., KÜGLER, S., LAGNADO, L., HEGEMANN, P., GOTTSCHALK, A., SCHREITER, E. R. & LOOGER, L. L. 2013. Genetically encoded calcium indicators for multi-color neural activity imaging and combination with optogenetics. *Frontiers in Molecular Neuroscience,* 6**,** 1-29.

AMANO, M., ITO, M., KIMURA, K., FUKATA, Y., CHIHARA, K., NAKANO, T., MATSUURA, Y. & KAIBUCHI, K. 1996. Phosphorylation and activation of myosin by Rho-associated kinase (Rho-kinase). *J Biol Chem,* 271**,** 20246-9.

ARNOLD, T. R., STEPHENSON, R. E. & MILLER, A. L. 2017. Rho GTPases and actomyosin: Partners in regulating epithelial cell-cell junction structure and function. *Experimental Cell Research***,** 1-11.

BALAJI, R., BIELMEIER, C., HARZ, H., BATES, J., STADLER, C., HILDEBRAND, A. & CLASSEN, A.-K. 2017. Calcium spikes, waves and oscillations in a large, patterned epithelial tissue. *Scientific Reports,* 7**,** 42786.

BAUMHOLTZ, A. I., SIMARD, A., NIKOLOPOULOU, E., OOSENBRUG, M., COLLINS, M. M., PIONTEK, A., KRAUSE, G., PIONTEK, J., GREENE, N. D. E. & RYAN, A. K. 2017. Claudins are essential for cell shape changes and convergent extension movements during neural tube closure. *Dev Biol,* 428**,** 25-38.

BELARDI, B., HAMKINS-INDIK, T., HARRIS, A. R., KIM, J., XU, K. & FLETCHER, D. A. 2020. A Weak Link with Actin Organizes Tight Junctions to Control Epithelial Permeability. *Dev Cell,* 54**,** 792-804 e7.

BEMENT, W. M., MILLER, A. L. & VON DASSOW, G. 2006. Rho GTPase activity zones and transient contractile arrays. *Bioessays,* 28**,** 983-93.

BENINK, H. A. & BEMENT, W. M. 2005. Concentric zones of active RhoA and Cdc42 around single cell wounds. *Journal of Cell Biology,* 168**,** 429-439.

BERRIDGE, M. J. 2006. Calcium microdomains: organization and function. *Cell Calcium,* 40**,** 405-12.

BEUTEL, O., MARASPINI, R., POMBO-GARCIA, K., MARTIN-LEMAITRE, C. & HONIGMANN, A. 2019. Phase Separation of Zonula Occludens Proteins Drives Formation of Tight Junctions. *Cell,* 179**,** 923-936 e11.

BISHOP, A. L. & HALL, A. 2000. Rho GTPases and their effector proteins. *Biochem J,* 348 Pt 2**,** 241-55.

BOULPAEP, E. L. & SEELY, J. F. 1971. Electrophysiology of proximal and distal tubules in the autoperfused dog kidney. *Am J Physiol,* 221**,** 1084-96.

BREZNAU, E. B., SEMACK, A. C., HIGASHI, T. & MILLER, A. L. 2015. MgcRacGAP restricts active RhoA at the cytokinetic furrow and both RhoA and Rac1 at cell-cell junctions in epithelial cells. *Mol Biol Cell,* 26**,** 2439-55.

BRODSKIY, P. A. & ZARTMAN, J. J. 2018. Calcium as a signal integrator in developing epithelial tissues. *Phys Biol,* 15**,** 051001.

BRUEWER, M., HOPKINS, A. M., HOBERT, M. E., NUSRAT, A. & MADARA, J. L. 2004. RhoA, Rac1, and Cdc42 exert distinct effects on epithelial barrier via selective structural and biochemical modulation of junctional proteins and F-actin. *American journal of physiology. Cell physiology,* 287**,** C327-35.

CANALES COUTINO, B. & MAYOR, R. 2021. Mechanosensitive ion channels in cell migration. *Cells Dev,* 166**,** 203683.

CANALES, J., MORALES, D., BLANCO, C., RIVAS, J., DIAZ, N., ANGELOPOULOS, I. & CERDA, O. 2019. A TR(i)P to Cell Migration: New Roles of TRP Channels in Mechanotransduction and Cancer. *Front Physiol,* 10**,** 757.

CAVANAUGH, K. J., JR., OSWARI, J. & MARGULIES, S. S. 2001. Role of stretch on tight junction structure in alveolar epithelial cells. *Am J Respir Cell Mol Biol,* 25**,** 584-91.

CHARRAS, G. T. 2008. A short history of blebbing. *Journal of Microscopy,* 231**,** 466-478.

CHEN, T. W., WARDILL, T. J., SUN, Y., PULVER, S. R., RENNINGER, S. L., BAOHAN, A., SCHREITER, E. R., KERR, R. A., ORGER, M. B., JAYARAMAN, V., LOOGER, L. L., SVOBODA, K. & KIM, D. S. 2013. Ultrasensitive fluorescent proteins for imaging neuronal activity. *Nature,* 499**,** 295-300.

CHOI, W., ACHARYA, B. R., PEYRET, G., FARDIN, M. A., MEGE, R. M., LADOUX, B., YAP, A. S., FANNING, A. S. & PEIFER, M. 2016. Remodeling the zonula adherens in response to tension and the role of afadin in this response. *J Cell Biol,* 213**,** 243-60.

CHRISTODOULOU, N. & SKOURIDES, P. A. 2015. Cell-Autonomous Ca(2+) Flashes Elicit Pulsed Contractions of an Apical Actin Network to Drive Apical Constriction during Neural Tube Closure. *Cell Rep,* 13**,** 2189-202.

CLARK, A. G., MILLER, A. L., VAUGHAN, E., YU, H. Y. E., PENKERT, R. & BEMENT, W. M. 2009. Integration of Single and Multicellular Wound Responses. *Current Biology,* 19**,** 1389-1395.

CLAUDE, P. & GOODENOUGH, D. A. 1973. Fracture faces of zonulae occludentes from "tight" and "leaky" epithelia. *J Cell Biol,* 58**,** 390-400.

COLOM, A., DERIVERY, E., SOLEIMANPOUR, S., TOMBA, C., MOLIN, M. D., SAKAI, N., GONZALEZ-GAITAN, M., MATILE, S. & ROUX, A. 2018. A fluorescent membrane tension probe. *Nat Chem,* 10**,** 1118-1125.

COSTE, B., MATHUR, J., SCHMIDT, M., EARLEY, T. J., RANADE, S., PETRUS, M. J., DUBIN, A. E. & PATAPOUTIAN, A. 2010. Piezo1 and Piezo2 Are Essential Components of Distinct Mechanically Activated Cation Channels. *Science,* 330**,** 55-60.

DAVENPORT, N. R., SONNEMANN, K. J., ELICEIRI, K. W. & BEMENT, W. M. 2016. Membrane dynamics during cellular wound repair. *Molecular Biology of the Cell,* 27**,** 2272-2285.

DENKER, B. M. & NIGAM, S. K. 1998. Molecular structure and assembly of the tight junction. *Am J Physiol,* 274**,** F1-9.

DIPAOLO, B. C. & MARGULIES, S. S. 2012. Rho kinase signaling pathways during stretch in primary alveolar epithelia. *Am J Physiol Lung Cell Mol Physiol,* 302**,** L992-1002.

EISENHOFFER, G. T., LOFTUS, P. D., YOSHIGI, M., OTSUNA, H., CHIEN, C.-B., MORCOS, P. A. & ROSENBLATT, J. 2012. Crowding induces live cell extrusion to maintain homeostatic cell numbers in epithelia. *Nature,* 484**,** 546-549.

ELLEFSEN, K. L., HOLT, J. R., CHANG, A. C., NOURSE, J. L., ARULMOLI, J., MEKHDJIAN, A. H., ABUWARDA, H., TOMBOLA, F., FLANAGAN, L. A., DUNN, A. R., PARKER, I. & PATHAK, M. M. 2019. Myosin-II mediated traction forces evoke localized Piezo1-dependent Ca(2+) flickers. *Commun Biol,* 2**,** 298.

FANNING, A. S. & ANDERSON, J. M. 2009. Zonula occludens-1 and -2 are cytosolic scaffolds that regulate the assembly of cellular junctions. *Ann N Y Acad Sci,* 1165**,** 113-20.

FANNING, A. S., JAMESON, B. J., JESAITIS, L. A. & ANDERSON, J. M. 1998. The tight junction protein ZO-1 establishes a link between the transmembrane protein occludin and the actin cytoskeleton. *J Biol Chem,* 273**,** 29745-53.

FANNING, A. S., VAN ITALLIE, C. M. & ANDERSON, J. M. 2012. Zonula occludens-1 and -2 regulate apical cell structure and the zonula adherens cytoskeleton in polarized epithelia. *Mol Biol Cell,* 23**,** 577-90.

FARQUHAR, M. G. & PALADE, G. E. 1963. Junctional complexes in various epithelia. *J Cell Biol,* 17**,** 375-412.

FROMTER, E. & DIAMOND, J. 1972. Route of passive ion permeation in epithelia. *Nat New Biol,* 235**,** 9-13.

FURUSE, M., SASAKI, H., FUJIMOTO, K. & TSUKITA, S. 1998. A single gene product, claudin-1 or -2, reconstitutes tight junction strands and recruits occludin in fibroblasts. *J Cell Biol,* 143**,** 391-401.

GARCIA-HERNANDEZ, V., QUIROS, M. & NUSRAT, A. 2017. Intestinal epithelial claudins: Expression and regulation in homeostasis and inflammation. *Annals of the New York Academy of Sciences,* 1397**,** 66-79.

GONZALEZ-MARISCAL, L., CHAVEZ DE RAMIREZ, B. & CEREIJIDO, M. 1985. Tight junction formation in cultured epithelial cells (MDCK). *J Membr Biol,* 86**,** 113-25.

GONZALEZ-MARISCAL, L., CONTRERAS, R. G., BOLIVAR, J. J., PONCE, A., CHAVEZ DE RAMIREZ, B. & CEREIJIDO, M. 1990. Role of calcium in tight junction formation between epithelial cells. *Am J Physiol,* 259**,** C978-86.

GUAN, Y., WATSON, A. J., MARCHIANDO, A. M., BRADFORD, E., SHEN, L., TURNER, J. R. & MONTROSE, M. H. 2011. Redistribution of the tight junction protein ZO-1 during physiological shedding of mouse intestinal epithelial cells. *Am J Physiol Cell Physiol,* 300**,** C1404-14.

GUDIPATY, S. A., LINDBLOM, J., LOFTUS, P. D., REDD, M. J., EDES, K., DAVEY, C. F., KRISHNEGOWDA, V. & ROSENBLATT, J. 2017. Mechanical stretch triggers rapid epithelial cell division through Piezo1. *Nature,* 543**,** 118-121.

GUDIPATY, S. A. & ROSENBLATT, J. 2017. Epithelial cell extrusion: Pathways and pathologies. *Semin Cell Dev Biol,* 67**,** 132-140.

GUMBINER, B. 1987. Structure, biochemistry, and assembly of epithelial tight junctions. *Am J Physiol,* 253**,** C749-58.

GUNZEL, D. 2017. Claudins: vital partners in transcellular and paracellular transport coupling. *Pflugers Arch,* 469**,** 35-44.

GUNZEL, D. & YU, A. S. 2013. Claudins and the modulation of tight junction permeability. *Physiol Rev,* 93**,** 525-69.

HARRIS, T. J. & TEPASS, U. 2010. Adherens junctions: from molecules to morphogenesis. *Nat Rev Mol Cell Biol,* 11**,** 502-14.

HASHIMOTO, Y., KINOSHITA, N., GRECO, T. M., FEDERSPIEL, J. D., JEAN BELTRAN, P. M., UENO, N. & CRISTEA, I. M. 2019. Mechanical Force Induces Phosphorylation-Mediated Signaling that Underlies Tissue Response and Robustness in Xenopus Embryos. *Cell Syst*.

HERRGEN, L., VOSS, O. P. & AKERMAN, C. J. 2014. Calcium-Dependent Neuroepithelial Contractions Expel Damaged Cells from the Developing Brain. *Developmental Cell,* 31**,** 599-613.

HIGASHI, T., ARNOLD, T. R., STEPHENSON, R. E., DINSHAW, K. M. & MILLER, A. L. 2016. Maintenance of the Epithelial Barrier and Remodeling of Cell-Cell Junctions during Cytokinesis. *Curr Biol,* 26**,** 1829-42.

HIGASHI, T., STEPHENSON, R. E. & MILLER, A. L. 2019. Comprehensive analysis of formin localization in Xenopus epithelial cells. *Mol Biol Cell,* 30**,** 82-95.

HIROKAWA, N. 1982. Organization of actin, myosin, and intermediate filaments in the brush border of intestinal epithelial cells. *The Journal of Cell Biology,* 94**,** 425-443.

HIROKAWA, N., KELLER, T. C., 3RD, CHASAN, R. & MOOSEKER, M. S. 1983. Mechanism of brush border contractility studied by the quick-freeze, deep-etch method. *J Cell Biol,* 96**,** 1325-36.

HULL, B. E. & STAEHELIN, L. A. 1976. Functional significance of the variations in the geometrical organization of tight junction networks. *J Cell Biol,* 68**,** 688-704.

ITOH, M., FURUSE, M., MORITA, K., KUBOTA, K., SAITOU, M. & TSUKITA, S. 1999. Direct binding of three tight junction-associated MAGUKs, ZO-1, ZO-2, and ZO-3, with the COOH termini of claudins. *J Cell Biol,* 147**,** 1351-63.

JAFFE, L. F. 2008. Calcium waves. *Philosophical Transactions of the Royal Society B: Biological Sciences,* 363**,** 1311-1317.

JOU, T. S., SCHNEEBERGER, E. E. & NELSON, W. J. 1998. Structural and functional regulation of tight junctions by RhoA and Rac1 small GTPases. *Journal of Cell Biology,* 142**,** 101-115.

KIMURA, K., ITO, M., AMANO, M., CHIHARA, K., FUKATA, Y., NAKAFUKU, M., YAMAMORI, B., FENG, J., NAKANO, T., OKAWA, K., IWAMATSU, A. & KAIBUCHI, K.

1996. Regulation of myosin phosphatase by Rho and Rho-associated kinase (Rho-kinase) - Abstract - Europe PubMed Central. *Science (New York, N.Y.),* 273**,** 245-8.

LUISSINT, A. C., PARKOS, C. A. & NUSRAT, A. 2016. Inflammation and the Intestinal Barrier: Leukocyte-Epithelial Cell Interactions, Cell Junction Remodeling, and Mucosal Repair. *Gastroenterology,* 151**,** 616-32.

LUO, M., K. Y. HO, K., TONG, Z., DENG, L. & P. LIU, A. 2019. Compressive Stress Enhances Invasive Phenotype of Cancer Cells via Piezo1 Activation. *bioRxiv***,** 513218.

MADARA, J. L. 1987. Intestinal absorptive cell tight junctions are linked to cytoskeleton. *Am J Physiol,* 253**,** C171-5.

MADARA, J. L. 1990. Maintenance of the macromolecular barrier at cell extrusion sites in intestinal epithelium: physiological rearrangement of tight junctions. *J Membr Biol,* 116**,** 177-84.

MADARA, J. L., BARENBERG, D. & CARLSON, S. 1986. Effects of cytochalasin D on occluding junctions of intestinal absorptive cells: further evidence that the cytoskeleton may influence paracellular permeability and junctional charge selectivity. *J Cell Biol,* 102**,** 2125-36.

MARCHIANDO, A. M., GRAHAM, W. V. & TURNER, J. R. 2010. Epithelial barriers in homeostasis and disease. *Annu Rev Pathol,* 5**,** 119-44.

MARCHIANDO, A. M., SHEN, L., GRAHAM, W. V., EDELBLUM, K. L., DUCKWORTH, C. A., GUAN, Y., MONTROSE, M. H., TURNER, J. R. & WATSON, A. J. 2011. The epithelial barrier is maintained by in vivo tight junction expansion during pathologic intestinal epithelial shedding. *Gastroenterology,* 140**,** 1208-1218 e1-2.

MARTINAC, B. 2004. Mechanosensitive ion channels: molecules of mechanotransduction. *J Cell Sci,* 117**,** 2449-60.

MILLER, A. L. & BEMENT, W. M. 2009. Regulation of cytokinesis by Rho GTPase flux. *Nat Cell Biol,* 11**,** 71-7.

MIYAMOTO, T., MOCHIZUKI, T., NAKAGOMI, H., KIRA, S., WATANABE, M., TAKAYAMA, Y., SUZUKI, Y., KOIZUMI, S., TAKEDA, M. & TOMINAGA, M. 2014. Functional role for Piezo1 in stretch-evoked Ca2+ influx and ATP release in Urothelial cell cultures. *Journal of Biological Chemistry,* 289**,** 16565-16575.

MORIWAKI, K., TSUKITA, S. & FURUSE, M. 2007. Tight junctions containing claudin 4 and 6 are essential for blastocyst formation in preimplantation mouse embryos. *Dev Biol,* 312**,** 509-22.

NAVIS, A. & BAGNAT, M. 2015. Developing pressures: fluid forces driving morphogenesis. *Curr Opin Genet Dev,* 32**,** 24-30.

NIGAM, S. K., RODRIGUEZ-BOULAN, E. & SILVER, R. B. 1992. Changes in intracellular calcium during the development of epithelial polarity and junctions. *Proc Natl Acad Sci U S A,* 89**,** 6162-6.

NOURSE, J. L. & PATHAK, M. M. 2017. How cells channel their stress: Interplay between Piezo1 and the cytoskeleton. *Seminars in Cell and Developmental Biology,* 71**,** 3-12.

NUSRAT, A., GIRY, M., TURNER, J. R., COLGAN, S. P., PARKOS, C. A., CARNES, D., LEMICHEZ, E., BOQUET, P. & MADARA, J. L. 1995. Rho protein regulates tight junctions and perijunctional actin organization in polarized epithelia. *Proc Natl Acad Sci U S A,* 92**,** 10629-33.

ODENWALD, M. A., CHOI, W., BUCKLEY, A., SHASHIKANTH, N., JOSEPH, N. E., WANG, Y., WARREN, M. H., BUSCHMANN, M. M., PAVLYUK, R., HILDEBRAND, J., MARGOLIS, B., FANNING, A. S. & TURNER, J. R. 2017. ZO-1 interactions with F-actin and occludin direct epithelial polarization and single lumen specification in 3D culture. *Journal of Cell Science,* 130**,** 243-259.

OTANI, T., NGUYEN, T. P., TOKUDA, S., SUGIHARA, K., SUGAWARA, T., FURUSE, K., MIURA, T., EBNET, K. & FURUSE, M. 2019. Claudins and JAM-A coordinately regulate tight junction formation and epithelial polarity. *J Cell Biol,* 218**,** 3372-3396.

PEIFER, M., MCCREA, P. D., GREEN, K. J., WIESCHAUS, E. & GUMBINER, B. M. 1992. The vertebrate adhesive junction proteins beta-catenin and plakoglobin and the Drosophila segment polarity gene armadillo form a multigene family with similar properties. *J Cell Biol,* 118**,** 681-91.

PITELKA, D. R. & TAGGART, B. N. 1983. Mechanical tension induces lateral movement of intramembrane components of the tight junction: studies on mouse mammary cells in culture. *J Cell Biol,* 96**,** 606-12.

PRIYA, R., GOMEZ, G. A., BUDNAR, S., VERMA, S., COX, H. L., HAMILTON, N. A. & YAP, A. S. 2015. Feedback regulation through myosin II confers robustness on RhoA signalling at E-cadherin junctions. *Nature Cell Biology,* 17**,** 1282-1293.

QUIROS, M. & NUSRAT, A. 2014. RhoGTPases, actomyosin signaling and regulation of the Epithelial Apical Junctional Complex. *Seminars in Cell and Developmental Biology,* 36**,** 194-203.

RALEIGH, D. R., BOE, D. M., YU, D., WEBER, C. R., MARCHIANDO, A. M., BRADFORD, E. M., WANG, Y., WU, L., SCHNEEBERGER, E. E., SHEN, L. &

TURNER, J. R. 2011. Occludin S408 phosphorylation regulates tight junction protein interactions and barrier function. *J Cell Biol,* 193**,** 565-82.

RANADE, S. S., QIU, Z., WOO, S.-H., HUR, S. S., MURTHY, S. E., CAHALAN, S. M., XU, J., MATHUR, J., BANDELL, M., COSTE, B., LI, Y.-S. J., CHIEN, S. & PATAPOUTIAN, A. 2014. Piezo1, a mechanically activated ion channel, is required for vascular development in mice. *Proceedings of the National Academy of Sciences,* 111**,** 10347-10352.

RATHEESH, A., GOMEZ, G. A., PRIYA, R., VERMA, S., KOVACS, E. M., JIANG, K., BROWN, N. H., AKHMANOVA, A., STEHBENS, S. J. & YAP, A. S. 2012. Centralspindlin and alpha-catenin regulate Rho signalling at the epithelial zonula adherens. *Nat Cell Biol,* 14**,** 818-828.

REYES, C. C., JIN, M., BREZNAU, E. B., ESPINO, R., DELGADO-GONZALO, R., GORYACHEV, A. B. & MILLER, A. L. 2014. Anillin regulates cell-cell junction integrity by organizing junctional accumulation of Rho-GTP and actomyosin. *Current Biology,* 24**,** 1263-1270.

ROSENBLATT, J., RAFF, M. C. & CRAMER, L. P. 2001. An epithelial cell destined for apoptosis signals its neighbors to extrude it by an actin- and myosin-dependent mechanism. *Curr Biol,* 11**,** 1847-57.

SACHS, F. 2017. Mechanical transduction by ion channels: A cautionary tale Sachs. *World Journal of Neurology,* 5**,** 74-87.

SAITO, A. C., HIGASHI, T., FUKAZAWA, Y., OTANI, T., TAUCHI, M., HIGASHI, A. Y., FURUSE, M. & CHIBA, H. 2021. Occludin and tricellulin facilitate formation of anastomosing tight-junction strand network to improve barrier function. *Mol Biol Cell,* 32**,** 722-738.

SAMAK, G., GANGWAR, R., CROSBY, L. M., DESAI, L. P., WILHELM, K., WATERS, C. M. & RAO, R. 2014. Cyclic stretch disrupts apical junctional complexes in Caco-2 cell monolayers by a JNK-2-, c-Src-, and MLCK-dependent mechanism. *Am J Physiol Gastrointest Liver Physiol,* 306**,** G947-58.

SASAKI, H., MATSUI, C., FURUSE, K., MIMORI-KIYOSUE, Y., FURUSE, M. & TSUKITA, S. 2003. Dynamic behavior of paired claudin strands within apposing plasma membranes. *Proc Natl Acad Sci U S A,* 100**,** 3971-6.

SCHWAYER, C., SHAMIPOUR, S., PRANJIC-FERSCHA, K., SCHAUER, A., BALDA, M., TADA, M., MATTER, K. & HEISENBERG, C. P. 2019. Mechanosensation of Tight Junctions Depends on ZO-1 Phase Separation and Flow. *Cell,* 179**,** 937-952 e18.

SHAO, X., LI, Q., MOGILNER, A., BERSHADSKY, A. D. & SHIVASHANKAR, G. V. 2015. Mechanical stimulation induces formin-dependent assembly of a perinuclear actin rim. *Proc Natl Acad Sci U S A,* 112**,** E2595-601.

SHEN, L., BLACK, E. D., WITKOWSKI, E. D., LENCER, W. I., GUERRIERO, V., SCHNEEBERGER, E. E. & TURNER, J. R. 2006. Myosin light chain phosphorylation regulates barrier function by remodeling tight junction structure. *J Cell Sci,* 119**,** 2095-106.

SHEN, L., WEBER, C. R., RALEIGH, D. R., YU, D. & TURNER, J. R. 2011. Tight junction pore and leak pathways: a dynamic duo. *Annu Rev Physiol,* 73**,** 283-309.

SHEN, L., WEBER, C. R. & TURNER, J. R. 2008. The tight junction protein complex undergoes rapid and continuous molecular remodeling at steady state. *J Cell Biol,* 181**,** 683-95.

SOTO, X., LI, J., LEA, R., DUBAISSI, E., PAPALOPULU, N. & AMAYA, E. 2013. Inositol kinase and its product accelerate wound healing by modulating calcium levels, Rho GTPases, and F-actin assembly. *Proc Natl Acad Sci U S A,* 110**,** 11029-34.

STAEHELIN, L. A., MUKHERJEE, T. M. & WILLIAMS, A. W. 1969. Freeze-etch appearance of the tight junctions in the epithelium of small and large intestine of mice. *Protoplasma,* 67**,** 165-84.

STEPHENSON, R. E., HIGASHI, T., EROFEEV, I. S., ARNOLD, T. R., LEDA, M., GORYACHEV, A. B. & MILLER, A. L. 2019. Rho Flares Repair Local Tight Junction Leaks. *Dev Cell,* 48**,** 445-459 e5.

STEPHENSON, R. E. & MILLER, A. L. 2017. Tools for live imaging of active Rho GTPases in Xenopus. *Genesis,* 55**,** 1-6.

STOOKE-VAUGHAN, G. A., DAVIDSON, L. A. & WOOLNER, S. 2017. Xenopus as a model for studies in mechanical stress and cell division. *Genesis,* 55**,** 1-11.

STUART, R. O., SUN, A., PANICHAS, M., HEBERT, S. C., BRENNER, B. M. & NIGAM, S. K. 1994. Critical role for intracellular calcium in tight junction biogenesis. *J Cell Physiol,* 159**,** 423-33.

SYEDA, R., XU, J., DUBIN, A. E., COSTE, B., MATHUR, J., HUYNH, T., MATZEN, J., LAO, J., TULLY, D. C., ENGELS, I. H., MICHAEL PETRASSI, H., SCHUMACHER, A. M., MONTAL, M., BANDELL, M. & PATAPOUTIAN, A. 2015. Chemical activation of the mechanotransduction channel Piezo1. *eLife,* 4**,** 1-11.

TAKEICHI, M. 1991. Cadherin cell adhesion receptors as a morphogenetic regulator. *Science,* 251**,** 1451-5.

TAKEICHI, M. 2014. Dynamic contacts: rearranging adherens junctions to drive epithelial remodelling. *Nat Rev Mol Cell Biol,* 15**,** 397-410.

TICE, L. W., CARTER, R. L. & CAHILL, M. B. 1979. Changes in tight junctions of rat intestinal crypt cells associated with changes in their mitotic activity. *Tissue Cell,* 11**,** 293-316.

TIRUPPATHI, C., AHMMED, G. U., VOGEL, S. M. & MALIK, A. B. 2006. Ca2+ signaling, TRP channels, and endothelial permeability. *Microcirculation,* 13**,** 693-708.

TSAI, F. C., KUO, G. H., CHANG, S. W. & TSAI, P. J. 2015. Ca2+ signaling in cytoskeletal reorganization, cell migration, and cancer metastasis. *Biomed Res Int,* 2015**,** 409245.

TSUKITA, S., FURUSE, M. & ITOH, M. 2001. Multifunctional strands in tight junctions. *Nat Rev Mol Cell Biol,* 2**,** 285-93.

TURKSEN, K. & TROY, T. C. 2004. Barriers built on claudins. *J Cell Sci,* 117**,** 2435-47.

TYLER, S. 2003. Epithelium--the primary building block for metazoan complexity. *Integr Comp Biol,* 43**,** 55-63.

UMEDA, K., IKENOUCHI, J., KATAHIRA-TAYAMA, S., FURUSE, K., SASAKI, H., NAKAYAMA, M., MATSUI, T., TSUKITA, S., FURUSE, M. & TSUKITA, S. 2006. ZO-1 and ZO-2 Independently Determine Where Claudins Are Polymerized in Tight-Junction Strand Formation. *Cell,* 126**,** 741-754.

VAN ITALLIE, C. M. & ANDERSON, J. M. 2014. Architecture of tight junctions and principles of molecular composition. *Semin Cell Dev Biol,* 36**,** 157-65.

VAN ITALLIE, C. M., FANNING, A. S., BRIDGES, A. & ANDERSON, J. M. 2009. ZO-1 stabilizes the tight junction solute barrier through coupling to the perijunctional cytoskeleton. *Mol Biol Cell,* 20**,** 3930-40.

VAN ITALLIE, C. M., TIETGENS, A. J. & ANDERSON, J. M. 2017. Visualizing the dynamic coupling of claudin strands to the actin cytoskeleton through ZO-1. *Mol Biol Cell,* 28**,** 524-534.

VAN ITALLIE, C. M., TIETGENS, A. J., KRYSTOFIAK, E., KACHAR, B. & ANDERSON, J. M. 2015. A complex of ZO-1 and the BAR-domain protein TOCA-1 regulates actin assembly at the tight junction. *Molecular Biology of the Cell.* American Society for Cell Biology.

VARADARAJAN, S., STEPHENSON, R. E. & MILLER, A. L. 2019. Multiscale dynamics of tight junction remodeling. *J Cell Sci,* 132.

WALLINGFORD, J. B., EWALD, A. J., HARLAND, R. M. & FRASER, S. E. 2001. Calcium signaling during convergent extension in Xenopus. *Current Biology,* 11**,** 652-661.

WALSH, S. V., HOPKINS, A. M., CHEN, J., NARUMIYA, S., PARKOS, C. A. & NUSRAT, A. 2001. Rho kinase regulates tight junction function and is necessary for tight junction assembly in polarized intestinal epithelia. *Gastroenterology,* 121**,** 566-579.

WATANABE, N., KATO, T., FUJITA, A., ISHIZAKI, T. & NARUMIYA, S. 1999. Cooperation between mDia1 and ROCK in Rho-induced actin reorganization. *Nat Cell Biol,* 1**,** 136-43.

WEBB, S. E. & MILLER, A. L. 2006. Ca2+ signaling and early embryonic patterning during the Blastula and Gastrula Periods of Zebrafish and Xenopus development. *Biochimica et Biophysica Acta - Molecular Cell Research.*

WEBER, E. W., HAN, F., TAUSEEF, M., BIRNBAUMER, L., MEHTA, D. & MULLER, W. A. 2015. TRPC6 is the endothelial calcium channel that regulates leukocyte transendothelial migration during the inflammatory response. *J Exp Med,* 212**,** 1883-99.

WEBER, E. W. & MULLER, W. A. 2017. Roles of transient receptor potential channels in regulation of vascular and epithelial barriers. *Tissue Barriers,* 5**,** e1331722.

WEI, C., WANG, X., CHEN, M., OUYANG, K., SONG, L. S. & CHENG, H. 2009. Calcium flickers steer cell migration. *Nature,* 457**,** 901-5.

YU, D., MARCHIANDO, A. M., WEBER, C. R., RALEIGH, D. R., WANG, Y., SHEN, L. & TURNER, J. R. 2010. MLCK-dependent exchange and actin binding region-dependent anchoring of ZO-1 regulate tight junction barrier function. *Proc Natl Acad Sci U S A,* 107**,** 8237-41.

YU, H. Y. E. & BEMENT, W. M. 2007. Control of local actin assembly by membrane fusion-dependent compartment mixing. *Nature Cell Biology,* 9**,** 149-159.

ZHAO, Q., ZHOU, H., CHI, S., WANG, Y., WANG, J., GENG, J., WU, K., LIU, W., ZHANG, T., DONG, M. Q., WANG, J., LI, X. & XIAO, B. 2018. Structure and mechanogating mechanism of the Piezo1 channel. *Nature,* 554**,** 487-492.

ZHONG, M., WU, W., KANG, H., HONG, Z., XIONG, S., GAO, X., REHMAN, J., KOMAROVA, Y. A. & MALIK, A. B. 2020. Alveolar Stretch Activation of Endothelial Piezo1 Protects Adherens Junctions and Lung Vascular Barrier. *Am J Respir Cell Mol Biol,* 62**,** 168-177.

Chapter 2 Mechanosensitive Calcium Signaling Promotes Epithelial Tight Junction Remodeling by Activating RhoA

This chapter describes work available as a preprint in bioRxiv

Varadarajan S., Stephenson R.E., Misterovich E.R., Wu J.L., Erofeev I.S., Goryachev A.B., and Miller A.L. Mechanosensitive calcium signaling promotes epithelial tight junction remodeling by activating RhoA. bioRxiv 2021.05.18.444663.

Author contributions are as follows:

S.Varadarajan and A.L.Miller conceptualized the study; S.Varadarajan, R.E.Stephenson, and A.L.Miller developed the methodology; S.Varadarajan performed the majority of experiments and data analysis; J.L.Wu performed the experiment and analyzed data for Figure S 2.3; E.R.Misterovich analyzed the data for Figure 2.2 E, Figure 2.5 F and F'; I.S.Erofeev constructed the kymographs for Figure 2.5 G; S.Varadarajan and A.L.Miller wrote the original draft of the manuscript with input from R.E.Stephenson; All authors revised the manuscript; A.L.Miller and A.B.Goryachev acquired funding; A.L.Miller supervised the study.

2.1 Abstract

Epithelia maintain an effective barrier by remodeling cell-cell junctions in response to mechanical stimuli. Cells often respond to mechanical stress through activating RhoA and remodeling actomyosin. Previously, we found that local leaks in the barrier are rapidly repaired by localized, transient activation of RhoA – "Rho flares" – but how Rho flares are initiated remains unknown. Here, we discovered that intracellular calcium flashes occur in *Xenopus laevis* epithelial cells undergoing Rho flare-mediated remodeling of tight junctions. Calcium flashes originate at the site of barrier leaks and

propagate into the cell. Depletion of intracellular calcium or inhibition of mechanosensitive calcium channels (MSC) reduced the amplitude of calcium flashes and diminished the activation of Rho flares. Furthermore, MSC-dependent calcium influx was necessary to maintain global barrier function by regulating local repair of tight junctions through efficient junction contraction. We propose that MSC-dependent calcium flashes are an important mechanism allowing epithelial cells to sense and respond to local leaks induced by mechanical stimuli.

2.2 Introduction

The ability of epithelial tissues to establish and maintain a selective paracellular barrier is crucial for development of multicellular organisms and proper function of vital organs (Marchiando et al., 2010, Moriwaki et al., 2007, Ivanov et al., 2010a, Luissint et al., 2016). The dynamic nature of epithelial tissues during development and organ homeostasis requires cells to change shape and remodel their cell-cell junctions during tissue-generated forces including cell division, extrusion, and intercalation (Varadarajan et al., 2019, Guillot and Lecuit, 2013, Gudipaty and Rosenblatt, 2016). Remarkably, epithelia are able to maintain barrier function despite this remodeling (Higashi et al., 2016, Stephenson et al., 2019, Rosenblatt et al., 2001). However, the mechanisms by which epithelial cells remodel their cell-cell junctions without compromising barrier function is not fully understood.

In vertebrates, epithelial barrier function is regulated by the apical junctional complex, including tight junctions (TJs) and adherens junctions (AJs) (Zihni et al., 2016). Claudins and Occludin, transmembrane TJ proteins, interact with their counterparts on neighboring cells and polymerize within the membrane to form a network of TJ strands that selectively regulate the passage of small ions and macromolecules between the cells (Claude and Goodenough, 1973, Furuse et al., 1998, Staehelin et al., 1969). TJ strands are connected to the underlying actomyosin array by the zonula occludens (ZO) family of scaffolding proteins, thereby coupling barrier function to actomyosin-mediated cells shape changes (Itoh et al., 1999, Van Itallie et al., 2017, Furuse et al., 1998, Fanning et al., 1998). Although it is known that mechanical stress leads to a global increase in permeability to macromolecules

(Cavanaugh et al., 2006, Samak et al., 2010, Cohen et al., 2008), much less is known about how cells respond to these leaks.

We recently reported the occurrence of short-lived leaks associated with cell-generated mechanical forces in the developing *Xenopus* epithelium (Stephenson et al., 2019). During *Xenopus* gastrulation, the epithelial monolayer covering the animal cap of the embryo undergoes frequent cell divisions and morphogenetic movements, requiring elongation of cell-cell junctions to accommodate cell shape changes. Leaks were associated with elongating junctions and happened at sites where TJ proteins were locally reduced. Leaks were dynamically repaired by localized, short-lived activations of the small GTPase RhoA, which we termed “Rho flares” (Stephenson et al., 2019). Rho flares are associated with local membrane protrusion at the site of leaks, suggesting that RhoA may be activated by a membrane tension-mediated mechanosensitive pathway.

Calcium signaling plays a key role in transducing mechanical forces into biochemical signals during cell shape changes (Christodoulou and Skourides, 2015, Sahu et al., 2017). Calcium signaling varies from long-range calcium waves to subcellular calcium transients, both of which are controlled precisely in space and time to modulate cytoskeleton-mediated cell shape changes. Calcium signaling is required for local RhoA activation during mechanical events including wound healing (Clark et al., 2009, Benink and Bement, 2005), cell migration (Pardo-Pastor et al., 2018), and dendritic spine enlargement (Murakoshi et al., 2011), suggesting the possibility of calcium-mediated RhoA activation during TJ remodeling.

Elevation of intracellular calcium following a mechanical stimulus is mediated by influx of extracellular calcium through mechanosensitive calcium channels (MSCs) in the plasma membrane or calcium release from the endoplasmic reticulum (ER) (Shao et al., 2015). Plasma membrane localized MSCs – including the Piezo and Transient Receptor Potential (TRP) families – allow calcium influx in response to local and/or global changes in membrane tension or curvature (Liu and Montell, 2015, Gudipaty et al., 2017, Miyamoto et al., 2014, Mochizuki et al., 2009, Coste et al., 2010, Shi et al., 2018). For example, during cell migration, MSCs mediate transient calcium influx at lamellipodia and focal adhesions to guide the direction of migration (Ellefsen et al., 2019, Wei et al., 2009). However, the role of MSCs in force-dependent remodeling of TJs has not been elucidated.

Here, we investigate whether calcium signaling and MSCs are involved in TJ remodeling using live imaging of the gastrula-stage *Xenopus* epithelium. We show that a local intracellular calcium increase follows paracellular leaks in response to cell-cell junction elongation. We demonstrate that this intracellular calcium increase is required for the Rho flare-mediated TJ repair pathway and is dependent on MSCs. Finally, we show that MSC-mediated calcium influx regulates local junction contraction through robust Rho activation and is required to repair and maintain an intact barrier during cell shape changes.

2.3 Results

2.3.1 Epithelial barrier leaks induce a local intracellular calcium increase

Intracellular calcium signaling has been implicated in TJ biogenesis, establishment of barrier function, and actomyosin-mediated cell shape changes (Gonzalez-Mariscal et al., 1990, Nigam et al., 1992, Christodoulou and Skourides, 2015, Suzuki et al., 2017). Thus, we hypothesized that intracellular calcium signaling might be involved in Rho flare-mediated TJ repair of local leaks. To test this idea, we performed Zinc-based Ultrasensitive Microscopic Barrier Assay (ZnUMBA (Stephenson et al., 2019)) in gastrula-stage *Xenopus* embryos (Nieuwkoop and Faber stage 10.5-12) expressing probes for intracellular calcium and active Rho (tagBFP-C2 (Yu and Bement, 2007) and mCherry-2xrGBD (Benink and Bement, 2005, Davenport et al., 2016). The C2 domain of PKCβ, when bound to calcium, is recruited from the cytoplasm to the plasma membrane, and is capable of detecting both local and global calcium increases. High-speed live imaging demonstrated that calcium increases locally at sites of leaks (Figure 2.1 and Figure S 2.1 A). FluoZin-3 intensity increased prior to the local calcium increase at the site of Rho flares, indicating a leak, (Figure 2.1 B) and returned to baseline following the increase in calcium and active Rho, indicating restoration of barrier function (Figure 2.1 B).

To better evaluate the spatial origin of the calcium increase at Rho flares, we generated a kymograph at the site of the Rho flare. The kymograph shows that the intracellular calcium increase originates at the plasma membrane and spreads asymmetrically into the cells adjacent to the membrane (Figure 2.1 D). Asymmetric intracellular calcium increase is proportional to the active Rho intensity in each of the

cells adjacent to the membrane (Figure 2.1, C-D). Because Rho flares precede TJ reinforcement (Stephenson et al., 2019), we next examined whether the local calcium increase precedes ZO-1 reinforcement. Indeed, quantification revealed that the local calcium increase precedes ZO-1 reinforcement (Figure 2.1, C and E). Together, these results show that the local calcium increase originates at sites of leaks and is followed by ZO-1 reinforcement.

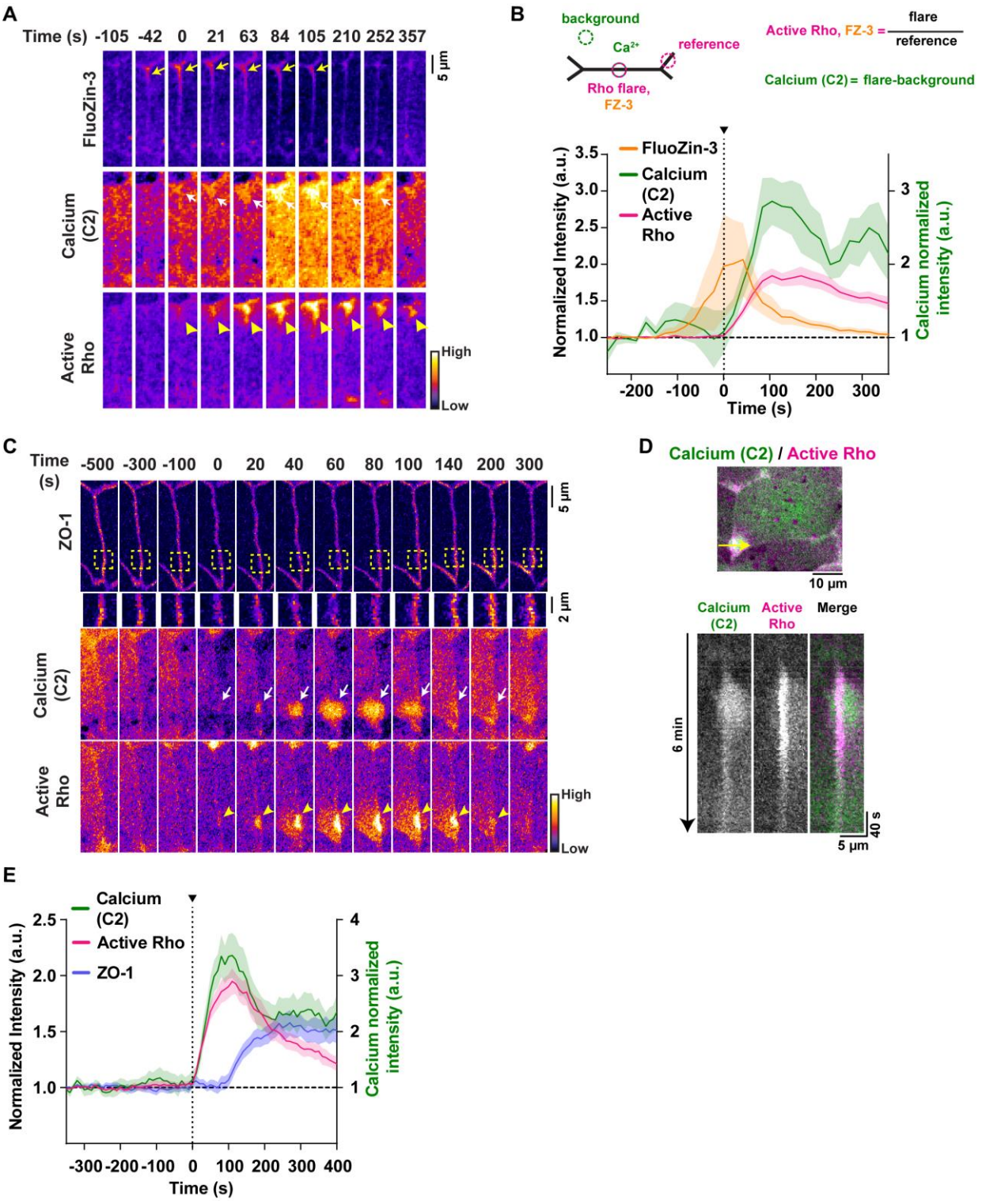

Figure 2.1: Epithelial paracellular leaks induce a local intracellular calcium increase.

(A) Time lapse images (Fire LUT) of FluoZin-3 dye, membrane calcium probe (tagBFP-PKC β-C2), and active Rho (mCherry-2xrGBD). Calcium increase (white arrows) follows a leak indicated by increase in FluoZin-3 fluorescence (yellow arrows) at the site of Rho flare (yellow arrowheads). Time 0 s represents start of Rho flare.

(B) Quantification of experiments shown in A. Top: Schematic showing regions of interest (ROIs) and used to quantify Rho flares, calcium (C2), and FluoZin-3. Bottom: Graph of mean normalized intensity shows the leak (FluoZin-3) precedes the increases in local calcium and active Rho. Shaded region represents S.E.M. n= 18 flares, 10 embryos, 6 experiments.
(C) Time lapse images (FIRE LUT) of BFP-ZO-1, membrane calcium probe (mNeon-PKC β-C2), and active Rho (mCherry-2xrGBD). Local calcium increase (white arrows) is spatially localized to the site of ZO-1 decrease (yellow boxed region) and Rho flare (yellow arrowheads).
(D) Top: Cell view of an embryo expressing membrane calcium probe (mNeon-PKCβ-C2, green) and active Rho probe (mCherry-2xrGBD, magenta). The yellow arrow indicates the 5-pixel wide region used to generate the kymograph. Bottom: Kymograph shows that calcium increase originates at the junction and spreads.
(E) Quantification of experiments shown in C. Graph of mean normalized intensity shows that local calcium increases simultaneously with the increase in active Rho. Shaded region represents S.E.M. n= 19 flares, 15 embryos, 8 experiments.

2.3.2 Intracellular calcium flash precedes Rho flares during local ZO-1 reinforcement

To better characterize the temporal dynamics of the intracellular calcium increase, we imaged GCaMP6m (Chen et al., 2013), a genetically encoded calcium probe with faster kinetics but reduced spatial sensitivity compared to C2. We detected a transient increase in calcium in cells adjacent to the junction with the Rho flare (Figure 2.2 A) with a duration of 72.72 ± 9.13 s (Figure 2.2 B), hereafter referred to as a “calcium flash”. Calcium flashes associated with Rho flares differ from calcium waves previously described during *Xenopus* gastrulation because they are restricted to the cells neighboring the junction exhibiting a Rho flare (Figure S 2.1, A-B). In contrast, calcium waves originate in 2-4 cells and propagate to neighboring cells within minutes (Wallingford et al., 2001) (Figure S 2.1, C-C’).

When observed with GCaMP6m, calcium flashes occur after the decrease in ZO-1 and precede Rho flares by ~40-50 s (Figure 2.2, C and D). The intensity of GCaMP6m decreases as reinstatement of ZO-1 is initiated (Figure 2.2 D). Next, to evaluate junction contraction in relation to the calcium flash, we measured the vertex-to-vertex junction distance of the cell-cell junctions where Rho flares occur over time. We found that junction elongation preceded the calcium flash, and a rapid contraction of the junction

immediately followed the calcium flash and Rho flare (blue trace, Figure 2.2 E). Of note, we observed that the initiation of junction contraction occurs during the peak of the calcium flash, and the stabilization of junction length occurs as the calcium level returns to baseline. Taken together, our results support a role for calcium flashes in promoting Rho flare-mediated TJ reinforcement through contraction and stabilization of cell-cell junctions.

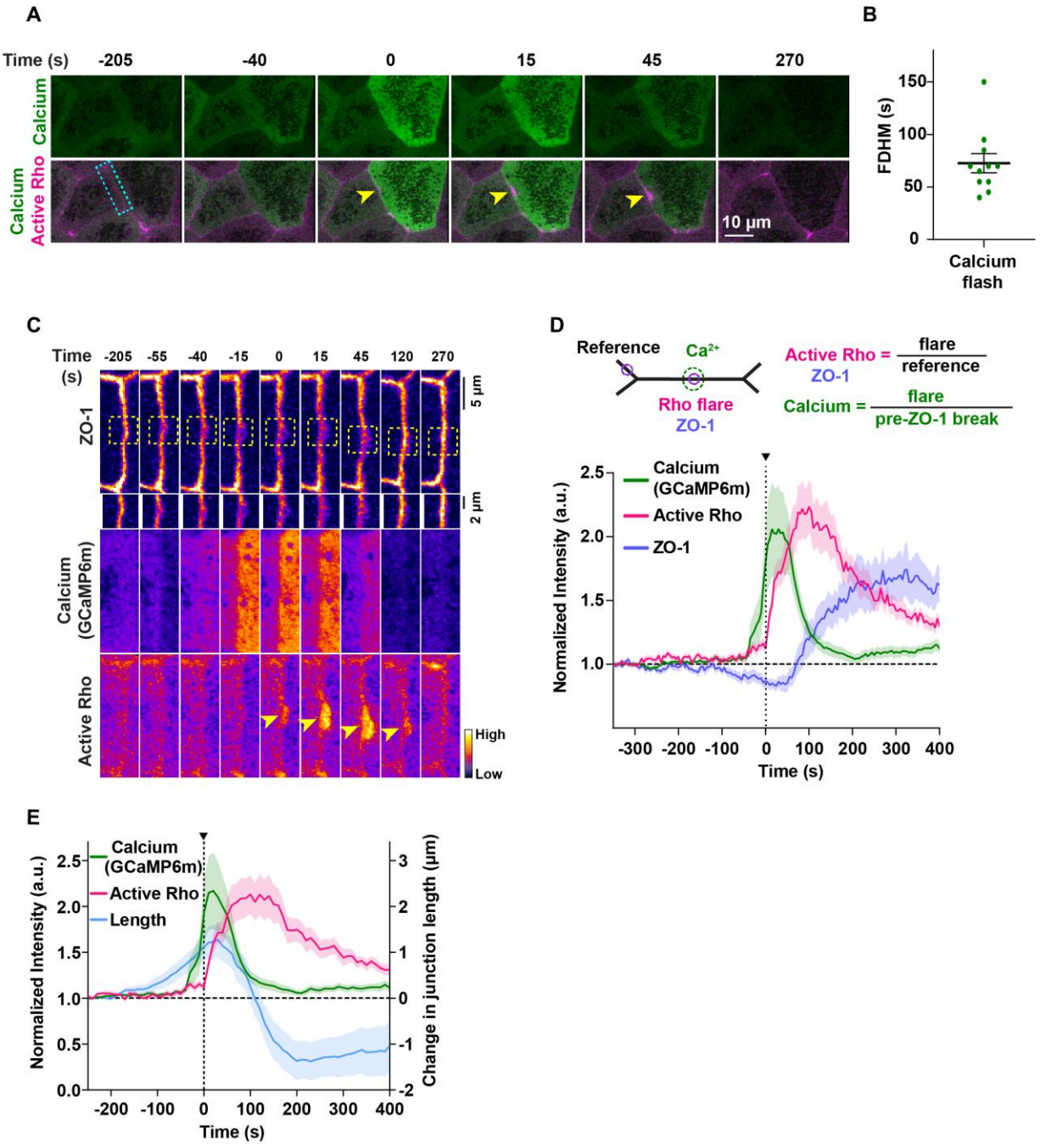

Figure 2.2: Intracellular calcium increase precedes Rho flares during local ZO-1 reinforcement. (A) Time lapse images of calcium (GCaMP6m, green) and active Rho (mCherry-2xrGBD, magenta). Calcium flash occurs in cells adjacent to the junction with the Rho flare (yellow arrowheads). Time 0 s represents start of Rho flare.(B) Dot plot of calcium flash duration (full duration at half maximum, FDHM). Error bar represents mean ± S.E.M. n= 11 flashes, 11 embryos, 10 experiments.

(C) Montage of the junction indicated by the blue box in A (FIRE LUT). A calcium flash (GCaMP6m) follows a local loss of ZO-1 (BFP-ZO-1, yellow boxed region, enlarged below) and precedes the Rho flare (mCherry-2xrGBD, yellow arrowhead).

(D) Quantification of experiments shown in C. Top: Schematic showing regions of interest (ROIs) used to quantify Rho flares, calcium, and ZO-1. Bottom: Graph showing calcium intensity increase follows a decrease in ZO-1 and precedes an increase in active Rho. Shaded region represents S.E.M. n= 20 flares, 15 embryos, 12 experiments.

(E) Graph showing calcium flash (GCaMP6m) follows junction elongation and precedes Rho-mediated junction contraction and stabilization of length. Shaded region represents S.E.M. n= 17 flares, 14 embryos, 11 experiments.

2.3.3 Intracellular calcium flash is required for Rho flare activation and ZO-1 reinforcement

Calcium is required for Rho activation during local cell shape changes including epithelial wound healing, cell migration, and dendritic spine enlargement (Clark et al., 2009, Murakoshi et al., 2011, Pardo-Pastor et al., 2018). However, whether calcium is required for local Rho activation and ZO-1 reinforcement at leaks remains unknown. To test this question, we chelated intracellular calcium using BAPTA-AM, a cell-permeable calcium chelator that chelates intracellular calcium without disrupting calcium-dependent cadherin adhesion. BAPTA-AM alone treatment led to an increase in the frequency of calcium waves (Figure S 2.2 A), which disrupted our ability to observe calcium flashes. Calcium waves are dependent on ER-mediated calcium release (Wallingford et al., 2001), so we blocked them using the IP3 channel blocker, 2-APB, in addition to chelating intracellular calcium with BAPTA-AM (Figure 2.3 A). Upon treatment with BAPTA-AM + 2-APB (Figure 2.3 A'), the intensity of calcium flashes was reduced compared to vehicle (DMSO) (Figure 2.3, B-D'). Active Rho was also significantly reduced at sites of ZO-1 loss when intracellular calcium was chelated (Figure 2.3, B, C, E, and E'). Finally, we observed that ZO-1 breaks were more severe, lasted longer, and failed to be reinstated in intracellular calcium chelated embryos compared to vehicle controls (Figure 2.3, B, C, F and F'). Together, our results suggest that intracellular calcium increase is required for both Rho flare activation and efficient ZO-1 reinforcement.

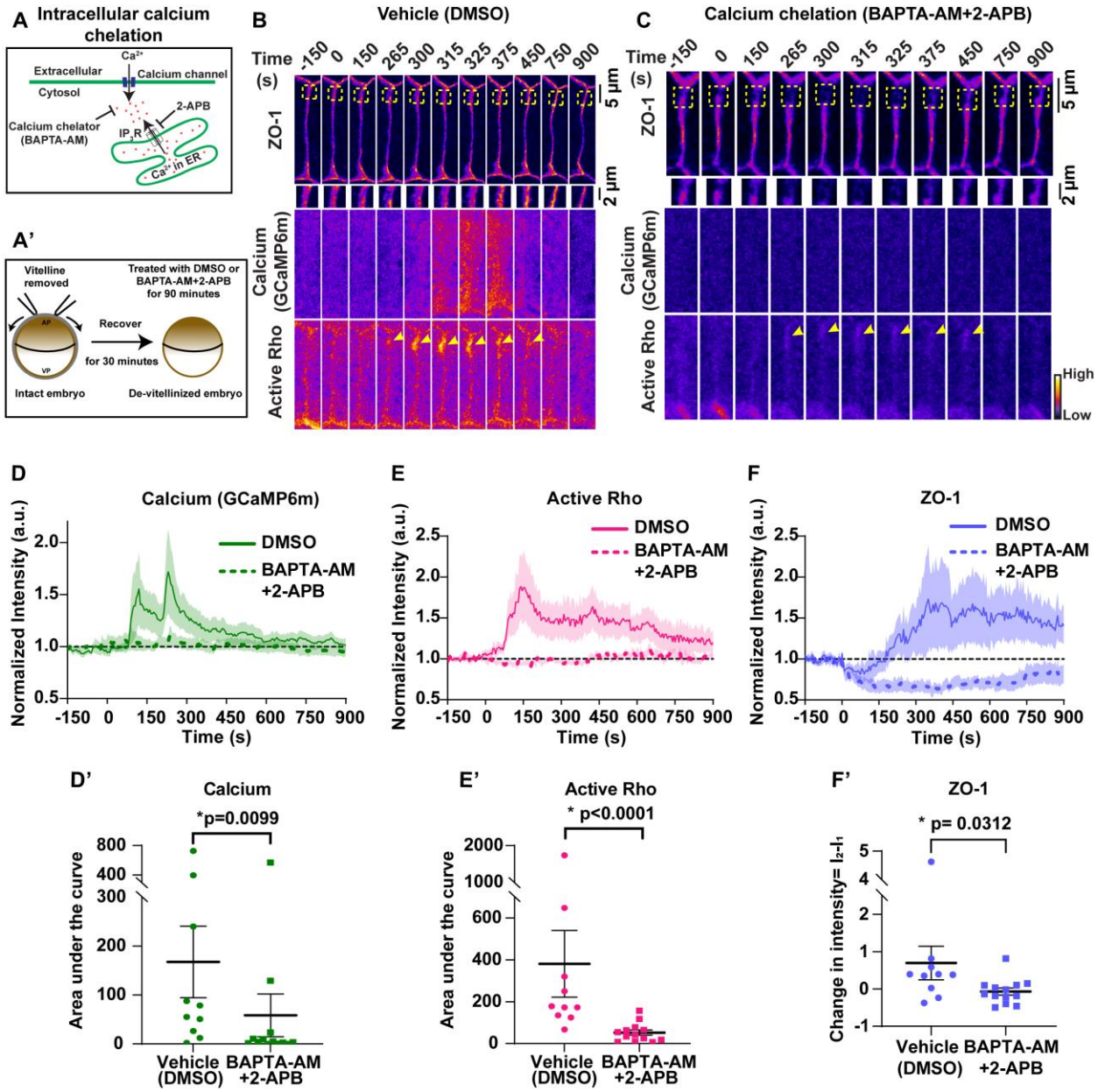

Figure 2.3: Intracellular calcium flash is required for Rho flare activation and ZO-1 reinforcement.(A) Schematic of cytosolic calcium chelation using BAPTA-AM and blocking IP_3R-mediated calcium release from the ER using 2-APB.

(A') Schematic showing BAPTA-AM and 2-APB treatment after removal of vitelline envelope.

(B-C) Time-lapse images (FIRE LUT) of BFP-ZO-1, calcium (GCaMP6m), and active Rho (mCherry-2xrGBD). Embryos were treated with 0.5% DMSO (vehicle, B) or 20 µM BAPTA-AM and 100 µM 2-APB (calcium chelation, C). Calcium chelation resulted in more severe ZO-1 breaks (yellow boxes, enlarged below) and decreased Rho activity (yellow arrowheads) at the site of ZO-1 loss. Time 0 s represents the start of ZO-1 decrease.

(D-F) Graphs of mean normalized intensity of calcium (GCaMP6m, D), active Rho (E) and ZO-1 (F) at the site of ZO-1 loss over time in vehicle (DMSO, solid lines) or calcium chelation (BAPTA-AM+2-APB, dashed lines) embryos. Shaded region represents S.E.M. DMSO: n= 10 flares, 7 embryos, 7 experiments; BAPTA-AM+2-APB: n=13 flares, 8 embryos, 8 experiments.

(D'-F') Area under the curve for calcium (D') and active Rho (E') was calculated from D and E, respectively. Scatter plot of change in ZO-1 intensity (F') was calculated from F. I_1 and I_2 represent average intensity of ZO-1 from individual traces from time 0-50 s and 400-450 s, respectively. Error bars represent mean ± S.E.M.; significance calculated using Mann-Whitney test.

2.3.4 Mechanosensitive calcium channel-dependent calcium influx is required for Rho-mediated reinforcement of ZO-1

Plasma membrane localized MSCs play an important role in mediating local calcium influx in response to changes in local membrane tension (Canales et al., 2019, Ellefsen et al., 2019). Rho flares occur following junction elongation (Figure 2.2 E) and loss of ZO-1 (Figure 2.2 D), a scaffolding protein that connects TJ transmembrane proteins to the underlying actin cytoskeleton, suggesting a possible change in membrane tension due to detachment of membrane from the underlying actin cytoskeleton. Furthermore, Rho flares are associated with apical plasma membrane deformation (Stephenson et al., 2019) and a local calcium increase that originates at the plasma membrane (Figure 2.1 D). Together, these observations suggest that calcium influx may be mediated by MSCs. First, we evaluated the temporal association of membrane protrusion (tagBFP-membrane) and Rho flares (mCherry-2xrGBD). The kymograph at the site of a Rho flare showed that membrane protrusion (blue, Figure 2.4 A) expands with a similar timing to the increase in Rho activation (magenta, Figure 2.4 A) supporting a mechanosensation-based mechanism. Therefore, to test if MSCs are responsible for the calcium flash preceding Rho flares, we blocked MSCs using Grammostola Mechanotoxin #4 (GsMTx4), a peptide from spider venom. GsMTx4 decreases the sensitivity of MSCs to changes in membrane tension, thereby blocking calcium influx mediated by Piezo1 and TRP channels (Figure 2.4 B) (Bae et al., 2011, Gnanasambandam et al., 2017, Bowman et al., 2007). MSC-mediated calcium transients are required for tissue homeostasis and proper development (Hunter et al., 2014). Therefore, we used GsMTx4 at a low concentration such that embryos successfully develop to gastrula

stage, and the overall morphology of cell-cell junctions is not altered. With GsMTx4-treatment, we observed a significant decrease in the calcium flash associated with Rho flares (Figure 2.4, C-E and E'), indicating that the calcium flashes preceding Rho flares are mediated by MSCs. Further, with GsMTx4 treatment, the amplitude and duration of Rho flares were significantly reduced compared to vehicle (water) (Figure 2.4, C-D, F, and F'). Although both vehicle- and GsMTx4-treated embryos showed an initial increase in active Rho at the site of ZO-1 loss, Rho flares were lower in intensity and short-lived in GsMTx4-treated embryos (Figure 2.4 F). In addition, by measuring the normalized intensity of ZO-1 over time, we found that the amount of ZO-1 loss prior to Rho activation was comparable between vehicle- and GsMTx4-treated embryos (I1, Figure 2.4 G). However, treatment with GsMTx4 significantly reduced ZO-1 reinforcement compared to vehicle controls (Figure 2.4, C-D, G, and G'). Of note, GsMTx4 treatment did not alter active RhoA accumulation at the contractile ring in dividing cells (Figure S 2.2 B), or steady state levels of active RhoA (Figure S 2.2, C-C'), or the downstream targets of active RhoA (Figure S 2.3, D-E) at cell-cell junctions. Together, these findings demonstrate that MSC-mediated calcium influx is required for both robust Rho flare activation and efficient reinforcement of ZO-1.

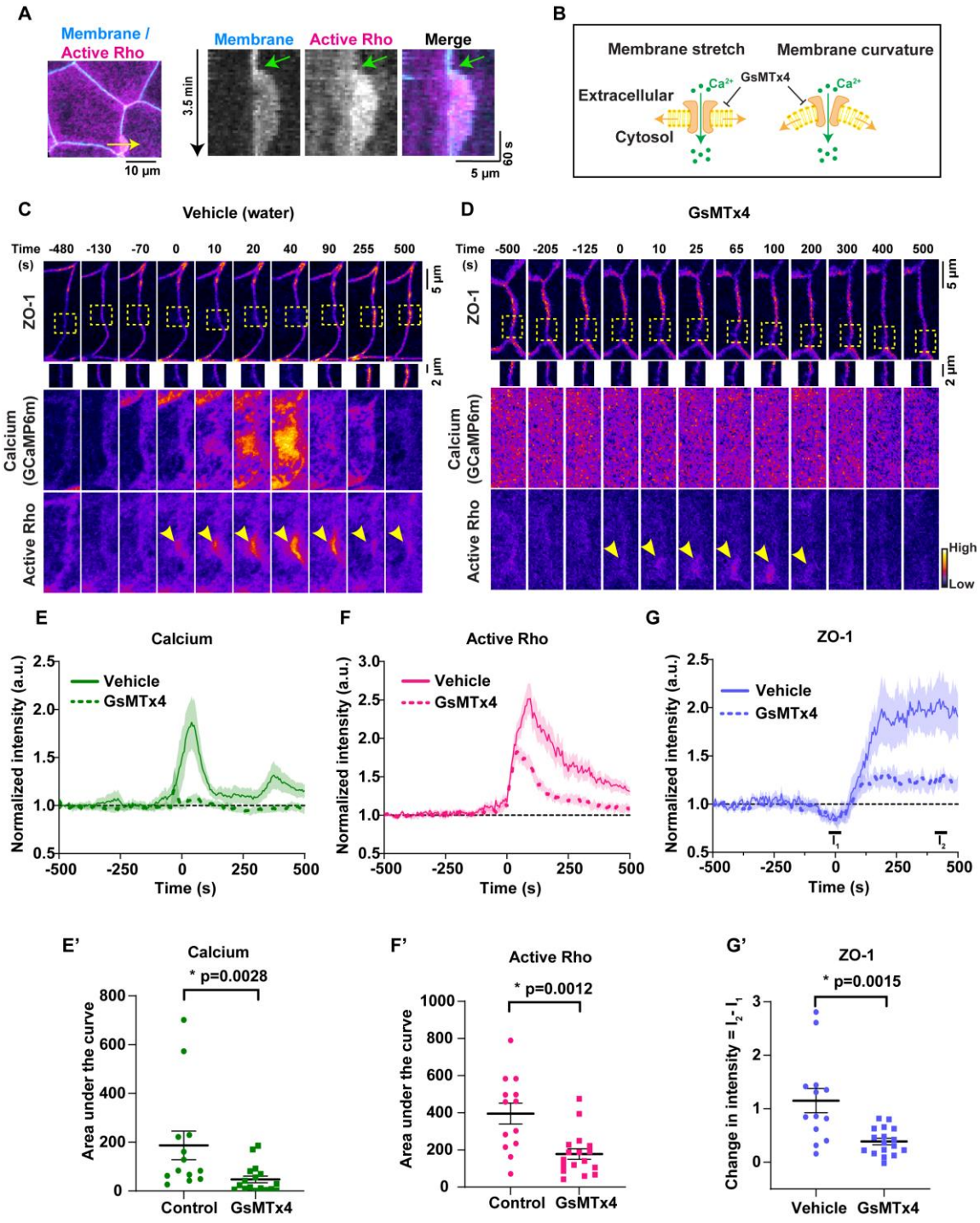

Figure 2.4: Mechanosensitive calcium channel-dependent calcium influx is required for Rho-mediated reinforcement of ZO-1.(A) Left: Cell view of an embryo expressing membrane probe (tagBFP-membrane, blue) and active Rho probe (mCherry-2xrGBD, magenta). Yellow arrow indicates the 2-pixel wide region used to generate the kymograph. Right: Kymograph shows that membrane protrusion increases with Rho flare. Green arrow indicates the start of membrane protrusion and Rho flare.
(B) Schematic showing that GsMTx4 inhibits MSC-mediated calcium influx in response to changes in membrane tension induced by stretch or curvature.
(C-D) Time-lapse images (FIRE LUT) of BFP-ZO-1, calcium (GCaMP6m), and active Rho (mCherry-2xrGBD). Embryos were treated with water (vehicle, C) or 12.5 µM GsMTx4 (MSC inhibitor, D). MSC inhibition resulted in a

decrease in calcium influx, short duration, low intensity Rho flares (yellow arrowheads), and decreased ZO-1 reinforcement at the site of ZO-1 loss (yellow boxes, enlarged below). Time 0 s represents the start of Rho flares. (E-G) Graphs of mean normalized intensity of calcium (GCaMP6m, E), active Rho (F), and ZO-1 (G) at the site of ZO-1 loss over time in vehicle (water, solid lines) or MSC inhibition (GsMTx4, dashed lines) embryos. Shaded region represents S.E.M. Vehicle: n= 13 flares, 6 embryos, 6 experiments; GsMTx4: n=17 flares, 7 embryos, 6 experiments. (E'-G') Area under the curve for calcium (E') and active Rho (F') were calculated from E and F, respectively. (G') Scatter plot of change in ZO-1 intensity (G') was calculated from G. I_1 and I_2 represent average intensity of ZO-1 from individual traces at time -25:25 s and 400:450 s, respectively. Error bars represent mean ± S.E.M.; significance calculated using Mann-Whitney test.

2.3.5 Mechanosensitive calcium channel-mediated calcium influx is required for proper epithelial barrier function and local junction contraction

Rho flare-mediated ZO-1 reinforcement is required to repair local leaks and maintain paracellular barrier integrity. Our results show that a calcium increase follows local leaks (Figure 2.1 B), and blocking MSCs leads to impaired Rho activation and ZO-1 reinforcement (Figure 2.4, F and G). Therefore, we hypothesized that MSC-mediated calcium influx is required to maintain an intact paracellular epithelial barrier. To detect transient leaks in the barrier, we performed ZnUMBA in vehicle- or GsMTx4-treated embryos. With GsMTx4 treatment, the whole-field intensity of FluoZin-3 increased over time compared to vehicle controls (Figure 2.5, A and B), indicating a global barrier disruption. However, global barrier disruption could be the result of failure to repair local leaks associated with ZO-1 loss. Therefore, we next analyzed the frequency of Rho flares in vehicle- and GsMTx4-treated embryos. The frequency of Rho flares increased significantly in GsMTx4-treated embryos compared to the matched controls (Figure 2.5 C), suggesting an increase in local leaks. To examine if local leaks were contributing to global barrier disruption, we analyzed individual junctions associated with local FluoZin-3 increase. With GsMTx4 treatment, local FluoZin-3 increased repeatedly at the site of ZO-1 loss (single and double white arrows, Figure 2.5 E) compared to vehicle controls where the local FluoZin-3 increase was resolved following robust activation of Rho flares and ZO-1 reinforcement (Figure 2.5, D-E). Of note, in GsMTx4-treated embryos, a

Rho flare failed to be activated following an initial increase in local FluoZin-3 (yellow arrow, Figure 2.5 E). Collectively, these findings suggest that MSC-mediated robust activation of Rho flares and ZO-1 reinforcement is required to resolve local leaks to maintain the overall paracellular barrier integrity.

Following TJ breaks, Myosin II activation through a Rho/ROCK-mediated signaling pathway is required for efficient ZO-1 reinforcement via local junction contraction (Stephenson et al., 2019). So, we asked whether reduced ZO-1 reinforcement observed in GsMTx4-treated embryos was a result of reduced junction contraction. We found that rapid contraction of the junction immediately following the Rho flare was significantly reduced in GsMTx4-treated embryos compared to vehicle controls (Figure 2.5, F and F'). Further, to track the local contractile regions within individual junctions, we generated kymographs of a cell-cell junction projected from vertex-to-vertex. In GsMTx4-treated embryos, we observed a dramatic loss of junction contraction and lack of ZO-1 reinforcement following Rho flares (black bracket, Figure 2.5 G) compared to robust contraction and ZO-1 reinforcement in controls. Additionally, kymographs highlighted that in GsMTx4-treated embryos there are many short-lived Rho flares, which often repeat at the same site and yet remain unable to reinforce ZO-1 (orange arrows, Figure 2.5 G and Figure S 2.3 A). Furthermore, we observed reduced F-actin accumulation at the site of short-lived Rho flares in GsMTx4-treated embryos (Figure S 2.3, B-C). Taken together, our results show that MSC-mediated calcium influx is required for actomyosin mediated local junction contraction through robust and sustained Rho activation, and thereby efficient reinforcement of ZO-1.

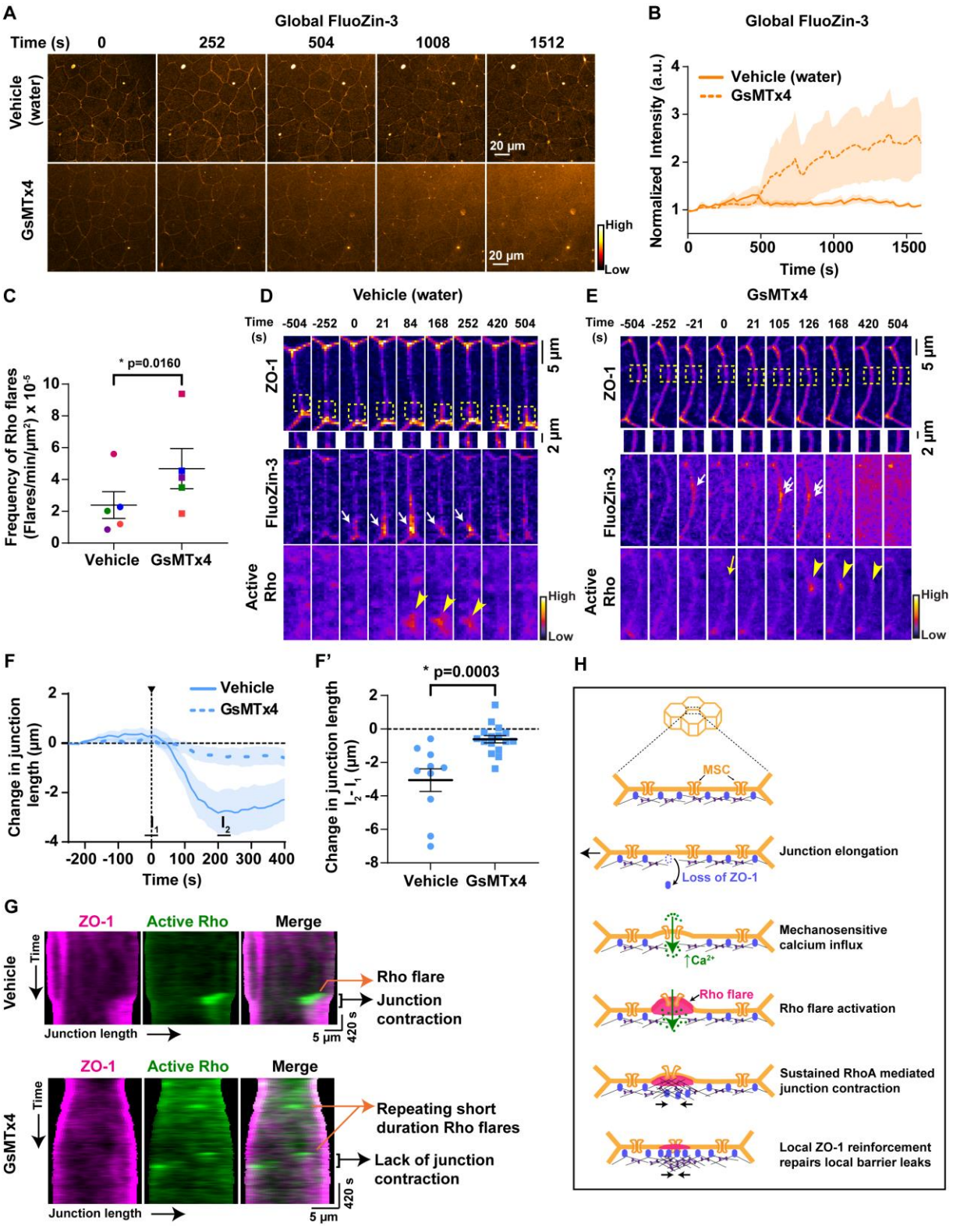

Figure 2.5: Mechanosensitive calcium channel-mediated calcium influx is required for proper epithelial barrier function and local junction contraction.(A) Time-lapse images (orange hot LUT) of epithelial permeability tested using ZnUMBA (FluoZin-3). Embryos were treated with water (vehicle, top) or 12.5 µM GsMTx4 (MSC inhibitor, bottom). Time 0 s represents the start of the time-lapse movie.

(B) Graph of mean normalized intensity of whole-field FluoZin-3 for vehicle (water) or GsMTx4-treated embryos. Blocking MSCs increased global FluoZin-3 intensity over time compared to vehicle. Shaded region represents S.E.M. Vehicle: n= 6 embryos, 4 experiments; GsMTx4: n= 6 embryos, 4 experiments.
(C) Frequency of Rho flares in vehicle (water) and GsMTx4-treated embryos. Frequencies from paired experiments are color matched. Error bars represent mean ± S.E.M.; significance calculated using paired two-tailed t-test; n=5 embryos, 4 experiments.
(D-E) Montage of representative junctions from A (FIRE LUT). Blocking MSCs with GsMTx4 causes repeated increases in local FluoZin-3 (white arrows), reduced ZO-1 (BFP-ZO-1) reinforcement (yellow boxes, enlarged below), and reduced duration of Rho flares (mCherry-2xrGBD, yellow arrowheads) at sites of ZO-1 loss. Repeated FluoZin-3 increase is indicated by double white arrows, and failure to activate Rho flare after FluoZin-3 increase is indicated by yellow arrow.
(F-F') Graph of change in junction length for junctions with Rho flares in vehicle (water) and GsMTx4-treated embryos. Shaded region represents S.E.M. (F') Scatter plot of change in junction length was calculated from F. I_1 and I_2 represent average length of junction from individual traces from time -20-20 s and 200-240 s, respectively. Error bars represent mean ± S.E.M.; significance calculated using Mann-Whitney test. Vehicle: n= 10 flares, 6 embryos, 6 experiments; GsMTx4: n=16 flares, 7 embryos, 6 experiments.
(G) Kymographs of BFP-ZO-1 (magenta) and active Rho (mChe-2xrGBD, green) from representative junctions projected vertex-to-vertex over time for vehicle (water) and GsMTx4-treated embryos. Kymographs highlight the repeating, short duration Rho flares, loss of local junction contraction, and reduced ZO-1 reinforcement upon GsMTx4 treatment.
(H) Model showing mechanism by which mechanosensitive calcium signaling regulates epithelial barrier function. Top: 3D view of epithelial cells. Bottom: *en face* view of the junction highlighted showing the spatiotemporal calcium and RhoA signaling following mechanical stimuli.

2.4 Discussion

Epithelial tissues adapt to mechanical cues by remodeling their cell-cell junctions and associated cytoskeleton to maintain tissue homeostasis and barrier function. We previously showed that physiological mechanical stimuli – like junction elongation that happens in response to cell shape changes – cause short-lived, local paracellular leaks (Stephenson et al., 2019). However, it was unclear how cells sense local leaks and remodel cell-cell junctions without compromising overall barrier integrity.

Using genetically encoded calcium probes, we observed intracellular calcium flashes during TJ remodeling. Calcium flashes in our study were of longer duration (72.72 ± 9.13 s) compared to single-cell calcium transients (~26-40 s) that mediate apical cell constriction during *Xenopus* neural tube closure (Suzuki et al., 2017, Christodoulou and Skourides, 2015). The difference in the duration of these calcium transients could be that during apical constriction, the calcium increase is mediated by intracellular calcium stores. Previous studies have shown that intracellular calcium increase precedes TJ formation and establishment of epithelial barrier function (Nigam et al., 1992, Gonzalez-Mariscal et al., 1990). However, these studies used a calcium switch model and found that the timescale of TJ formation following calcium increase is significantly slower (~50 minutes) than that of TJ reinstatement following a barrier breach and calcium flash described here (~1-2 minutes). In addition, we demonstrate that local leaks and ZO-1 reduction precede the calcium flash, suggesting that the calcium increase is a consequence of paracellular leak rather than a cause. Thus, our work is the first to suggest that intracellular calcium is a critical regulator of barrier function when cells change shape in an intact epithelium.

Our results also revealed that the intracellular calcium increase originated at the plasma membrane following a leak (Figure 2.1, D, and Figure S 2.1, D-E), suggesting that the calcium increase could be mediated locally by plasma membrane-localized calcium channels or a local membrane rupture. However, previous work from our lab suggested that the plasma membrane is indeed intact at the site of leak (Stephenson et al., 2019). Furthermore, we think it is likely that plasma membrane tension changes locally when the transmembrane TJ proteins uncouple from the cortical actin cytoskeleton upon loss of the scaffolding protein, ZO-1. We demonstrated that calcium increase following local ZO-1 loss is mediated by MSCs, supporting the idea that in epithelial cells, change in local membrane tension led to local activation of MSCs (Shi et al., 2018). Given that both the Piezo and TRP families are mammalian MSCs capable of gating calcium influx, it will be interesting in future studies to investigate the relative role of MSCs blocked by GsMTx4, specifically Piezo1 and TRPC6, in TJ remodeling (Spassova et al., 2006, Bae et al., 2011). Further, it is clear that local calcium increase spreads throughout the cell, thus we cannot rule out the possibility that MSC-mediated calcium influx induces calcium release from intracellular calcium stores.

Both calcium transients and RhoA activation are modulated locally and globally in response to mechanical stimuli (Clark et al., 2009, Benink and Bement, 2005, Pardo-Pastor et al., 2018, Acharya et al., 2018). Our results demonstrate intracellular calcium increase as a key signal for activation of Rho flares. We observed that perturbation of intracellular calcium using a cytoplasmic calcium chelator in conjunction with an IP_3R blocker (BAPTA-AM+2-APB) reduced RhoA activation at sites of ZO-1 loss to a greater extent compared to the MSC blocker (GsMTx4). The difference in the degree of

inhibition could be potentially due to altered tissue tension resulting from physical removal of the vitelline for BAPTA-AM+2-APB but not GsMTx4 experiments, or due to a calcium-independent effect of BAPTA-AM on the actin cytoskeleton (Saoudi et al., 2004). Furthermore, our results show that despite the spreading of calcium throughout the cell, Rho flares are spatially confined to the site of paracellular leaks. This suggests that calcium may regulate RhoA activity by modulating the activity of a specific Rho GEF or Rho GAP, not by direct regulation of RhoA. For example, intracellular calcium increase could activate RhoA via PKCα-mediated activation of a Rho GEF (Holinstat et al., 2003), or CaMKII-mediated crosstalk between active Cdc42 and RhoA (Murakoshi et al., 2011, Benink and Bement, 2005). Interestingly, our observation that in GsMTx4-treated cells, Rho flares were activated but at a significantly lower intensity and shorter duration, suggests an additional calcium-independent mechanism to initiate activation of RhoA.

In addition to regulating the activity of RhoA, MSC-mediated intracellular calcium increase is important for reinforcement of ZO-1, given that both intracellular calcium chelation, and blocking MSCs, inhibited reinforcement of ZO-1. This loss of ZO-1 reinforcement is due to reduced active RhoA-mediated junction contraction, presumably due to the loss of ROCK/Myosin II activation at the site of leaks (Stephenson et al., 2019). Previous studies have demonstrated that chelation of intracellular calcium or inhibition of RhoA activity hinder the association of ZO-1 with the actin cytoskeleton (Stuart et al., 1994, Nusrat et al., 1995b). Thus, our study is the first to reveal that calcium promotes ZO-1 recruitment and reinforcement at TJs by regulating RhoA activation. Given that myosin light chain kinase (MLCK) is activated by

calcium/calmodulin, and active MLCK stabilizes ZO-1 at TJs (Yu et al., 2010), it is possible that calcium regulates ZO-1 reinforcement at TJs via MLCK activation in parallel to RhoA activation.

Expression and activity of MSCs, including Piezo1 and TRPV4, enhanced global barrier function by up-regulation or post-translational modification of junctional proteins (Zhong et al., 2020, Sokabe et al., 2010, Akazawa et al., 2013). Consistent with this finding, using live imaging and a highly sensitive barrier assay, we observed MSC-mediated calcium influx is required to maintain global barrier function. Interestingly, the increased global paracellular permeability appears to be a cumulative effect of failure to fix local leaks. When MSCs were blocked, Rho flares often failed to be activated immediately following the leak, and when Rho flares were weakly activated, they tended to repeat at the site of the leak in attempts to reinforce ZO-1.

In conclusion, we find mechanically-triggered calcium influx is an important feature of the mechanism by which epithelial cells sense and respond to transient leaks in barrier function (Figure 2.5 H). Calcium flashes mediated by MSCs are required for local junction contraction through robust and sustained Rho activation and thereby efficient TJ reinforcement. However, when local leaks fail to be repaired by low intensity, short duration Rho flares, global barrier function is weakened. Thus, MSC-mediated local calcium influx may serve as a mechanotransduction mechanism to specifically relay biochemical signals only to sites of paracellular leaks, without affecting overall TJ structure and function in a dynamic epithelial tissue undergoing various cell shape changes.

2.5 Materials and Methods

DNA constructs and mRNA preparation:

GCaMP6m was generated by PCR amplifying the GCaMP6m sequence from pGP-CMV-GCaMP6m (Addgene plasmid #40754, (Chen et al., 2013)) and ligating it into the *BamH1* and *EcoR1* sites in pCS2+. BFP-PKC-β-C2 and mNeon-PKC-β-C2 were generated by PCR amplifying the C2 domain of *Xenopus laevis* PKC-β from pCS2+/eGFP-PKC-β-C2 (Yu and Bement, 2007) and ligating into the *XhoI* and *EcoR1* sites in pCS2+/N-tagBFP2.0 and pCS2+/N-mNeon, respectively. All constructs were verified by sequencing. pCS2+/mCherry-2xrGBD (probe for active Rho, (Davenport et al., 2016)), pCS2+/BFP-ZO-1 (human ZO-1, (Stephenson et al., 2019)), and pCS2+/tagBFP-membrane (probe for membrane, (Higashi et al., 2016)) were previously reported. All plasmid DNAs were linearized with *NotI*, except BFP-ZO-1 which was linearized using *KpnI*. mRNA was *in vitro* transcribed from linearized pCS2+ plasmids using the mMessage mMachine SP6 Transcription kit (Ambion) and purified using the RNeasy Mini kit (Qiagen). Transcript size was verified on 1% agarose gel containing 0.05% bleach and Millennium RNA markers (Invitrogen).

Xenopus embryos and microinjection:

All studies conducted using *Xenopus laevis* embryos strictly adhered to the compliance standards of the U.S. Department of Health and Human Services Guide for the Care and Use of Laboratory Animals and were approved by the University of Michigan Institutional Animal Care and Use Committee. Eggs from *Xenopus* were collected, *in vitro* fertilized, and dejellied as previously reported (Woolner et al., 2009, Miller and Bement, 2009). Dejellied embryos were stored at 15°C in 0.1x Mark's Modified Ringers

solution (MMR) containing 10 mM NaCl, 0.2 mM KCl, 0.2 mM $CaCl_2$, 0.1 mM $MgCl_2$, and 0.5 mM HEPES, pH 7.4. Embryos were microinjected in the animal hemisphere with mRNA either twice per cell at the two-cell or once per cell at the four-cell stage. Injected embryos were allowed to develop to gastrula stage (Nieuwkoop and Faber stage 10.5–12) at 15°C or 17°C. The amount of mRNA per 5nl of microinjection volume was as follows: BFP-PKC-β-C2, 100 pg; mNeon-PKC-β-C2, 100 pg; GCaMP6m, 500 pg; mCherry-2xrGBD, 50 pg; BFP-ZO-1, 50 pg; BFP-membrane, 12.5 pg and Lifeact-GFP 10 pg.

Microscope image acquisition:

Live imaging of gastrula stage *Xenopus* embryos was performed on an inverted Olympus Fluoview 1000 Laser Scanning Confocal Microscope equipped with a 60X supercorrected Plan Apo N 60XOSC objective (numerical aperture (NA) = 1.4, working distance = 0.12mm) using mFV10-ASW software. Embryos were imaged in a custom chamber made of a 0.8 mm thick metal slide with a 5 mm hole in the center and two coverslips stuck on both sides of the hole with a thin layer of vacuum grease, lightly compressing the embryo between the coverslips. Embryos were mounted in 0.1x MMR, and the imaging chamber was inverted to image the epithelial cells in the animal hemisphere at room temperature using the Olympus Fluoview 1000 as previously described (Reyes et al., 2014).

Live imaging of calcium and Rho flares was generally captured by scanning the top 3 apical Z- planes (step size of 0.5 µm) and acquired sequentially by line scanning to avoid bleed-through between channels. Global calcium (GCaMP6m), Rho flares, and ZO-1 were acquired at a 2 µs/pixel scanning speed, 5 s time interval, and 1.5-2x zoom.

Local calcium (mNeon-PKC-β-C2), Rho flares, and membrane or ZO-1 were acquired at a 4 µs/pixel scanning speed, 10 s time interval, and 2x zoom. For ZnUMBA, 8 apical Z-planes were acquired at an 8 µs/pixel scanning speed, 21 s time interval, and 1.5x zoom.

Drug treatments:

The intracellular calcium chelator BAPTA-AM (Cayman, 15551) and IP_3R blocker 2-APB (Sigma, D9754) were resuspended in DMSO as a 20 mM or 25 mM stock, respectively, aliquoted and stored at -20°C. Prior to treatment, the translucent vitelline envelope of gastrula-stage embryos was physically removed using sharp forceps as previously described (Sive et al., 2007). Naked embryos were allowed to recover in 0.1x MMR for 30 minutes. Following recovery, embryos were incubated for 1 hour prior to imaging at 15°C in either 0.5% DMSO (vehicle) or a mixture of 20 µM BAPTA-AM and 100 µM 2-APB in 0.1x MMR.

The MSC blocker GsMTx4 (Smartox, 08GSM001) was resuspended in water as a 500 µM stock, aliquoted, and stored at -20°C. Prior to use, GsMTx4 was diluted to a concentration of 25 µM in water, mixed with mRNA, and a total of 1ng was microinjected into each embryo at the 2-4 cell stage.

Live imaging barrier assay:

Zinc-based Ultrasensitive Microscopic Barrier Assay (ZnUMBA) was performed as previously reported (Stephenson et al., 2019). Gastrula-stage albino embryos expressing mCherry-2xrGBD and BFP-ZO-1 or BFP-PKC-β-C2 were microinjected with 10 nl of 1 mM FluoZin-3 containing 100 µM $CaCl_2$ and 100 µM EDTA into the blastocoel. FluoZin-3-injected embryos were allowed to recover from microinjection for 5

minutes in 0.1x MMR. Following recovery, embryos were mounted in 0.1x MMR containing 1 mM $ZnCl_2$ and imaged immediately using confocal microscopy.

Immunofluorescence staining:

Albino embryos injected with vehicle (water) or 12.5 µM GsMTx4 were fixed and immunostained as previously reported (Arnold et al., 2019). At gastrula-stage, embryos were fixed overnight at room temperature with a mix of 1.5% PFA , 0.25% glutaraldehyde, 0.2% Triton X-100, Alexa Fluor 647 phalloidin (1:1000, Thermo Fisher Scientific, # A22287) in a 0.88x MT buffer containing 80 mM K-PIPES, 5 mM EGTA, and 1 mM $MgCl_2$, pH 6.8 with KOH. Fixed embryos were quenched for 1 hour at room temperature with 100mM sodium borohydride in 1x PBS and blocked overnight in 10% FBS, 5% DMSO and 0.1% NP-40 in 1x Tris-buffered Saline. Animal hemisphere of the bisected embryos were incubated overnight in anti-P-MLC (1:100, Cell Signaling Technologies, # 3671) in blocking solution, washed 3x with blocking solution, and incubated overnight in anti-rabbit Alexa 488 IgG (1:200, Thermo Fisher Scientific, # A11008) and Alexa Fluor 647 phalloidin (1:1000). Embryos were washed and mounted in VECTASHIELD (VWR, # 101098-042).

Image processing and quantification:

Image processing and analysis were performed using Image J (Fiji). Sum intensity projections of the Z-series were used for all quantification, and confocal images of time-lapse movies represented in all figures are sum projections of 3 apical Z-planes (1.5 µm), with the exception of FluoZin-3 (8 apical Z-planes, 4 µm).

Quantification of calcium dynamics during Rho flares:

Calcium dynamics at Rho flares were measured using a circular region of interest of 2.5 µm diameter drawn at the site of flares, spanning the membrane and cytoplasm adjacent to the membrane, manually tracked over every frame to account for in-plane drifting in live tissue, and normalized to baseline of 1. Cytosolic calcium (GCaMP6m) was calculated for each frame using the formula, $F_{normalized} = (F/F_{baseline})$, where $F_{baseline}$ represents the average calcium intensity of the first 150 s. Local calcium (PKC-C2) was calculated for each frame using the formula, $F = (F_{flare} – F_{background})$ and normalized to a baseline of 1, where $F_{baseline}$ represents the average calcium intensity of first 100 s and $F_{background}$ represents the cytoplasmic C2 intensity measured using an ROI of same size. An average of three independent measurements of calcium dynamics at each Rho flare was considered one data point (n=1).

For accurate measurement of calcium flash dynamics using the cytoplasmic soluble calcium probe (GCaMP6m), Rho flares were selected from cells that exhibited an isolated Rho flare that was not interrupted by a multicellular travelling calcium wave for 500 s prior to and after the initiation of Rho flares.

Intensity and duration of Rho flares and ZO-1 were measured at the site of Rho flares using a small circular ROI (GCaMP6m: 0.8 µm; PKC-C2: 2.5 µm; and Fluozin-3: 2.2 µm) and normalized to a nearby reference junction without Rho flares using ROI of same size to account for photobleaching and drifting in the Z-plane. The increase in Rho activity at the start of the Rho flare was aligned to time 0 s as previously described (Stephenson et al., 2019), with the exception of Figure 2.3. For Figure 2.3, as calcium chelation (BAPTA-AM + 2-APB) significantly reduced the intensity of Rho flares, we adopted an alternate method to align time 0 s in the graph to the frame before the rapid

decrease in ZO-1; the decrease in ZO-1 was defined as a 5% decrease in normalized ZO-1 intensity for at least 3 out of 4 consecutive frames.

Duration of calcium flash:

Duration of the calcium flash was quantified by measuring the full duration at half-maximum (FDHM) of the individual normalized calcium flashes at sites of Rho flares. FDHM (seconds) was measured manually by calculating the duration at 50% of the maximum amplitude above the baseline of 1 on the ascent and descent of the calcium transient. Experiments where calcium increased less than two-fold over the baseline were eliminated from the analysis. FDHM was plotted in a scatter plot.

Area under the curve:

Area under the curve for active Rho flares and calcium flashes was quantified using GraphPad Prism 9.0 by applying area under the curve (AUC) analysis of the individual traces. AUC analysis was applied to all points in the peaks above the baseline of 1, and peaks less than 10% of the increase from the baseline to the maximum Y-value were ignored. Individual AUC values for each Rho flare or calcium flash were plotted in a scatter plot.

Frequency of Rho flares:

Rho flare frequency was measured manually using Image J, by counting the number of Rho flare occurrences at cell-cell junctions in the whole field of imaging from the start of the time-lapse movie. Rho flares where the local active RhoA intensity increased and was sustained at the junctions for a span of 4-5 frames (84 s-105 s) was included in the analysis.

Global barrier function:

Global barrier function was quantified by measuring the whole field intensity of Fluozin-3 signal, including junctional and cytoplasmic, over time using an ROI of 141.12x141.12 µm. Time 0 s represents the start of image acquisition, which began immediately following mounting of the embryo injected with Fluozin-3 in 0.1x MMR containing 1 mM $ZnCl_2$. Each timepoint was measured, and baseline was normalized to 1 by dividing the individual value by the average of the first 84 seconds.

Junction length:

Length of the cell-cell junction was quantified using ZO-1 as junctional marker. Using Image J, a 0.3 µm wide segmented line was drawn on the junction with Rho flares to trace the junction from vertex-to-vertex. Length of the line was measured for every other frame by manually advancing and adjusting the line to accommodate cell shape changes through the time lapse movie. Each junction was measured in triplicate, and baseline was normalized to 1 by dividing the individual value by the average of the first 6 data points.

Construction of kymographs:

Kymographs from vertex-to-vertex of a cell-cell junction were constructed as previously described (Stephenson et al., 2019). Briefly, cell-cell junctions were digitized using ZO-1 as junctional marker. Each horizontal line in the kymograph was generated by measuring the intensity of ZO-1 and active Rho using 0.75 µm circular ROIs positioned at points along the length of the cell-cell junction. Kymographs were constructed by stacking and center aligning the horizontal lines from successive time frames.

Apical cell perimeter:

Apical perimeter of the cell was quantified using ZO-1 to identify cell boundaries. Using Image J, a segmented line was drawn to trace the boundary of the cells with a calcium flash and neighboring cells without a calcium flash over time. The perimeter of the cell was measured for every time point by manually adjusting the line to accommodate cell shape changes. Change in apical perimeter was calculated by subtracting the current perimeter from the initial perimeter (average perimeter over the first 3 time points).

Intensity of F-actin and P-MLC:

Junctional and cytoplasmic intensity of F-actin and P-MLC were quantified in Image J. Junctional intensity was measured using a 2.07 μm wide segmented line to trace a bicellular junction (excluding vertices) and the matched cytoplasmic intensity was measured using a 10.4 μm circular ROI. Ratio of junctional/cytoplasmic F-actin or P-MLC was calculated by dividing the intensity at the junction by the intensity in the cytoplasm for each cell.

Statistical analysis:

Statistical analysis and standard error of the mean (S.E.M.) were calculated in GraphPad Prism 9.0. Statistical analysis between two groups was measured using a two-tailed, unpaired Mann-Whitney U test, with the exception of flare frequency and intensity of actomyosin. The statistical significance of frequency of Rho flares was measured using a two-tailed, paired Student's *t*-test. Statistical significance of F-actin and P-MLC intensity at the junctions and junction/cytoplasm ratio was measured using a One-way ANOVA test.

2.6 Supplemental figures

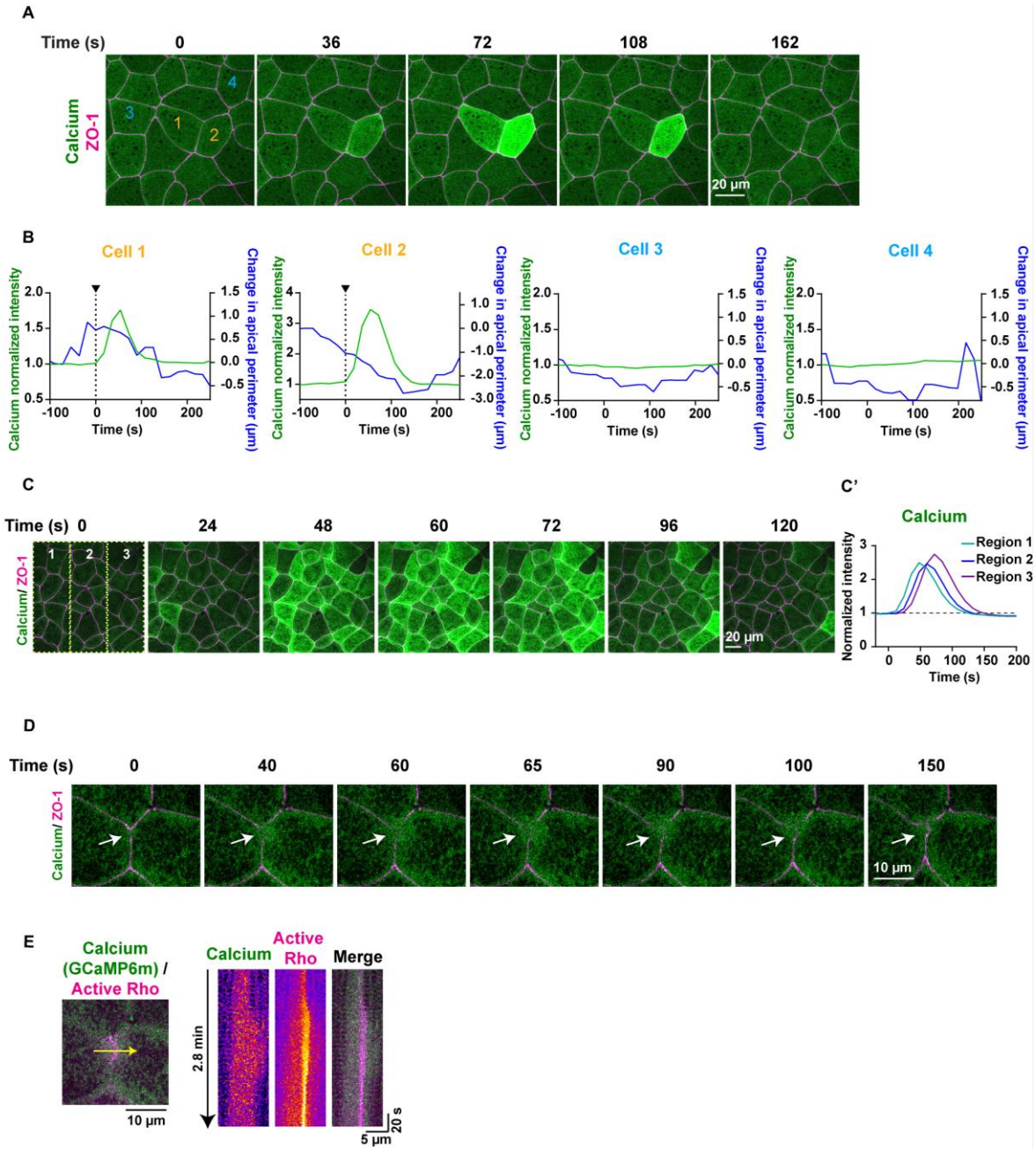

Figure S 2.1: Dynamics of calcium flash and calcium waves in gastrula-stage *Xenopus laevis* epithelium.(A) Live imaging of calcium (GCaMP6m, green) and ZO-1 (BFP-ZO-1, magenta) in the animal cap epithelium of gastrula-stage *Xenopus* embryos. Calcium flash is short-lived and restricted to cell 1 and cell 2 (orange numbers). Time 0 s represents the start of the calcium flash.
(B) Graphs showing change in cellular apical perimeter and calcium intensity in 4 different cells shown in A over time. Cells experiencing calcium flash (cells 1 and 2) decrease in apical perimeter compared to control cells (cells 3 and 4).
(C-C') Live imaging of calcium (GCaMP6m, green) and ZO-1 (BFP-ZO-1, magenta) in the animal cap epithelium of gastrula-stage *Xenopus* embryos. Travelling calcium wave starts at time 0 s in region 1, propagates through regions

2 and 3, and subsides in ~120 s. (C') Graph showing the increase in calcium intensity over time in regions marked in the first frame of C.
(D) Live imaging of calcium (GCaMP6m, green) and ZO-1 (BFP-ZO-1, magenta) showing a local calcium increase (white arrows) in cells expressing a reduced amount of GCaMP6m. Time 0 s represents the start of the calcium increase.
(E) Left: Cell view of embryo expressing calcium probe (GCaMP6m, green) and active Rho probe (mCherry-2xrGBD, magenta). 5-pixel wide yellow arrow indicates the region used to generate the kymograph. Right: Kymograph shows that cytosolic calcium increases locally at the site of the Rho flare. Individual images are shown using FIRE LUT.

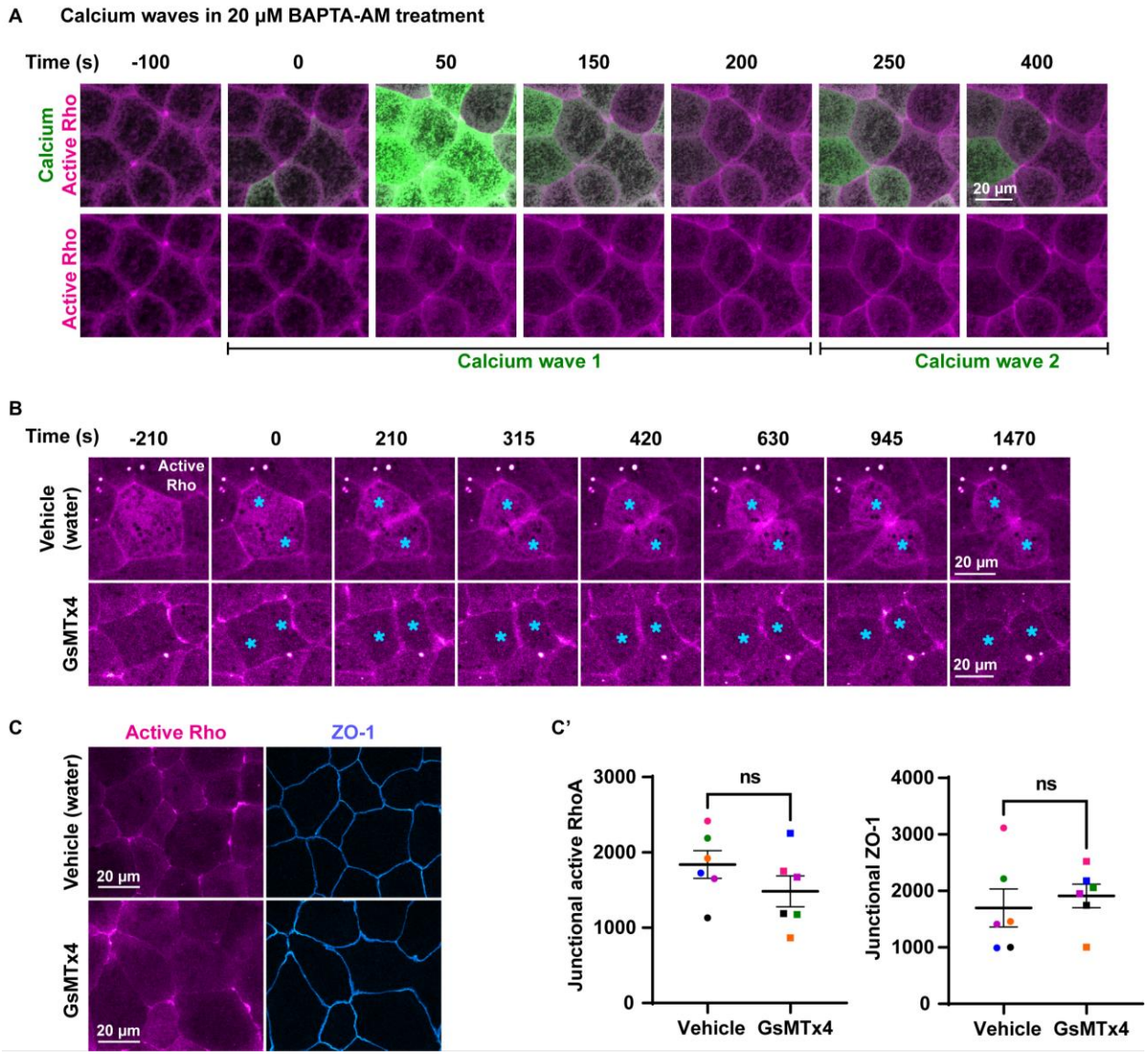

Figure S 2.2: Mechanosensitive calcium channel-mediated calcium influx is not required for baseline junctional Rho activity or Rho activation at the contractile ring.(A) Live imaging of calcium (GCaMP6m, green) and active Rho probe (mCherry-2xrGBD, magenta) in the animal cap epithelium of gastrula-stage *Xenopus* embryos treated with 20 µM BAPTA-AM in DMSO after vitelline removal. Montage shows recurring calcium waves within a span of 500 s. First calcium wave starts at time 0 s, and second calcium wave starts at ~200 s.
(B) Live imaging of active Rho (mCherry-2xrGBD, magenta) in embryos treated with vehicle (water) or 12.5 µM GsMTx4 (MSC inhibitor). Montage shows MSC inhibition does not affect Rho activity at the contractile ring, and cells complete cytokinesis successfully. Blue asterisk indicates dividing cells. Time 0 s represents the start of contractile ring formation.
(C-C') Live imaging of ZO-1 (BFP-ZO-1, blue) and active Rho (mCherry-2xrGBD, magenta) in embryos treated with vehicle (water) or 12.5 µM GsMTx4. (C') Quantification shows that MSC inhibition does not significantly affect baseline junctional RhoA activity at apical cell-cell junctions. Junctional intensity of active Rho and ZO-1 from paired experiments are color matched. Error bars represent mean ± S.E.M.; significance calculated using Wilcoxon matched-pairs test; n=30 junctions, 6 experiments.

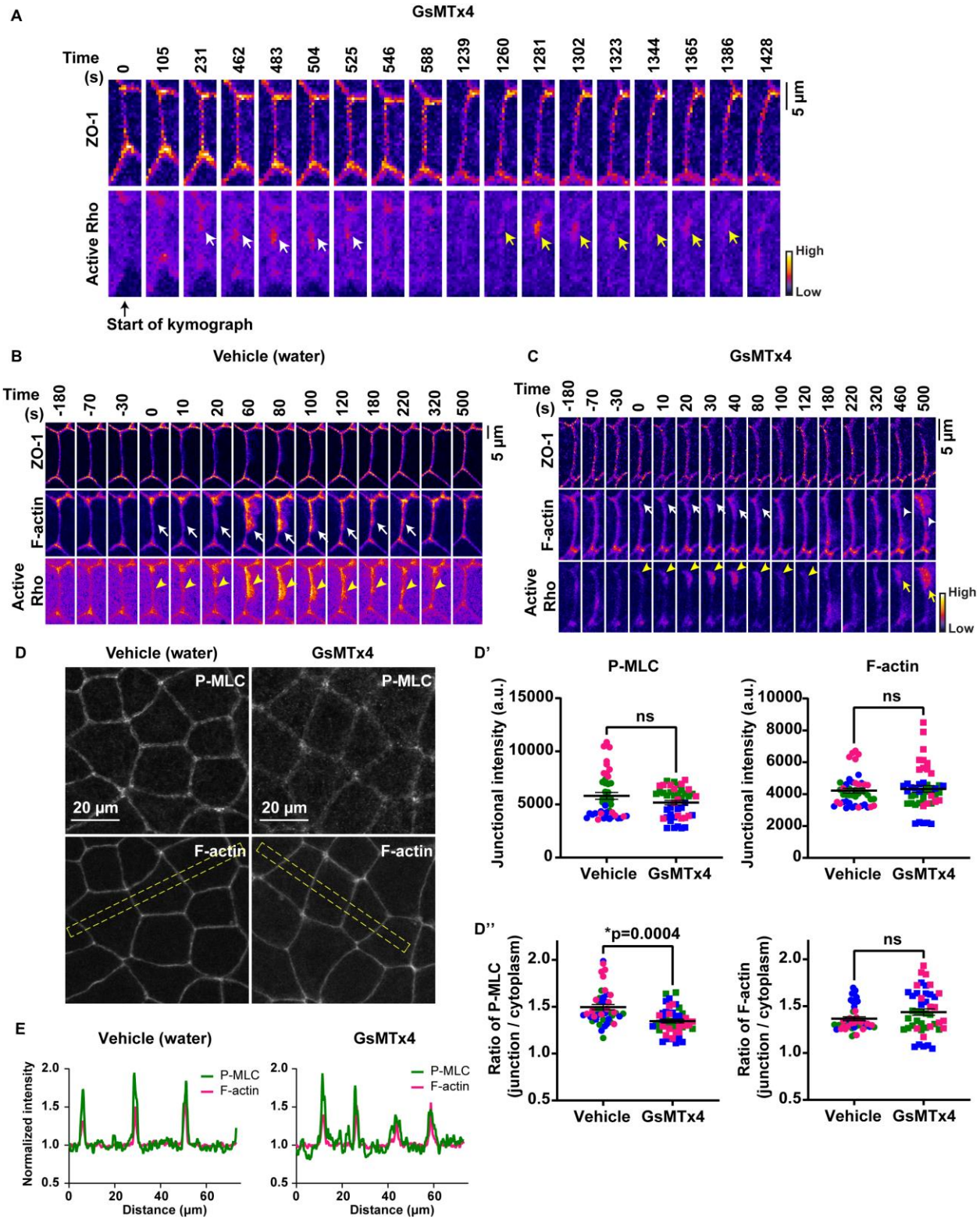

Figure S 2.3: Sustained Rho flares are required for robust F-actin accumulation and successful reinforcement of ZO-1.(A) Montage of a representative junction used to construct kymograph in Figure 2.5G (FIRE LUT). Blocking MSCs with 12.5 µM GsMTx4 causes repeated increases in active Rho at the site of reduced ZO-1 at time 231 s (first flare, white arrows) and 1260 s (second flare, yellow arrows). Note that ZO-1 is partially reinforced

following the first flare but breaks at the same site prior to activation of second flare. Time 0 s represents the start of kymograph in Figure 2.5G.
(B-C) Time-lapse images (FIRE LUT) of ZO-1 (BFP-ZO-1), F-actin (Lifeact-GFP), and active Rho (mCherry-2xrGBD) in embryos treated with vehicle (water) or 12.5 μM GsMTx4. Blocking MSCs with 12.5 μM GsMTx4 causes reduced F-actin accumulation (C, white arrows) at the site of Rho flares (C, yellow arrowheads) compared to vehicle control in B. Note the robust F-actin accumulation (C, white arrowhead) scales with a higher intensity repeating Rho flare (C, yellow arrow). Time 0 s represents the start of Rho flare.
(D-D'') Sum projection of fixed staining for P-MLC (anti-pMLC) and F-actin (Alexa Fluor 647 phalloidin) in embryos treated with vehicle (water) or 12.5 μM GsMTx4. (D') Quantification shows that MSC inhibition does not significantly affect the junctional intensity of P-MLC and F-actin at cell-cell junctions compared to vehicle control. (D'') MSC inhibition reduces the junction/cytoplasm ratio of P-MLC compared to vehicle, but does not affect the junction/cytoplasm ratio for F-actin. Data points from paired experiments are color matched. Error bars represent mean ± S.E.M.; significance calculated using One-way ANOVA test; n=45 junctions, 3 experiments.
(E) Line scan of P-MLC (green) and F-actin (magenta) across multiple junctions for representative image shown in D (yellow boxes) shows that intensity and width of P-MLC and F-actin peaks at cell-cell junctions in GsMTx4-treated embryos are comparable to vehicle controls.

2.7 Acknowledgements

We thank W.M.Bement for pCS2+/ mCherry-2xrGBD and pCS2+/ eGFP-PKC-β-C2 constructs as well as current and former members of the A.L.Miller laboratory for providing helpful discussion and feedback on experiments. This work was supported by NIH grant (2R01 GM112794) to A.L.Miller, a predoctoral fellowship from the American Heart Association (20PRE35120588) to S.Varadarajan, and BBSRC grants BB/P01190X and BB/P006507 to A.B.Goryachev.

2.8 References

ACHARYA, B. R., NESTOR-BERGMANN, A., LIANG, X., GUPTA, S., DUSZYC, K., GAUQUELIN, E., GOMEZ, G. A., BUDNAR, S., MARCQ, P., JENSEN, O. E., BRYANT, Z. & YAP, A. S. 2018. A Mechanosensitive RhoA Pathway that Protects Epithelia against Acute Tensile Stress. *Dev Cell,* 47**,** 439-452 e6.

AKAZAWA, Y., YUKI, T., YOSHIDA, H., SUGIYAMA, Y. & INOUE, S. 2013. Activation of TRPV4 strengthens the tight-junction barrier in human epidermal keratinocytes. *Skin Pharmacol Physiol,* 26**,** 15-21.

ARNOLD, T. R., SHAWKY, J. H., STEPHENSON, R. E., DINSHAW, K. M., HIGASHI, T., HUQ, F., DAVIDSON, L. A. & MILLER, A. L. 2019. Anillin regulates epithelial cell mechanics by structuring the medial-apical actomyosin network. *Elife,* 8.

BAE, C., SACHS, F. & GOTTLIEB, P. A. 2011. The mechanosensitive ion channel Piezo1 is inhibited by the peptide GsMTx4. *Biochemistry,* 50**,** 6295-6300.

BENINK, H. A. & BEMENT, W. M. 2005. Concentric zones of active RhoA and Cdc42 around single cell wounds. *Journal of Cell Biology,* 168**,** 429-439.

BOWMAN, C. L., GOTTLIEB, P. A., SUCHYNA, T. M., MURPHY, Y. K. & SACHS, F. 2007. Mechanosensitive ion channels and the peptide inhibitor GsMTx-4: history, properties, mechanisms and pharmacology. *Toxicon,* 49**,** 249-70.

CANALES, J., MORALES, D., BLANCO, C., RIVAS, J., DIAZ, N., ANGELOPOULOS, I. & CERDA, O. 2019. A TR(i)P to Cell Migration: New Roles of TRP Channels in Mechanotransduction and Cancer. *Front Physiol,* 10**,** 757.

CAVANAUGH, K. J., COHEN, T. S. & MARGULIES, S. S. 2006. Stretch increases alveolar epithelial permeability to uncharged micromolecules. *Am J Physiol Cell Physiol,* 290**,** C1179-88.

CHEN, T. W., WARDILL, T. J., SUN, Y., PULVER, S. R., RENNINGER, S. L., BAOHAN, A., SCHREITER, E. R., KERR, R. A., ORGER, M. B., JAYARAMAN, V., LOOGER, L. L., SVOBODA, K. & KIM, D. S. 2013. Ultrasensitive fluorescent proteins for imaging neuronal activity. *Nature,* 499**,** 295-300.

CHRISTODOULOU, N. & SKOURIDES, P. A. 2015. Cell-Autonomous Ca(2+) Flashes Elicit Pulsed Contractions of an Apical Actin Network to Drive Apical Constriction during Neural Tube Closure. *Cell Rep,* 13**,** 2189-202.

CLARK, A. G., MILLER, A. L., VAUGHAN, E., YU, H. Y. E., PENKERT, R. & BEMENT, W. M. 2009. Integration of Single and Multicellular Wound Responses. *Current Biology,* 19**,** 1389-1395.

CLAUDE, P. & GOODENOUGH, D. A. 1973. Fracture faces of zonulae occludentes from "tight" and "leaky" epithelia. *J Cell Biol,* 58**,** 390-400.

COHEN, T. S., CAVANAUGH, K. J. & MARGULIES, S. S. 2008. Frequency and peak stretch magnitude affect alveolar epithelial permeability. *Eur Respir J,* 32**,** 854-61.

COSTE, B., MATHUR, J., SCHMIDT, M., EARLEY, T. J., RANADE, S., PETRUS, M. J., DUBIN, A. E. & PATAPOUTIAN, A. 2010. Piezo1 and Piezo2 Are Essential Components of Distinct Mechanically Activated Cation Channels. *Science,* 330**,** 55-60.

DAVENPORT, N. R., SONNEMANN, K. J., ELICEIRI, K. W. & BEMENT, W. M. 2016. Membrane dynamics during cellular wound repair. *Molecular Biology of the Cell,* 27**,** 2272-2285.

ELLEFSEN, K. L., HOLT, J. R., CHANG, A. C., NOURSE, J. L., ARULMOLI, J., MEKHDJIAN, A. H., ABUWARDA, H., TOMBOLA, F., FLANAGAN, L. A., DUNN, A. R., PARKER, I. & PATHAK, M. M. 2019. Myosin-II mediated traction forces evoke localized Piezo1-dependent Ca(2+) flickers. *Commun Biol,* 2**,** 298.

FANNING, A. S., JAMESON, B. J., JESAITIS, L. A. & ANDERSON, J. M. 1998. The tight junction protein ZO-1 establishes a link between the transmembrane protein occludin and the actin cytoskeleton. *J Biol Chem,* 273**,** 29745-53.

FURUSE, M., SASAKI, H., FUJIMOTO, K. & TSUKITA, S. 1998. A single gene product, claudin-1 or -2, reconstitutes tight junction strands and recruits occludin in fibroblasts. *J Cell Biol,* 143**,** 391-401.

GNANASAMBANDAM, R., GHATAK, C., YASMANN, A., NISHIZAWA, K., SACHS, F., LADOKHIN, A. S., SUKHAREV, S. I. & SUCHYNA, T. M. 2017. GsMTx4: Mechanism of Inhibiting Mechanosensitive Ion Channels. *Biophysical Journal,* 112**,** 31-45.

GONZALEZ-MARISCAL, L., CONTRERAS, R. G., BOLIVAR, J. J., PONCE, A., CHAVEZ DE RAMIREZ, B. & CEREIJIDO, M. 1990. Role of calcium in tight junction formation between epithelial cells. *Am J Physiol,* 259**,** C978-86.

GUDIPATY, S. A., LINDBLOM, J., LOFTUS, P. D., REDD, M. J., EDES, K., DAVEY, C. F., KRISHNEGOWDA, V. & ROSENBLATT, J. 2017. Mechanical stretch triggers rapid epithelial cell division through Piezo1. *Nature,* 543**,** 118-121.

GUDIPATY, S. A. & ROSENBLATT, J. 2016. Epithelial cell extrusion: Pathways and pathologies. *Seminars in Cell and Developmental Biology*.

GUILLOT, C. & LECUIT, T. 2013. Mechanics of epithelial tissue homeostasis and morphogenesis. *Science,* 340**,** 1185-9.

HIGASHI, T., ARNOLD, T. R., STEPHENSON, R. E., DINSHAW, K. M. & MILLER, A. L. 2016. Maintenance of the Epithelial Barrier and Remodeling of Cell-Cell Junctions during Cytokinesis. *Curr Biol,* 26**,** 1829-42.

HOLINSTAT, M., MEHTA, D., KOZASA, T., MINSHALL, R. D. & MALIK, A. B. 2003. Protein kinase Calpha-induced p115RhoGEF phosphorylation signals endothelial cytoskeletal rearrangement. *J Biol Chem,* 278**,** 28793-8.

HUNTER, G. L., CRAWFORD, J. M., GENKINS, J. Z. & KIEHART, D. P. 2014. Ion channels contribute to the regulation of cell sheet forces during Drosophila dorsal closure. *Development,* 141**,** 325-334.

ITOH, M., FURUSE, M., MORITA, K., KUBOTA, K., SAITOU, M. & TSUKITA, S. 1999. Direct binding of three tight junction-associated MAGUKs, ZO-1, ZO-2, and ZO-3, with the COOH termini of claudins. *J Cell Biol,* 147**,** 1351-63.

IVANOV, A. I., PARKOS, C. A. & NUSRAT, A. 2010. Cytoskeletal Regulation of Epithelial Barrier Function During Inflammation. *The American Journal of Pathology,* 177**,** 512-524.

LIU, C. & MONTELL, C. 2015. Forcing open TRP channels: Mechanical gating as a unifying activation mechanism. *Biochem Biophys Res Commun,* 460**,** 22-5.

LUISSINT, A. C., PARKOS, C. A. & NUSRAT, A. 2016. Inflammation and the Intestinal Barrier: Leukocyte-Epithelial Cell Interactions, Cell Junction Remodeling, and Mucosal Repair. *Gastroenterology,* 151**,** 616-32.

MARCHIANDO, A. M., GRAHAM, W. V. & TURNER, J. R. 2010. Epithelial barriers in homeostasis and disease. *Annu Rev Pathol,* 5**,** 119-44.

MILLER, A. L. & BEMENT, W. M. 2009. Regulation of cytokinesis by Rho GTPase flux. *Nat Cell Biol,* 11**,** 71-7.

MIYAMOTO, T., MOCHIZUKI, T., NAKAGOMI, H., KIRA, S., WATANABE, M., TAKAYAMA, Y., SUZUKI, Y., KOIZUMI, S., TAKEDA, M. & TOMINAGA, M. 2014. Functional role for Piezo1 in stretch-evoked Ca2+ influx and ATP release in Urothelial cell cultures. *Journal of Biological Chemistry,* 289**,** 16565-16575.

MOCHIZUKI, T., SOKABE, T., ARAKI, I., FUJISHITA, K., SHIBASAKI, K., UCHIDA, K., NARUSE, K., KOIZUMI, S., TAKEDA, M. & TOMINAGA, M. 2009. The TRPV4 cation channel mediates stretch-evoked Ca2+ influx and ATP release in primary urothelial cell cultures. *J Biol Chem,* 284**,** 21257-64.

MORIWAKI, K., TSUKITA, S. & FURUSE, M. 2007. Tight junctions containing claudin 4 and 6 are essential for blastocyst formation in preimplantation mouse embryos. *Dev Biol,* 312**,** 509-22.

MURAKOSHI, H., WANG, H. & YASUDA, R. 2011. Local, persistent activation of Rho GTPases during plasticity of single dendritic spines. *Nature,* 472**,** 100-104.

NIGAM, S. K., RODRIGUEZ-BOULAN, E. & SILVER, R. B. 1992. Changes in intracellular calcium during the development of epithelial polarity and junctions. *Proc Natl Acad Sci U S A,* 89**,** 6162-6.

NUSRAT, A., GIRY, M., TURNER, J. R., COLGAN, S. P., PARKOS, C. A., CARNES, D., LEMICHEZ, E., BOQUET, P. & MADARA, J. L. 1995. Rho protein regulates tight junctions and perijunctional actin organization in polarized epithelia. *Proceedings of the National Academy of Sciences of the United States of America,* 92**,** 10629-10633.

PARDO-PASTOR, C., RUBIO-MOSCARDO, F., VOGEL-GONZÁLEZ, M., SERRA, S. A., AFTHINOS, A., MRKONJIC, S., DESTAING, O., ABENZA, J. F., FERNÁNDEZ-FERNÁNDEZ, J. M., TREPAT, X., ALBIGES-RIZO, C., KONSTANTOPOULOS, K. & VALVERDE, M. A. 2018. Piezo2 channel regulates RhoA and actin cytoskeleton to promote cell mechanobiological responses. *Proceedings of the National Academy of Sciences,* 115**,** 1925-1930.

REYES, C. C., JIN, M., BREZNAU, E. B., ESPINO, R., DELGADO-GONZALO, R., GORYACHEV, A. B. & MILLER, A. L. 2014. Anillin regulates cell-cell junction integrity by organizing junctional accumulation of Rho-GTP and actomyosin. *Current Biology,* 24**,** 1263-1270.

ROSENBLATT, J., RAFF, M. C. & CRAMER, L. P. 2001. An epithelial cell destined for apoptosis signals its neighbors to extrude it by an actin- and myosin-dependent mechanism. *Curr Biol,* 11**,** 1847-57.

SAHU, S. U., VISETSOUK, M. R., GARDE, R. J., HENNES, L., KWAS, C. & GUTZMAN, J. H. 2017. Calcium signals drive cell shape changes during zebrafish midbrain–hindbrain boundary formation. *Molecular Biology of the Cell,* 28**,** 875-882.

SAMAK, G., SUZUKI, T., BHARGAVA, A. & RAO, R. K. 2010. c-Jun NH2-terminal kinase-2 mediates osmotic stress-induced tight junction disruption in the intestinal epithelium. *Am J Physiol Gastrointest Liver Physiol,* 299**,** G572-84.

SAOUDI, Y., ROUSSEAU, B., DOUSSIERE, J., CHARRASSE, S., GAUTHIER-ROUVIERE, C., MORIN, N., SAUTET-LAUGIER, C., DENARIER, E., SCAIFE, R., MIOSKOWSKI, C. & JOB, D. 2004. Calcium-independent cytoskeleton disassembly induced by BAPTA. *Eur J Biochem,* 271**,** 3255-64.

SHAO, X., LI, Q., MOGILNER, A., BERSHADSKY, A. D. & SHIVASHANKAR, G. V. 2015. Mechanical stimulation induces formin-dependent assembly of a perinuclear actin rim. *Proc Natl Acad Sci U S A,* 112**,** E2595-601.

SHI, Z., GRABER, Z. T., BAUMGART, T., STONE, H. A. & COHEN, A. E. 2018. Cell Membranes Resist Flow. *Cell,* 175**,** 1769-1779 e13.

SIVE, H. L., GRAINGER, R. M. & HARLAND, R. M. 2007. Removing the Vitelline Membrane from Xenopus laevis Embryos. *CSH Protoc,* 2007**,** pdb prot4732.

SOKABE, T., FUKUMI-TOMINAGA, T., YONEMURA, S., MIZUNO, A. & TOMINAGA, M. 2010. The TRPV4 channel contributes to intercellular junction formation in keratinocytes. *J Biol Chem,* 285**,** 18749-58.

SPASSOVA, M. A., HEWAVITHARANA, T., XU, W., SOBOLOFF, J. & GILL, D. L. 2006. A common mechanism underlies stretch activation and receptor activation of TRPC6 channels. *Proceedings of the National Academy of Sciences,* 103**,** 16586-16591.

STAEHELIN, L. A., MUKHERJEE, T. M. & WILLIAMS, A. W. 1969. Freeze-etch appearance of the tight junctions in the epithelium of small and large intestine of mice. *Protoplasma,* 67**,** 165-84.

STEPHENSON, R. E., HIGASHI, T., EROFEEV, I. S., ARNOLD, T. R., LEDA, M., GORYACHEV, A. B. & MILLER, A. L. 2019. Rho Flares Repair Local Tight Junction Leaks. *Dev Cell,* 48**,** 445-459 e5.

STUART, R. O., SUN, A., PANICHAS, M., HEBERT, S. C., BRENNER, B. M. & NIGAM, S. K. 1994. Critical role for intracellular calcium in tight junction biogenesis. *J Cell Physiol,* 159**,** 423-33.

SUZUKI, M., SATO, M., KOYAMA, H., HARA, Y., HAYASHI, K., YASUE, N., IMAMURA, H., FUJIMORI, T., NAGAI, T., CAMPBELL, R. E. & UENO, N. 2017. Distinct intracellular Ca(2+) dynamics regulate apical constriction and differentially contribute to neural tube closure. *Development,* 144**,** 1307-1316.

VAN ITALLIE, C. M., TIETGENS, A. J. & ANDERSON, J. M. 2017. Visualizing the dynamic coupling of claudin strands to the actin cytoskeleton through ZO-1. *Mol Biol Cell,* 28**,** 524-534.

VARADARAJAN, S., STEPHENSON, R. E. & MILLER, A. L. 2019. Multiscale dynamics of tight junction remodeling. *J Cell Sci,* 132.

WALLINGFORD, J. B., EWALD, A. J., HARLAND, R. M. & FRASER, S. E. 2001. Calcium signaling during convergent extension in Xenopus. *Current Biology,* 11**,** 652-661.

WEI, C., WANG, X., CHEN, M., OUYANG, K., SONG, L. S. & CHENG, H. 2009. Calcium flickers steer cell migration. *Nature,* 457**,** 901-5.

WOOLNER, S., MILLER, A. L. & BEMENT, W. M. 2009. Imaging the cytoskeleton in live Xenopus laevis embryos. *Methods Mol Biol,* 586**,** 23-39.

YU, D., MARCHIANDO, A. M., WEBER, C. R., RALEIGH, D. R., WANG, Y., SHEN, L. & TURNER, J. R. 2010. MLCK-dependent exchange and actin binding region-dependent anchoring of ZO-1 regulate tight junction barrier function. *Proc Natl Acad Sci U S A,* 107**,** 8237-41.

YU, H. Y. E. & BEMENT, W. M. 2007. Control of local actin assembly by membrane fusion-dependent compartment mixing. *Nature Cell Biology,* 9**,** 149-159.

ZHONG, M., WU, W., KANG, H., HONG, Z., XIONG, S., GAO, X., REHMAN, J., KOMAROVA, Y. A. & MALIK, A. B. 2020. Alveolar Stretch Activation of Endothelial Piezo1 Protects Adherens Junctions and Lung Vascular Barrier. *Am J Respir Cell Mol Biol,* 62**,** 168-177.

ZIHNI, C., MILLS, C., MATTER, K. & BALDA, M. S. 2016. Tight junctions: From simple barriers to multifunctional molecular gates. *Nature Reviews Molecular Cell Biology,* 17**,** 564-580.

Chapter 3 Piezo1's Role in Maintaining and Remodeling Epithelial Cell-Cell Junctions

Contributions to this work are as follows:

Varadarajan.S.: conceptualized the study, developed the methodology, performed experiments except Figure 3.6, wrote the original draft of the chapter

Wu. J.L. (undergraduate student, who I mentored): performed some experiments for Figure 3.2 and Figure 3.6, analyzed data for Figure 3.1, Figure 3.2, and Figure 3.6

Misterovich. E.R. (recent UM graduate, who I supervised): analyzed data for Figure 3.3, Figure 3.4, and Figure 3.6

Miller, A.L.: conceptualized the study, developed the methodology, acquired funding, supervised the study, revised the chapter

3.1 Abstract

Proper barrier function of epithelial tissues requires epithelial cells to sense a range of mechanical forces and respond by remodeling their cell-cell junctions. How tension is sensed and transduced is an area of active research. Mechanosensitive calcium channels (MSCs) are capable of sensing changes in mechanical tension and converting the mechanical stimuli into biochemical signals. Previous work from our lab shows that calcium influx mediated by MSCs is required to maintain proper barrier function in epithelia. Here, we explore the localization and function of a MSC, Piezo1, at cell-cell junctions. Using the gastrula-stage *Xenopus laevis* epithelium, we found that Piezo1 localizes to apical cell-cell junctions in a homogenous population as well as in bright clusters along junctions. Piezo1 co-localizes with E-cadherin at adherens junctions

(AJs). Using fluorescence recovery after photobleaching (FRAP), we show that junctional Piezo1 is highly dynamic with a mobile fraction of 79.17% ± 1.73%, comparable to the previously reported mobile fraction for E-cadherin at AJs. Further, stimulation with extracellular ATP addition to increase actomyosin-mediated cellular contraction decreased junctional Piezo1 without altering its mobility. Finally, knock down of Piezo1 with an antisense morpholino increased the frequency of barrier leaks associated with tight junction (TJ) breaks without compromising global barrier function, possibly due to weakening of cell-cell junctions. These data suggest that Piezo1 is important for strengthening epithelial cell-cell junctions in response to mechanical tension.

3.2 Introduction

Based on the results from my previous chapter, we know that calcium influx mediated by MSCs is required to maintain an intact barrier in epithelium (Varadarajan et al., 2021). However, the specific channel(s) involved in epithelial barrier regulation remain unknown. In this chapter, I characterize the role of a MSC, Piezo1, which is expressed in epithelial cells and implicated in maintaining epithelial homeostasis, in maintaining and remodeling epithelial cell-cell junctions.

MSCs are transmembrane proteins that detect mechanical force in cells and allow calcium ions pass through the membrane (Ranade et al., 2015). Two eukaryotic MSCs, Piezo1 and Piezo2, were identified in 2010 and were found to be expressed in variety of tissues including bladder, colon, kidney, lung, and skin (Coste et al., 2010, Coste et al., 2012, Xiao and Xu, 2010). Endogenous mechanosensation by Piezo1 is required for epithelial homeostasis (Gudipaty et al., 2017, Eisenhoffer et al., 2012), vascular development (Ranade et al., 2014), vascular physiology (Zhong et al., 2020, Friedrich et al., 2019, Rode et al., 2017, Li et al., 2014), and neuronal differentiation (Pathak et al., 2014), among other processes. Abnormal function of Piezo1 leads to impaired development (Ranade et al., 2014), tumor formation (Gudipaty et al., 2017), and inflammation (Bai et al., 2017). Thus, it is important to understand the functions of Piezo1 during diverse biological processes.

In mammals, Piezo1 is ~2500 amino acids long with 38 predicted transmembrane domains, and Piezo1 assembles into a homotrimer in the plasma membrane to form a channel, consisting of a dynamic three bladed propeller with a central pore (Wang et al., 2018, Saotome et al., 2018). Upon a mechanical stimulus that

induces membrane stretch or a change in membrane curvature, Piezo1 senses a change in membrane tension and allows the passage of calcium ions through the pore module of the trimeric channel (Zhao et al., 2016, Wang et al., 2018). Piezo1 can mediate a range of calcium signals, from local calcium flickers to whole-cell calcium transients depending on the scale of the mechanical stimulus. For instance, Piezo1 mediates local calcium increases observed naturally at focal adhesions or by experimentally poking or pulling the membrane (Ellefsen et al., 2019, Shi et al., 2018). Tissue stretching, tissue compression, and osmotic stress induce Piezo1-dependent whole-cell calcium transients (Coste et al., 2010, Ellefsen et al., 2019, Pathak et al., 2014, Shi et al., 2018, Syeda et al., 2016, Cox et al., 2016, Luo et al., 2019). The scale of Piezo1 activation thereby regulates the spatio-temporal dynamics of downstream calcium signaling to regulate biological functions either locally or globally in a cell (Canales Coutino and Mayor, 2021, Heisenberg, 2017, Nourse and Pathak, 2017).

Notably, Piezo1 is expressed in a number of epithelial cell types that experience cell-scale tension generated by actomyosin forces and tissue-scale tension during their physiological function including uroepithelial, alveolar, and colonic epithelial cells, (Stewart and Davis, 2019, Miyamoto et al., 2014, Piddini, 2017). Functionally, Piezo1 is required to regulate epithelial tissue homeostasis by balancing cell extrusion and cell division, events that require rapid remodeling of cell-cell junctions (Eisenhoffer et al., 2012, Gudipaty et al., 2017). Additionally, Piezo1 is highly expressed in uroepithelium, where it mediates calcium influx into the cell in response to stretch (Miyamoto et al., 2014). However, it is not known if the stretch-mediated calcium influx through Piezo1 directly regulates the structure and function of epithelial cell-cell junctions.

In epithelial cells, tight junctions (TJs) and adherens junctions (AJs), are coupled to an underlying actomyosin array (Arnold et al., 2017, Higashi et al., 2019). These apical cell-cell junctions are rapidly remodeled in response to mechanical forces to maintain tissue structure and barrier function (Gomez et al., 2011, Varadarajan et al., 2019, Stephenson et al., 2019). For instance, in response to global and local mechanical stimuli, epithelial cells stabilize E-cadherin-mediated cell-cell adhesion, thereby maintaining an intact barrier (Acharya et al., 2018, Acharya et al., 2017, Higashi et al., 2016, Rosenblatt et al., 2001, Teo et al., 2020). Intracellular calcium signaling is required for remodeling of TJ and regulating barrier function (Varadarajan et al., 2021, Stuart et al., 1994, Bhat et al., 1993). Thus, it is of interest to understand if cell-cell junctions are regulated by Piezo1-mediated calcium signaling.

In this study, we use the gastrula-stage *Xenopus laevis* epithelium as a model vertebrate epithelium to explore the localization, dynamics, and function of Piezo1 at epithelial cell-cell junctions. Further, we investigate the mechanism by which Piezo1 regulates epithelial barrier function.

3.3 Results and Discussion

3.3.1 Piezo1 localizes to apical cell-cell junctions in the gastrula-stage *Xenopus* epithelium

Piezo1 is enriched at cell-cell junctions and the endoplasmic reticulum in monolayers of cultured epithelial cells (Gudipaty et al., 2017), but the expression and distribution of endogenous Piezo1 in an intact epithelium experiencing tissue scale forces is not known. Thus, we characterized the localization of Piezo1 in the epithelium of gastrula-stage *Xenopus laevis* embryos. In order to evaluate the endogenous expression and localization of Piezo1, we immunostained gastrula-stage embryos expressing a membrane marker (mCherry-Farnesyl) with a Piezo1 antibody and DNA stain (DAPI). We found that endogenous Piezo1 is expressed in the gastrula-stage epithelium and is enriched at cell-cell junctions (Figure 3.1, A and B). Upon comparing the intensity of Piezo1 at bicellular junctions and tricellular junctions, which are known to be sites of increased tension (Higashi and Miller, 2017), we found that the distribution of Piezo1 is comparable between the two sites (Figure 3.1 C), suggesting that this level of tension difference does not detectably affect Piezo1 localization.

Piezo1 is a transmembrane protein that localizes to plasma membrane in various cells, including red blood cells, fibroblasts, endothelial cells, and neural stem cells (Coste et al., 2010, Zarychanski et al., 2012, Ellefsen et al., 2019). To test whether Piezo1 localization exhibits apicobasal polarization similar to junctional proteins or homogenous localization along the apical-basal length of the junctions, we co-immunostained gastrula-stage embryos with antibodies for Piezo1 and the TJ protein ZO-1. Piezo1 generally localizes to apical cell-cell junctions near ZO-1, rather than

basolateral cell-cell junctions (Figure 1D). Interestingly, a non-junctional population of Piezo1 formed clusters in the medial apical area of the cell and in the cytoplasm (bright green puncta, Figure 3.1 D).

To knock down (KD) Piezo1, we injected a translation blocking Piezo1 morpholino (MO) targeting the 5' untranslated region (UTR) of Piezo1.S. We decided to target the Piezo1.S alloalele, as mRNA of the Piezo1.S. alloallele is expressed ~2-20 fold more than the Piezo1.L alloallelle during the early stages of *Xenopus laevis* development (Session et al., 2016). Injection of Piezo1 MO significantly decreased the intensity of endogenous Piezo1 at cell-cell junctions to 49.84% ± 7.90% compared to controls (Figure 3.1, E and E'). Additionally, we observed that the Piezo1 KD cells were larger in size compared to controls (membrane, Figure 3.1 E), but did not display multinucleation (DAPI stain, Figure 3.1 E). Taken together, our results show that Piezo1 is expressed in the gastrula-stage epithelium and localizes to apical cell-cell junctions. Additionally, our results show that Piezo1 KD cells are larger, suggesting a role for Piezo1 in regulating cell size.

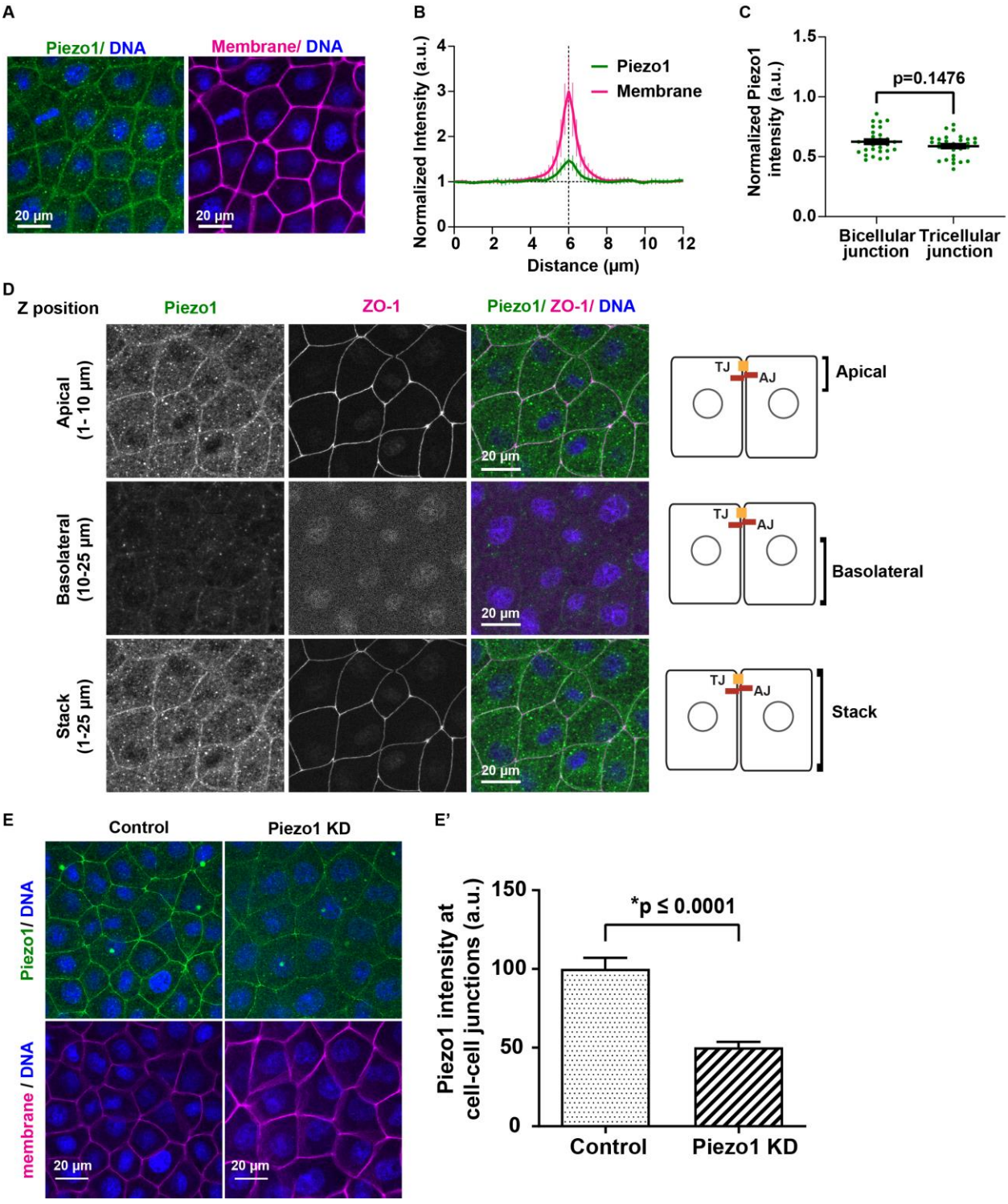

Figure 3.1: Piezo1 localizes to apical cell-cell junctions in the gastrula-stage *Xenopus* epithelium

(A) Immunostaining of endogenous Piezo1 (anti-Piezo1, green), membrane (anti-mCherry, magenta) and DNA (DAPI, blue) in the animal cap epithelium of gastrula-stage *Xenopus laevis* embryos expressing membrane probe (mCherry-Farnesyl). Stacked projections show endogenous Piezo1 localizes to cell-cell junctions in the *Xenopus* epithelium.

(B) Graph of relative intensity of Piezo1 (green) and membrane (magenta) at cell-cell junctions. Averaged line scans across the cell-cell junction and cytoplasm on either side of the junction show that the intensity of Piezo1 is increased at cell-cell junctions. Vertical line represents center of the cell-cell junction, and error bars represent S.D. n=10 junctions, 10 embryos, 3 experiments.
(C) Graph of intensity of Piezo1 at bicellular junctions and tricellular junctions in the animal cap epithelium of gastrula-stage *Xenopus laevis* embryos expressing membrane probe (mCherry-Farnesyl). Graph shows that the Piezo1 intensity at bicellular junctions is comparable to the intensity at tricellular junctions. Error bars represent mean ± S.E.M.; significance calculated using t-test with Welch's correction. n= 30 junctions, 8 embryos, 3 experiments.
(D) Immunostaining of Piezo1 (anti-Piezo1, green), TJ protein (anti-ZO-1, magenta), and DNA (DAPI, blue) in gastrula-stage *Xenopus* epithelial cells. Stacked projections (sum) show Piezo1 intensity is higher at apical cell-cell junctions (top) marked by ZO-1 compared to basolateral cell-cell junctions (middle). (Right) Schematic specifies the region along the Z-axis used to make stacked projections.
(E-E') Immunostaining of embryos injected with membrane probe with or without Piezo1 MO targeting the Piezo1.S alloallele. Gastrula-stage embryos immunostained for Piezo-1 (anti-Piezo1, green), membrane (anti-mCherry, magenta), and DNA (DAPI, blue). (E') Graph shows endogenous Piezo1 is reduced at cell-cell junctions in Piezo1 MO injected embryos (Piezo1 KD) compared to controls. Error bars represent mean ± S.E.M.; significance calculated using t-test with Welch's correction. n= 40 junctions, 10 embryos, 3 experiments.

3.3.2 Piezo1 localizes to adherens junctions in the gastrula-stage *Xenopus* epithelium

In the vertebrate apical junctional complex, TJs are localized most apically, and AJs are localized basal to TJs. To examine the precise localization of Piezo1 at apical cell-cell junctions, we co-expressed eGFP-tagged Piezo1 along with a TJ protein (tagBFP-ZO-1), and AJ proteins (PLEKHA-7-mCherry or E-Cadherin-3xmCherry) in gastrula-stage *Xenopus* epithelial cells. We observed that eGFP-Piezo1 localized to cell-cell junctions (green, Figure 3.2 A), consistent with the localization of endogenous Piezo1. Co-expression of eGFP-Piezo1 with BFP-ZO-1, shows that Piezo1 (green, Figure 3.2 A) localizes basal to the level of the TJ (magenta, Figure 3.2 A). Quantification of fluorescence intensity along the Z-axis using an approach previously developed in our lab (Higashi et al., 2019) shows that the peak intensity of Piezo1 is ~1-1.5 µm basal to the ZO-1 peak (2 µm) (Figure 3.2 A'), demonstrating that Piezo1 is not enriched at TJs. Next, upon co-expression of Piezo1 with the AJ proteins (PLEKHA-7 or E-Cadherin), we found that Piezo1 partially co-localizes with PLEKHA-7 (Figure 3.2, B and B'), and strongly co-localizes with E-cadherin (Figure 3.2, C and C'). Unlike E-cadherin,

PLEKHA-7 is an AJ protein that localizes specifically to the ZA (*Zonula adhaerens*) and not to the basolateral region of AJs (Pulimeno et al., 2010). Thus, Piezo1 is not restricted to the ZA, but spans the junction laterally similar to E-Cadherin. Though the peak of Piezo1 (3-3.5 µm) is basal to the peak of E-Cadherin (2.5 µm), a significant fraction of Piezo1 signal overlaps with AJ, ZA and TJ. The box and whisker plot of Piezo1 distribution shows that, ~95-98% is at AJ, ~77% is at ZA, and ~40% is at TJ (Figure 3.2, D and D'). Together, our results show that Piezo1 localizes to apical cell-cell junctions, with enrichment at the AJ. Consistent with our data, recent work using immunoprecipitation experiments shows that Piezo1 interacts directly with E-Cadherin in MDCK cells (Wang et al., 2020).

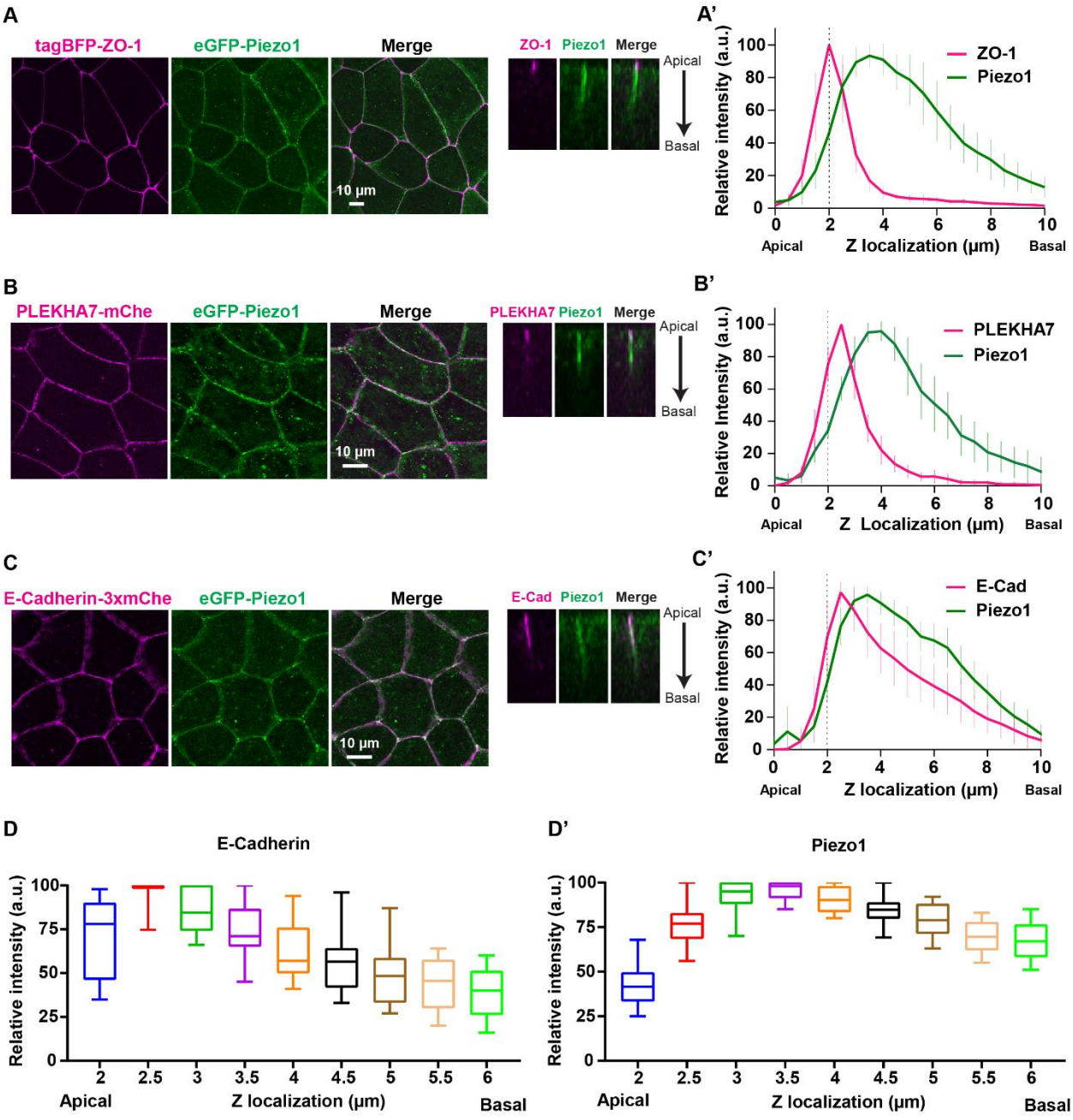

Figure 3.2: Piezo1 localizes to adherens junction in gastrula-stage *Xenopus* epithelium

(A-C) Localization of Piezo1 with TJ (A) and AJ (B-C) proteins in gastrula-stage *Xenopus laevis* embryos expressing eGFP-Piezo1 together with tagBFP-ZO-1 (TJ marker, A), PLEKHA7-mCherry (ZA marker, B), or E-Cadherin-3xmCherry (AJ marker, C). En-face views (left) of cell-cell junctions show Piezo1 localizes to cell-cell junctions and side views (right) show Piezo-1 localizes to AJs.
(A'-C') Graph shows the mean relative intensity of ZO-1 (tagBFP-ZO-1, magenta), PLEKHA7 (PLEKHA7-mCherry, magenta), E-cadherin (E-cadherin-3xmCherry, magenta) with Piezo1 (eGFP-Piezo1, green) and along the Z-axis at cell-cell junctions. Piezo1 localizes to apical cell-cell junctions with strong localization to AJs (3-4 µm) and weaker localization to TJ (2 µm). Vertical dotted lines indicate peak intensity of ZO-1 at 2 µm. Error bars represents S.D. n= 16 junctions, 4 embryos, 2 experiments.

(D-D') Box and whisker plot showing the intensity of E-cadherin (D) and Piezo1 (D') along the Z-axis quantified from C'. Graph shows the tight distribution of Piezo1 at AJ (3-4 µm). Whiskers indicate the 5-95 percentile range of the intensity values.

3.3.3 Junctional localization of Piezo1 is dependent on actomyosin-mediated tension

We next asked if junctional localization of Piezo1 is influenced by tension at cell-cell junctions. Because contractility of the apical actomyosin array alters the structure and function of cell-cell junctions (Arnold et al., 2017), we examined whether localization of Piezo1 is influenced by actomyosin-mediated tension. Although Piezo1 has been proposed to differentially localize to the plasma membrane, nuclear envelope, or the cytoplasm, depending on the crowding of epithelial cells (Gudipaty et al., 2017), its dynamic localization in response to cell and tissue level forces remains unclear.

Extracellular ATP has been used to increase contractility in various cells and tissues, including epithelial cells, endothelial cells, and cardiac muscle (Kim et al., 2014). In *Xenopus* embryos, addition of extracellular ATP induces rapid contraction of epithelial tissue, thereby reinforcing the connection of E-cadherin to the underlying actomyosin array (Joshi and Davidson, 2010, Kim et al., 2014, Arnold et al., 2019, Higashi et al., 2016). We treated embryos expressing eGFP-Piezo1, tagBFP-ZO-1, and mCherry-membrane with either control conditions (0.1x MMR) or 500 µM ATP (in 0.1x MMR) for 10 minutes. Using confocal imaging, we observed that upon extracellular ATP treatment, ZO-1 signal at TJs appeared "wavy" compared to relatively straight junctions in control cells (Figure 3.3, A and A'), confirming that junctions are indeed under increased tension in response to ATP. Interestingly, we found that the intensity of Piezo1 appeared reduced at cell-cell junctions in response to ATP compared to control

(blue LUT, Figure 3.3 A). With ATP treatment, Piezo1 junctional clusters seen in control cells (yellow arrowhead, Figure 3.3 A') were dramatically reduced, and the junctional localization of Piezo1 appeared homogenous (Figure 3.3 A').

To better understand if the change in the intensity of Piezo1 at junctions is due to a change in the amount of membrane at junctions, we normalized eGFP-Piezo1 signal to the mCherry-membrane signal (Figure 3.3 B). Consistent with our fixed staining (Figure 3.1 A'), eGFP-Piezo1 was not significantly different between bicellular and tricellular junctions in control cells (blue, Figure 3.3 B). However, following extracellular ATP treament, Piezo1 was significantly reduced at both bicellular and tricellular junctions compared to controls (magenta, Figure 3.3 B), suggesting that actomyosin-mediated cellular contractility removes Piezo1 from the cell-cell junctions.

Next, we asked if the change in junctional tension leads to redistribution of Piezo1 along the apical-basal axis of cell-cell junctions. Both, TJ and AJ transmembrane proteins have been shown to diffuse laterally along the cell-cell junction in response to cytoskeletal tension changes (Shen et al., 2008b). We found that Piezo1 distribution along the Z-axis was comparable between control and ATP-treated embryos (green, Figure 3.3, C and C').

Taken together, our results show that Piezo1 localization at AJs is inversely correlated with actomyosin-mediated junctional contraction: more Piezo1 is present at junctions under lower tension, and less Piezo1 is present at junctions with increased tension. Notably, we observed that the apical perimeter of the cells treated with extracellular ATP was reduced compared to controls. We previously showed that ATP treatment increases medial apical actomyosin, which apically constricts epithelial cells

(Arnold et al., 2019). During apical constriction, excess membrane from the apical cell surface is removed by endocytosis (Lee and Harland, 2010). Thus, the decrease in Piezo1 at cell-cell junctions following ATP treatment might be caused by endocytosis of the apical membrane.

Under baseline tension, Piezo1 has been shown to form clusters on the surface of red blood cells and human neuronal stem cell progenitors at sites of actin attachement to the membrane (Dumitru et al., 2021, Ellefsen et al., 2019). Additionally, local calcium influx was observed at regions of Piezo1 clusters (Ellefsen et al., 2019), suggesting that clustering of Piezo1 in the membrane might be a mechanism to amplify local calcium influx mediated by Piezo1. However, our data shows that with ATP treatment Piezo1 clusters were dramatically reduced. Thus, it's possible that Piezo1 clusters are targeted for removal from the plasma membrane and degraded to dampen the calcium influx that is induced by ATP treatment (data not shown). This hypothesis is based on a recent finding that degradation of Piezo1 via the proteosome is a mechanism by which endothelial cells turn off calcium influx following application of long-term stretch (30 minutes) (Miroshnikova et al., 2021).

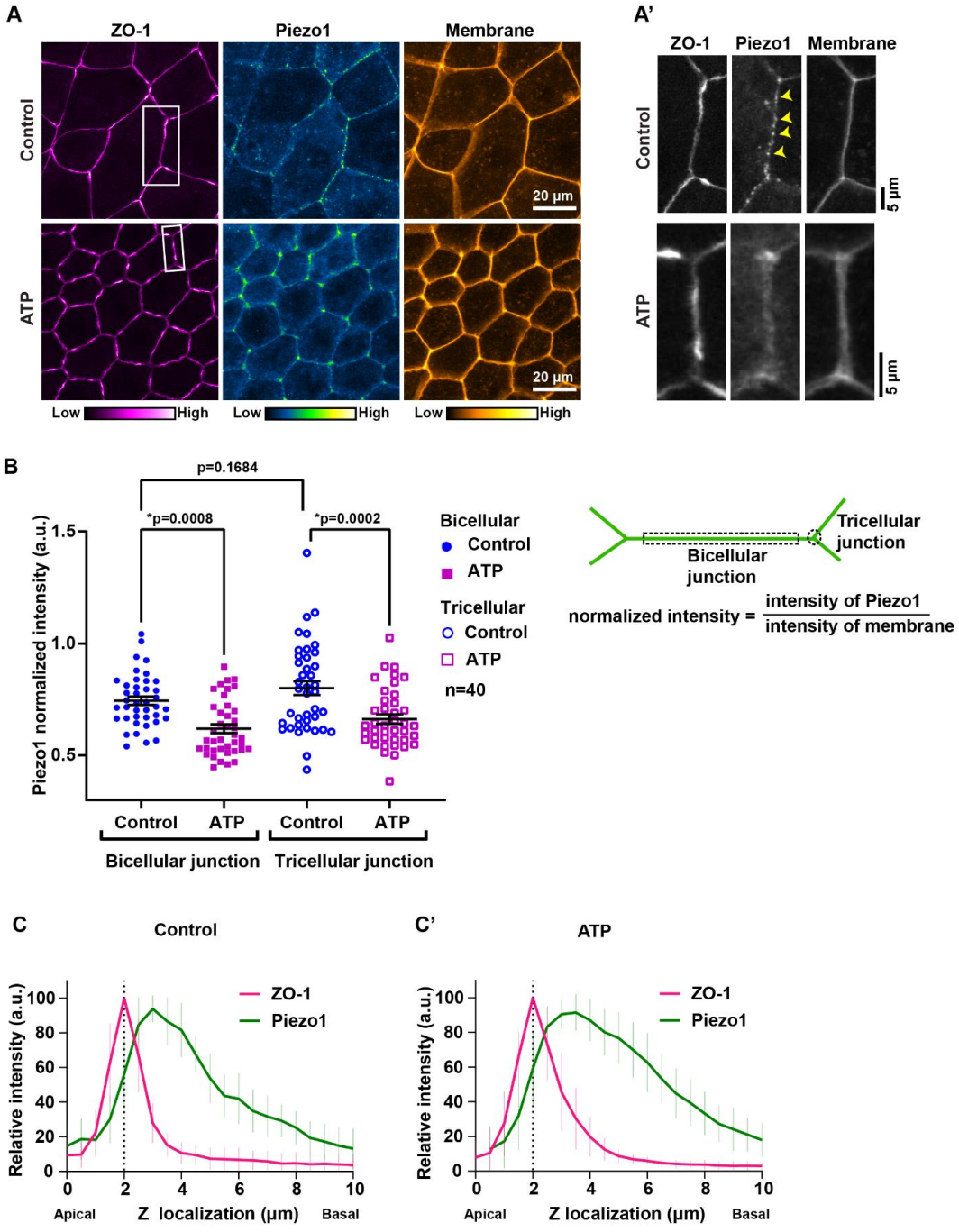

Figure 3.3: Junctional localization of Piezo1 is dependent on actomyosin-mediated tension

(A-A') Sum projection of embryos expressing BFP-ZO-1, eGFP-Piezo1, and membrane probe (mCherry-membrane) shown in LUT. Embryos were treated with either control condition (0.1x MMR, baseline tension) or 500 µM ATP (in 0.1x MMR, increased junction tension) for 10 minutes prior to imaging. (A) Increased tension changed the localization of Piezo1 and ZO-1 along the cell-cell junctions. (A') Zoomed in views of junctions highlighted in A (white boxes). In control embryos, Piezo1 localizes as clusters along the length of the junction (indicated by yellow arrowheads). When tension is increased with ATP treatment, Piezo1 distributes evenly along the length of the cell-cell junction compared to controls.

(B) Quantification of experiments shown in (A) along the length of bicellular junctions and at tricellular junctions. (Left) Graph of relative intensity of Piezo1 shows no significant difference at bicellular and tricellular junctions under

baseline tension (blue circles). Increased tension with ATP treatment reduces Piezo1 intensity at both bicellular and tricellular junctions (magenta squares) compared to control. Error bars represent mean ± S.E.M.; significance calculated using One-way ANOVA. n= 40 junctions, 8 embryos, 2 experiments. (Right) Schematic showing regions of interest (ROIs) used to quantify intensity at the bicellular and tricellular junctions.
(C-C') Graphs show the mean relative intensity of Piezo1 (eGFP-Piezo1, green), and ZO-1 (tagBFP-ZO-1, magenta) along the Z-axis at cell-cell junctions under baseline and increased tension. Distribution of Piezo1 along the Z-axis under increased tension (ATP) is comparable to baseline tension (control). Vertical dotted line indicates peak intensity of ZO-1 at 2 μm. Error bars represents S.D. Control: n= 12 junctions, 4 embryos, 1 experiment; ATP: n= 16 junctions, 4 embryos, 1 experiment.

3.3.4 High mobility of junctional Piezo1 is independent of actomyosin-mediated tension

Time-lapse imaging of eGFP-Piezo1 demonstrated that Piezo1 clusters observed at cell-cell junctions and in the cytoplasm are highly dynamic (data not shown). Using Total Internal Reflection Fluorescence (TIRF) microscopy, previous work showed that Piezo1 clusters at the plasma membrane of neuronal stem cells exhibited decreased mobility at focal adhesions, sites where actomyosin is connected to the plasma membrane (Ellefsen et al., 2019). Therefore, we next examined the mobility of Piezo1 at AJs by fluorescence recovery after photobleaching (FRAP) of eGFP-Piezo1. Our results show that the majority of Piezo1 at AJs exchanges with a mobile fraction of 79.17% ± 1.73% (Figure 3.4, A-C) via a rapid two-phase recovery (fast $t_{1/2}$ of 4.51 ± 2.08s, slow $t_{1/2}$ of 50.1 ± 9.4s) (Figure 3.4, D and D'). Our FRAP results for Piezo1 are comparable to the mobility and exchange of E-cadherin in the same tissue (mobile fraction: 73.2%-80.5%, slow $t_{1/2}$: 49.5 ± 9.9 s) (Higashi et al., 2016). Furthermore, junctional E-cadherin has been shown to form nano-clusters (Truong Quang et al., 2013) similar to the Piezo1 clusters we observed in this study. Together, these data along with our localization data support the idea that Piezo1 might directly interact with E-cadherin or be part of an E-cadherin-associated complex.

Since both E-cadherin and ZO-1 are stabilized at cell-cell junctions in response to increased cytoskeletal-mediated tension (Higashi et al., 2016, Yu et al., 2010), we next tested if the mobility of Piezo1 is altered by increased tension. We found that in ATP-treated embryos, the mobile fraction (75.02% ± 1.71%, Figure 3.4, B and C) and $t_{1/2}$ of Piezo1 (fast $t_{1/2}$ of 4.56 ± 3.88 s, slow $t_{1/2}$ of 49.57 ± 8.11 s, Figure 3.4, D and D') was unchanged compared to controls. Thus, although ATP-mediated cytoskeletal tension does reduce the amount of Piezo1 at cell-cell junctions, it does not alter the mobility or exchange rate of remaining Piezo1 at AJs, suggesting that the high mobility of Piezo1 at AJs is independent of actomyosin-mediated tension.

Given that activation of Piezo1 is dependent on the direction of mechanical force (Gaub and Müller, 2017), and Piezo1 reacts differently to compressive versus tensile forces (Gudipaty et al., 2017), it is possible that ATP-mediated radial tension acting perpendicular to the cell-cell junction (Arnold et al., 2019) might not have an effect on the mobility of Piezo1. Thus, further studies are required to determine if Piezo1 localization or mobility is influenced by actomyosin-mediated tension generated by tensile stress that increases actomyosin-mediated tension in plane with the junctions. Previous studies have shown that tensile stress induced by the small molecule calyculin A, which inhibits myosin phosphatase (Higashi et al., 2016, Acharya et al., 2017), or uniaxial stretching of epithelial cells (Nestor-Bergmann et al., 2019, Acharya et al., 2018), increases tension along the length of the junctions. Thus, testing the mobility and localization of Piezo1 with these methods would be of great interest for future studies.

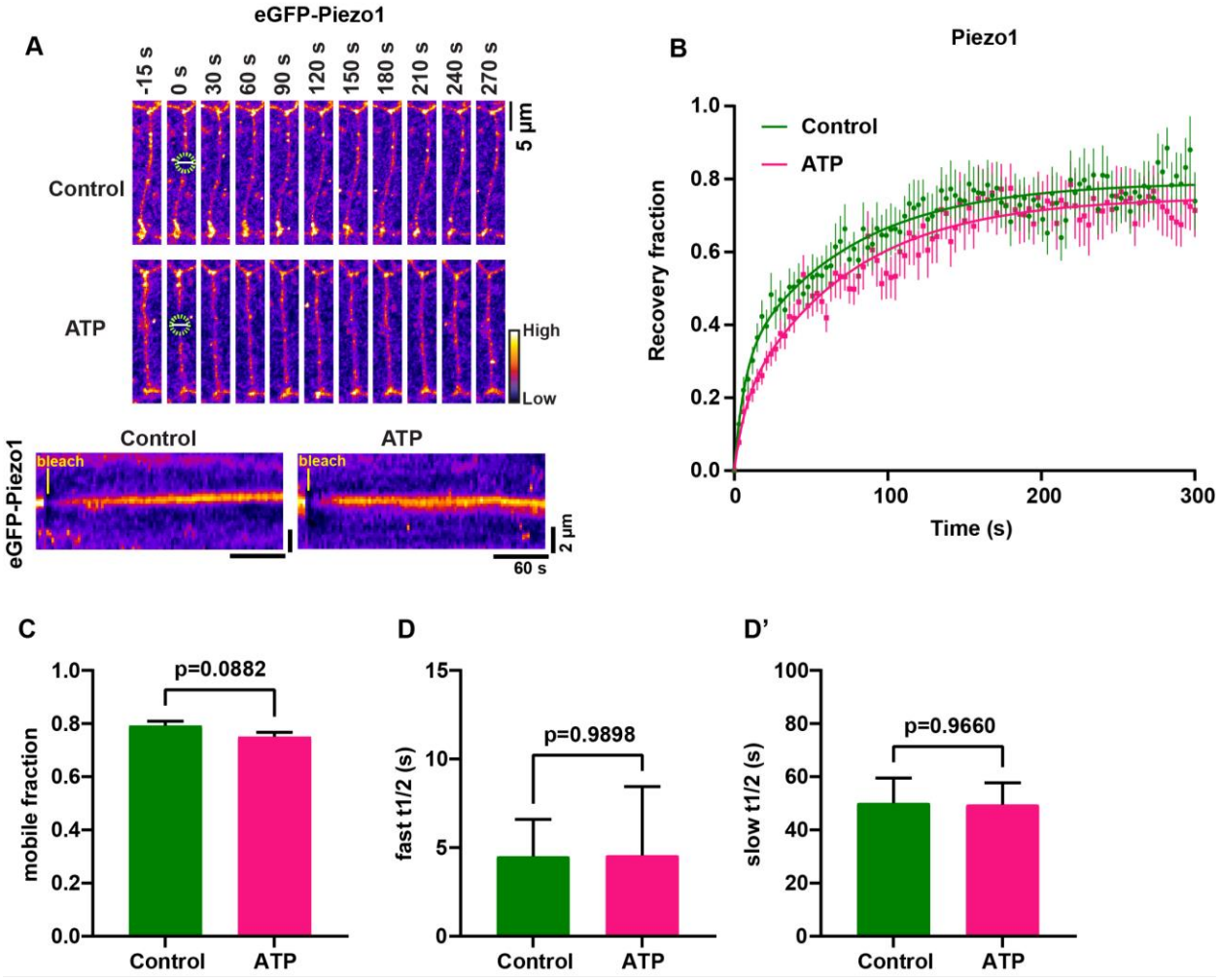

Figure 3.4: Piezo1 is a highly dynamic at the apical cell-cell junctions

(A) Time-lapse images and kymograph of eGFP-Piezo1 FRAP (FIRE LUT) at apical cell-cell junctions in embryos treated with either control condition (0.1x MMR, baseline tension) or 500 µM ATP (in 0.1x MMR, increased junction tension) for 10 minutes prior to imaging. (Top) Montage of Piezo1 FRAP shows that Piezo1 recovers rapidly. Green dotted circle represents bleached area, and white line represents the region used to construct kymograph. (Bottom) Kymograph shows rapid recovery of Piezo1 in control and ATP-treated conditions.
(B) A double exponential curve fitted to eGFP-Piezo1 FRAP under baseline (control, green) and increased tension (ATP, magenta). Points indicate the average, and bars represent the S.E.M. Control: n= 14 junctions, 14 embryos, 2 experiments; ATP: n= 12 junctions, 12 embryos, 2 experiments.
(C-D') Graph of mobile fraction (C), fast half-time of recovery ($t_{1/2}$) (D), and slow $t_{1/2}$ (D') of eGFP-Piezo1 calculated from the double exponential curves in (B). Graphs show that Piezo1 is a highly dynamic protein at apical cell-cell junctions. Error bars represent mean ± S.E.M.; significance calculated using t-test with Welch's correction.

3.3.5 Piezo1 is required to maintain the integrity of cell-cell junctions

Based on our results that Piezo1 localizes to apical cell-cell junctions and the recent finding that MSC-mediated calcium influx is required to maintain epithelial barrier

function (Varadarajan et al., 2021), we next asked if Piezo1 regulates epithelial barrier function. To test the importance of Piezo1 in regulating barrier function, we performed a highly-sensitive live imaging barrier assay (ZnUMBA), which can detect local, transient leaks in the barrier and can assess the global integrity of the epithelial barrier. With ZnUMBA, leaks in the barrier are detected in real time when the fluorescent dye Fluozin-3 comes in contact with Zn^{++}, thereby increasing in fluorescence intensity (Stephenson et al., 2019). Using ZnUMBA, we found no significant increase in the whole-field intensity of Fluozin-3 over time between control and Piezo1 KD embryos (orange, Figure 3.5 A). This suggests that the global barrier function of the epithelium is intact in Piezo1 KD embryos. However, we noticed that the frequency of local barrier leaks was increased in Piezo1 KD embryos (data not shown). As local barrier leaks were followed by Rho flares in control and Piezo1 KD embryos, we used Rho flares as an indicator of sites of local leaks (Stephenson et al., 2019), and constructed a time projection of Rho flares. In agreement with increased barrier leaks, we observed that the frequency of Rho flares was significantly higher in Piezo1 KD embryos compared to controls (Figure 3.5 B).

The increased frequency of Rho flares in Piezo1 KD embryos could be due to changes in junctional actomyosin, which weaken apical cell-cell junctions and increase the number of leak sites, or it could be due to repeated activation of Rho flares at a limited number of leak sites in repeated attempts to fix TJ breaks.

To assess if the local TJ breaks were repaired when Piezo1 is KD, we imaged cells expressing tagBFP-ZO-1 and probe for active Rho (mCherry-2xrGBD) in control and Piezo1 KD embryos. We found that in Piezo1 KD cells, Rho flares (Figure 3.5 C',

time 0s) were initiated at sites of ZO-1 loss, and following the activation of Rho flares, ZO-1 was reinforced (Figure 3.5 C', time 100 s) at levels comparable to controls (Figure 3.5 C), suggesting that Piezo1 is not required for local repair of TJ breaks and barrier leaks. However, we found that in Piezo1 KD cells, Rho flares were significantly bigger in size compared to controls (active Rho, Figure 3.5, C and C'), suggesting that Piezo1 KD might be altering junctional and tissue-level tension. Larger Rho flares could be a result of reduced tissue level tension due to alteration of junctional and/or cortical actomyosin.

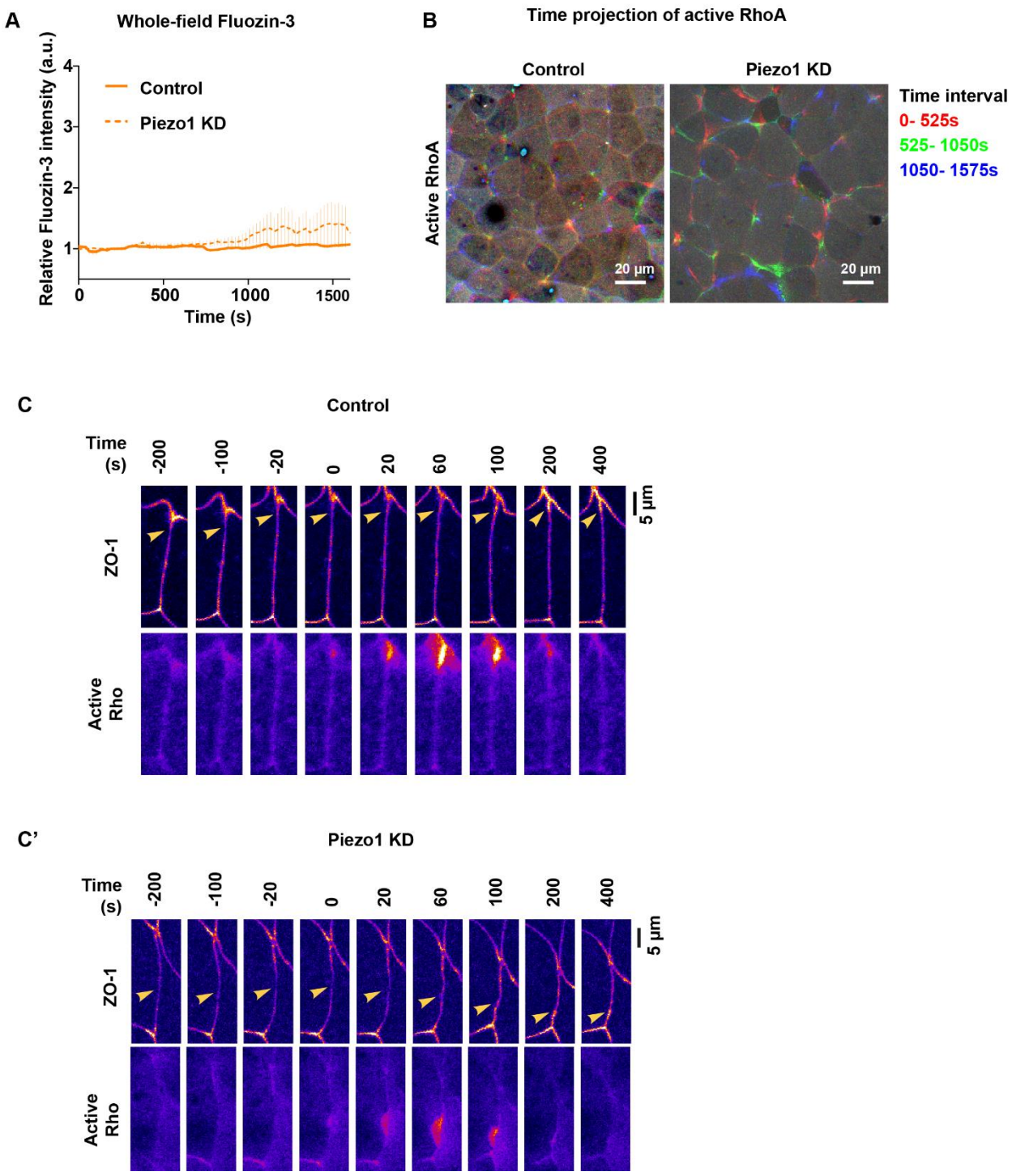

Figure 3.5: Piezo1 is required to maintain the integrity of cell-cell junctions

(A) Graph of mean normalized intensity of whole-field FluoZin-3 for control and Piezo1 KD embryos. Global FluoZin-3 intensity over time stayed close to the baseline for both control and Piezo1 KD and was comparable between the two groups. Shaded region represents S.E.M. Vehicle: n= 5 embryos, 4 experiments; Piezo1 KD: n= 7 embryos, 4 experiments.

(B) Time projection of active RhoA shows increased frequency of Rho flares in Piezo1 KD embryos compared to controls over the span of 1500s. Max projection of Rho flares occurring between time 0-525s, 525-1050s, and 1050-1575s are shown in red, green and blue, respectively.
(C-C') Time-lapse images (FIRE LUT) of ZO-1 (tagBFP-ZO-1), and active Rho (mCherry-2xrGBD) in control (C) or Piezo1 KD (C') embryos. Rho flares are activated at the site of ZO-1 decrease (yellow arrow heads) in both control and Piezo1 KD embryos. ZO-1 reinforcement was observed by time 100s in both control and Piezo1 KD embryos. Time 0 s represents the start of Rho flares.

To test this idea, we next stained gastrula-stage control and Piezo1 KD embryos for F-actin and P-MLC (phosphorylated non-muscle myosin II light chain). We found that the organization of junctional P-MLC was disrupted in Piezo1 KD embryos compared to controls (magenta, Figure 3.6, A and A'), with no observable difference in F-actin (green, Figure 3.6, A and A'). Specifically, we observed that the two-track localization of P-MLC (a band on either side of the junction) seen in controls was lost in Piezo1 KD embryos (magenta, Figure 3.6 A'). Further, quantification of the junctional to cytoplasmic ratio of P-MLC and F-actin, shows that junctional:cytoplasmic ratio of P-MLC is significantly reduced in Piezo1 KD compared to controls (Figure 6B), with no change in F-actin (Figure 3.6 B'). This suggests that Piezo1 is required for proper organization of non-muscle myosin II (NMII) at cell-cell junctions. In sum, our results suggest that Piezo1 regulates the integrity of cell-cell junctions by regulating the distribution of junctional NMII.

Proper organization and activity of NMII is required for the stability of apical cell junctions (Priya et al., 2015). Improper organization of NMII could be the result of nano-scale disorganization of F-actin, which is not visible by the limited resolution of confocal microscopy, or altered upstream activators of NMII. MLC phosphorylation mediated by Rho/ROCK or MLCK can alter apical actomyosin organization and thereby alter barrier function (Nusrat et al., 1995; Clayburgh et al., 2004). Of note, both ROCK and MLCK are activated by calcium/calmodulin (Lazar and Garcia, 1999, Uehata et al., 1997); thus,

future studies should test if Piezo1-mediated barrier regulation is dependent on Rho/ROCK or MLCK.

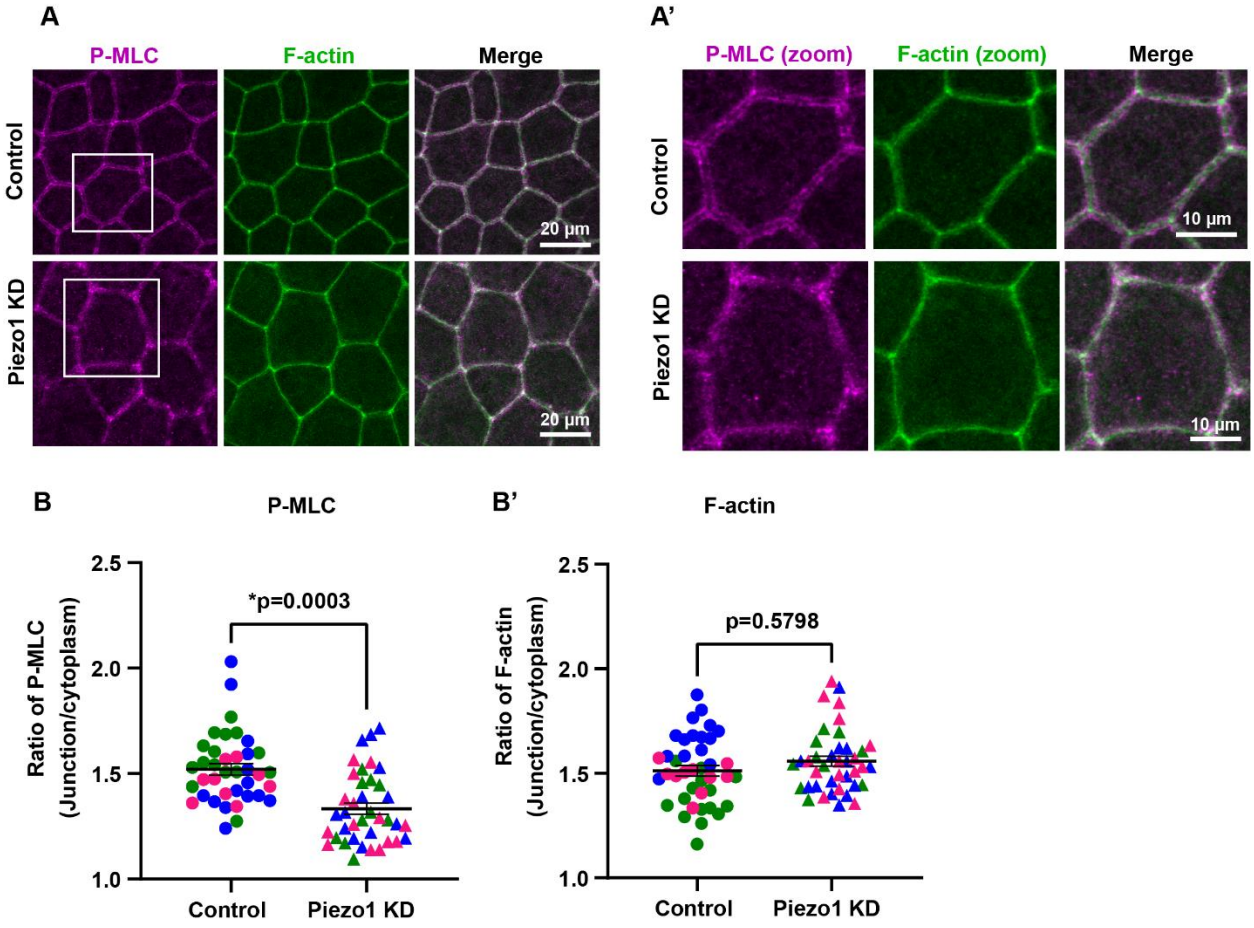

Figure 3.6: Piezo1 regulates the distribution of junctional NMII

(A-A') Fixed staining of P-MLC and F-actin using anti-P-MLC and Phalloidin respectively, in control and Piezo1 KD embryos. Representative images of P-MLC (magenta) and F-actin (green) shows that Piezo1 KD reduces P-MLC at cell-cell junctions compared to control without affecting junctional F-actin. (A') Zoomed in view of regions highlighted in A (white boxes). In Piezo1 KD, prominent P-MLC track-like organization on either side of junctional F-actin is reduced or lost compared to control embryos.
(B-B') Graph shows the ratio of P-MLC (B) or F-actin (B') at cell-cell junctions to the cytoplasm in control (circles) and Piezo1 KD (triangle) embryos. Junction to cytoplasm ration of P-MLC is reduced in Piezo1 KD embryos vs. control embryos, with no significant difference in F-actin. Error bars represent mean ± S.E.M.; significance calculated using One-way ANOVA. Data from independent experiments are color-matched. For P-MLC, Control: n= 38 junctions, 3 experiments and Piezo1 KD: n= 38 junctions, 3 experiments. For F-actin, Control: n= 40 junctions, 3 experiments and Piezo1 KD: n= 40 junctions, 3 experiments.

3.4 Conclusion

Prior to our work, Piezo1 had been shown to localize to epithelial cell-cell junctions and regulate tissue homeostasis by regulating cell extrusion and cell division (Gudipaty et al., 2017, Eisenhoffer et al., 2012). Our study suggests that Piezo1 also regulates the integrity of epithelial cell-cell junctions when epithelial tissues are subjected to mechanical stimuli like tensile stress. We propose that Piezo1 alters E-cadherin-mediated cell-cell adhesion to strengthen cell-cell junctions in response to tensile stress. In support of our hypotheis, recent work has shown that E-cadherin increases at AJs in response to tensile stress (Acharya et al., 2018), and Piezo1 interacts directly with E-Cadherin in MDCK cells (Wang et al., 2020). Though it has been proposed that Piezo1 activation is mediated by lipid bilayer tension (Syeda et al., 2016, Cox et al., 2016), interaction of Piezo1 with E-cadherin might be a mechanism by which Piezo1 is regulated by actomyosin-generated tensile forces in the epithelium. If true, this suggests that crosstalk between mechanosensitive calcium channels and cell-cell junctions may help maintain the integrity of epithelia during mechanical stretch caused by physiological and pathophysiological events including filling and voiding of the urinary bladder, expansion of the lungs, mucosal wound healing, and cancer cell metastasis.

3.5 Future directions

Work presented in this chapter is ongoing research and I propose carrying out the following experiments in the future. First, to assess the effect of Piezo1 on the integrity of cell-cell junctions, I will immunostain for TJ (ZO-1) and AJ (E-Cadherin) proteins in control and Piezo1 KD embryos. Additionally, I will increase the tensile stress in the epithelium by treating embryos with CalA or applying uniaxial stretch to explants using a tissue stretcher to quantify the localization and exchange rate of junctional Piezo1 under increased tension in plane with the junctions. Further, to assess if Piezo1-mediated calcium influx is required for dynamic remodeling of cell-cell junctions in response to tensile stress, I will assess the dynamics of intracellular calcium signaling and the localization and dynamics of TJ and AJ proteins in control and Piezo1 KD embryos. Together, these experiments will help us directly test our hypothesis that Piezo1 alters E-cadherin-mediated cell-cell adhesion to strengthen cell-cell junctions in response to tensile stress.

3.6 Materials and Methods

DNA constructs, mRNA preparation and Piezo1 morpholino:

pCS2+/eGFP-Piezo1 was generated by PCR amplifying the eGFP-Piezo1 sequence from pcDNA3.1-eGFP-mousePiezo1 (gift from Ardem Patapoutian's lab) and ligating it into the *BstBI* and *XbaI* sites in pCS2+ vector. A point mutation at nucleotide 3354 C-T was corrected using site-directed mutagenesis kit and verified by sequencing. pCS2+/PLEKHA-7-mCherry (Higashi et al., 2019), pCS2+/E-Cadherin-3xmCherry (Higashi et al., 2016), pCS2+/mCherry-2xrGBD (probe for active Rho (Davenport et al., 2016)), pCS2+/BFP-ZO-1 (human ZO-1 (Stephenson et al., 2019)), and pCS2+/BFP-membrane (probe for membrane (Higashi et al., 2016)) were previously reported. All plasmid DNA were linearized with *NotI*, except for eGFP-Piezo1 which was linearized using *NsiI*, and BFP-ZO-1 which was linearized using *KpnI*. mRNA was *in vitro* transcribed from linearized pCS2+ plasmids using the mMessage mMachine SP6 Transcription kit (Ambion) and purified using the RNeasy Mini kit (Qiagen). Transcript size was verified on 1% agarose gels containing 0.05% bleach and Millennium RNA markers (Invitrogen). Translation blocking morpholino to knock down Piezo1 was designed by Gene Tools to target the 5'UTR of the Piezo1.S. alloallele with the sequence: 5'- GATGTCACTAACTGTGCAGCTCTGA-3'.

Xenopus embryos and microinjection:

All studies conducted using *Xenopus laevis* embryos strictly adhered to the compliance standards of the U.S. Department of Health and Human Services Guide for the Care and Use of Laboratory Animals and were approved by the University of Michigan Institutional Animal Care and Use Committee (IACUC). Eggs from *Xenopus laevis* were

collected, *in-vitro* fertilized and dejellied as previously reported (Woolner et al., 2009, Miller and Bement, 2009). Dejellied embryos were stored at 15°C in 0.1x Mark's Modified Ringers solution (MMR) containing 10 mM NaCl, 0.2 mM KCl, 0.2 mM $CaCl_2$, 0.1 mM $MgCl_2$, and 0.5 mM HEPES, pH 7.4. Embryos were microinjected in the animal hemisphere with mRNA either twice per cell at two-cell or once per cell at four-cell stage. Injected embryos were allowed to develop to gastrula stage (Nieuwkoop and Faber stage 10.5–12) at 15°C or 17°C. Amounts of mRNA per 5nl of microinjection volume were as follows: eGFP-Piezo1, 100 pg; BFP-ZO-1, 50 pg; PLEKHA-7-mCherry, 25 pg; E-Cadherin-3xmCherry, 20 pg; mCherry-2xrGBD, 50 pg; and BFP-membrane, 12.5 pg.

Immunostaining:

For immunostaining of endogenous Piezo1 and ZO-1, albino embryos were injected at the twoo-cell stage with water (control) or 2.5 mM Piezo1 MO along with mRNA for mCherry-Farnesyl (membrane probe) as a lineage tracer and allowed to develop at 15°C overnight. Gastrula-stage embryos were fixed using tricholoroacetic acid (TCA) fixative as reported previously (Reyes et al., 2014) and immunostained. Briefly, embryos were fixed for 2 hours at room temperature (RT) in TCA fixative (2%TCA in 1x Phospho-buffered Saline (PBS)), with gentle shaking for even fixation. Fixed embryos were washed thrice with 1x PBS and bisected with a sharp scalpel to remove the vegetal hemisphere. Bisected animal caps were permeabilized for 20 minutes at RT in a mix of 1% Triton X-100 in 1x PBS followed by a 20-minute incubation in 0.01% Triton X-100 in 1x PBS. Permeabilized embryos were blocked overnight at 4°C in blocking solution (5% Fetal bovine serum (FBS), and 0.01% Triton X-100 in 1x PBS) with shaking. After

blocking, animal caps were incubated in primary antibodies in blocking solution overnight at 4°C. After four washes (5 min, 15 min, 2 h, and overnight), animal caps were incubated in secondary antibodies in blocking solution overnight at 4°C. Animal caps were stained for DNA using 10 µg/ml DAPI (Invitrogen, # D1306) for 30 minutes at RT, washed and mounted in VECTASHIELD (VWR, # 101098-042) for imaging. For F-actin and P-MLC, immunostaining was performed as described previously (Varadarajan et al., 2021).

Primary antibodies used for immunostaining were anti-Piezo1 (1:200, Novus, # NBP1-78537), anti-ZO-1 (1:500, T8-754, a gift from Dr. Masahiko Itoh), and anti-mCherry (1:200, Abcam, # ab125096). Secondary antibodies used were anti-rabbit Alexa 488 IgG (1:200, Thermo Fisher Scientific, # A11008) and anti-mouse Alexa Fluor 568 IgG (1:200, # A11004).

Barrier assay:

Zinc-based Ultrasensitive Microscopic Barrier Assay (ZnUMBA) was performed as previously reported (Stephenson et al., 2019) in gastrula-stage albino embryos expressing mCherry-2xrGBD and BFP-ZO-1.

Fluorescence recovery after photobleaching (FRAP):

FRAP of Piezo1 was performed using a 405-nm laser in the below-mentioned microscope. Piezo1 at cell-cell junctions was bleached using a circular region of interest (ROI, 3.6 x 3.6 µm) with a laser power of 50% for 800 ms. Following photobleach, recovery of Piezo1 signal was determined by acquiring time-lapse images at the level of AJs at an 8 µs/pixel scanning speed, 3 s time interval, and 2x zoom.

Microscope image acquisition:

Live and fixed imaging of gastrula-stage *Xenopus laevis* embryos were performed on an inverted Olympus Fluoview 1000 Laser Scanning Confocal Microscope equipped with a 60X supercorrected Plan Apo N 60XOSC objective (numerical aperture (NA) = 1.4, working distance = 0.12 mm) using mFV10-ASW software as previously described (Reyes et al., 2014). Three-channel imaging (blue, green, and red) was acquired sequentially by line scanning to avoid bleed through between channels.

Z-stacks of live and fixed imaging of Piezo1 were acquired at 8 µs/pixel scanning speed and 2x zoom. For ZnUMBA, 8 apical Z-planes were acquired at an 8 µs/pixel scanning speed, 21 s time interval, and 1.5x zoom. For figure 5C, live imaging of BFP-ZO-1 and Rho flares was imaged by scanning the top 8 apical Z-planes with a step size of 0.5 µm at 4 µs/pixel scanning speed, 10 s time interval, and 2x zoom.

Image processing, figure preparation and statistical analysis:

Image processing and analysis were performed using ImageJ (Fiji) and Volocity (PerkinElmer). Sum intensity projection of the Z-stacks was used for all quantification: Z projections (X-Z or Y-Z) were generated using Volocity. Figures 3 and 6 were made using the QuickFigures plugin in ImageJ (Mazo, 2020). Statistical analysis, standard deviation (S.D.), and standard error of the mean (S.E.M.) were calculated in GraphPad Prism 9.0.

Time projections of Rho flares:

Time projections of Rho flares were generated using max projections in ImageJ as described previously (Reyes et al., 2014). Flares from time 0-525 s were color coded red, 525-1050 s were color coded green, and 1050-1575 s were color coded blue.

Individual time interval max projections were merged to display the number and distribution of Rho flares over time.

Global barrier function:

Global barrier function was quantified by measuring the whole field intensity of Fluozin-3 signal, including junctional and cytoplasmic signal, over time. Time 0 s represents the start of the movie, immediately following mounting of the embryo injected with Fluozin-3 in 0.1x MMR containing 1 mM $ZnCl_2$. Each timepoint was measured, and baseline was normalized to 1 by dividing the individual value by the average of the first 84 seconds.

FRAP analysis:

FRAP analysis was performed in ImageJ as previously reported (Higashi et al., 2016), with following exceptions. A circular ROI of 0.9 µm was used to measure the intensity of eGFP-Piezo1 at the site of bleach and a nearby reference junction (unbleached). Each measurement was repeated 3 times both at the bleach area and the reference junction and the average considered n=1. Average intensity data was fitted using a double exponential curve in GraphPad to derive the t1/2 (slow and fast) and mobile fraction of Piezo1. Curves were fitted using the following constraints: plateau must be less that 1 and Y0 must be equal to 0. All data points below 0 and above 1 were eliminated from analysis.

Intensity of Piezo1 at cell-cell junctions:

Intensity of Piezo1 and membrane probe at cell-cell junctions was quantified using ImageJ. Intensity at cell-cell junctions was measured using a 1.64 µm wide segmented line to trace the junction from one vertex to another.

For quantifying Piezo1 at bicellular and tricellular junctions, intensity at bicellular junctions was measured using a 1.64 µm wide segmented line to trace the junction (excluding vertices), and intensity at tricellular junctions was measured using a 2.957 µm wide circular ROI. Junctions slanted in the Z-direction and junctions of dividing cells were excluded from the analysis. Normalized intensity of Piezo1 was calculated by dividing the intensity of Piezo1 by the intensity of the membrane probe for the respective junctions.

Line scan of Piezo1 at cell-cell junctions:

Using ImageJ, a straight line of 12 µm length and 1.64 µm width was drawn perpendicular to the junction such that the center of the line is at the junction and the ends of the line are in the cytoplasm. Intensity of Piezo1 and membrane probe was measured using Plot profile. Individual values were normalized to the average of the first 5 and last 5 intensity values along the length of the line for the respective channels.

Z-localization quantification:

Z-localization of Piezo1, ZO-1, PLEKHA-7 and E-Cadherin was quantified as previously reported (Higashi et al., 2019). Relative intensity of the proteins along the Z-axis of cell-cell junctions were aligned such that the maximum intensity of ZO-1 of individual junctions is at 2 µm from the apical plane.

3.7 Acknowledgements

We thank Dr. Ardem Patapoutian (The Scripps Research Institute, California) for the eGFP-mouse Piezo1 construct; Dr. Tomohito Higashi for developing the methodology for X-Z localization of proteins; Dr. Rachel Stephenson for reading and providing critical feedback; current and former members of A.L. Miller laboratory for providing helpful discussion and feedback on experiments. This work was supported by NIH grant (R01 GM112794) to A.L. Miller, a predoctoral fellowship from the American Heart Association (20PRE35120588) to S. Varadarajan, and a University of Michigan Rackham Dissertation Fellowship to S.Varadarajan.

3.8 References

ACHARYA, B. R., NESTOR-BERGMANN, A., LIANG, X., GUPTA, S., DUSZYC, K., GAUQUELIN, E., GOMEZ, G. A., BUDNAR, S., MARCQ, P., JENSEN, O. E., BRYANT, Z. & YAP, A. S. 2018. A Mechanosensitive RhoA Pathway that Protects Epithelia against Acute Tensile Stress. *Dev Cell,* 47**,** 439-452 e6.

ACHARYA, B. R., WU, S. K., LIEU, Z. Z., PARTON, R. G., GRILL, S. W., BERSHADSKY, A. D., GOMEZ, G. A. & YAP, A. S. 2017. Mammalian Diaphanous 1 Mediates a Pathway for E-cadherin to Stabilize Epithelial Barriers through Junctional Contractility. *Cell Rep,* 18**,** 2854-2867.

ARNOLD, T. R., SHAWKY, J. H., STEPHENSON, R. E., DINSHAW, K. M., HIGASHI, T., HUQ, F., DAVIDSON, L. A. & MILLER, A. L. 2019. Anillin regulates epithelial cell mechanics by structuring the medial-apical actomyosin network. *Elife,* 8.

ARNOLD, T. R., STEPHENSON, R. E. & MILLER, A. L. 2017. Rho GTPases and actomyosin: Partners in regulating epithelial cell-cell junction structure and function. *Experimental Cell Research***,** 1-11.

BAI, T., LI, Y., XIA, J., JIANG, Y., ZHANG, L., WANG, H., QIAN, W., SONG, J. & HOU, X. 2017. Piezo2: A Candidate Biomarker for Visceral Hypersensitivity in Irritable Bowel Syndrome? *J Neurogastroenterol Motil,* 23**,** 453-463.

BHAT, M., TOLEDO-VELASQUEZ, D., WANG, L., MALANGA, C. J., MA, J. K. & ROJANASAKUL, Y. 1993. Regulation of tight junction permeability by calcium mediators and cell cytoskeleton in rabbit tracheal epithelium. *Pharm Res,* 10**,** 991-7.

CANALES COUTINO, B. & MAYOR, R. 2021. Mechanosensitive ion channels in cell migration. *Cells Dev,* 166**,** 203683.

COSTE, B., MATHUR, J., SCHMIDT, M., EARLEY, T. J., RANADE, S., PETRUS, M. J., DUBIN, A. E. & PATAPOUTIAN, A. 2010. Piezo1 and Piezo2 Are Essential Components of Distinct Mechanically Activated Cation Channels. *Science,* 330**,** 55-60.

COSTE, B., XIAO, B., SANTOS, J. S., SYEDA, R., GRANDL, J., SPENCER, K. S., KIM, S. E., SCHMIDT, M., MATHUR, J., DUBIN, A. E., MONTAL, M. & PATAPOUTIAN, A. 2012. Piezo proteins are pore-forming subunits of mechanically activated channels. *Nature,* 483**,** 176-181.

COX, C. D., BAE, C., ZIEGLER, L., HARTLEY, S., NIKOLOVA-KRSTEVSKI, V., ROHDE, P. R., NG, C.-A., SACHS, F., GOTTLIEB, P. A. & MARTINAC, B. 2016. Removal of the mechanoprotective influence of the cytoskeleton reveals PIEZO1 is gated by bilayer tension. *Nature Communications,* 7**,** 10366.

DAVENPORT, N. R., SONNEMANN, K. J., ELICEIRI, K. W. & BEMENT, W. M. 2016. Membrane dynamics during cellular wound repair. *Molecular Biology of the Cell,* 27**,** 2272-2285.

DUMITRU, A. C., STOMMEN, A., KOEHLER, M., CLOOS, A. S., YANG, J., LECLERCQZ, A., TYTECA, D. & ALSTEENS, D. 2021. Probing PIEZO1 Localization upon Activation Using High-Resolution Atomic Force and Confocal Microscopy. *Nano Lett,* 21**,** 4950-4958.

EISENHOFFER, G. T., LOFTUS, P. D., YOSHIGI, M., OTSUNA, H., CHIEN, C.-B., MORCOS, P. A. & ROSENBLATT, J. 2012. Crowding induces live cell extrusion to maintain homeostatic cell numbers in epithelia. *Nature,* 484**,** 546-549.

ELLEFSEN, K. L., HOLT, J. R., CHANG, A. C., NOURSE, J. L., ARULMOLI, J., MEKHDJIAN, A. H., ABUWARDA, H., TOMBOLA, F., FLANAGAN, L. A., DUNN, A. R., PARKER, I. & PATHAK, M. M. 2019. Myosin-II mediated traction forces evoke localized Piezo1-dependent Ca(2+) flickers. *Commun Biol,* 2**,** 298.

FRIEDRICH, E. E., HONG, Z., XIONG, S., ZHONG, M., DI, A., REHMAN, J., KOMAROVA, Y. A. & MALIK, A. B. 2019. Endothelial cell Piezo1 mediates pressure-induced lung vascular hyperpermeability via disruption of adherens junctions. *Proc Natl Acad Sci U S A,* 116**,** 12980-12985.

GAUB, B. M. & MÜLLER, D. J. 2017. Mechanical Stimulation of Piezo1 Receptors Depends on Extracellular Matrix Proteins and Directionality of Force. *Nano Letters,* 17**,** 2064-2072.

GOMEZ, G. A., MCLACHLAN, R. W. & YAP, A. S. 2011. Productive tension: Force-sensing and homeostasis of cell-cell junctions. *Trends in Cell Biology,* 21**,** 499-505.

GUDIPATY, S. A., LINDBLOM, J., LOFTUS, P. D., REDD, M. J., EDES, K., DAVEY, C. F., KRISHNEGOWDA, V. & ROSENBLATT, J. 2017. Mechanical stretch triggers rapid epithelial cell division through Piezo1. *Nature,* 543**,** 118-121.

HEISENBERG, C.-P. 2017. Cell biology: Stretched divisions. *Nature*.

HIGASHI, T., ARNOLD, T. R., STEPHENSON, R. E., DINSHAW, K. M. & MILLER, A. L. 2016. Maintenance of the Epithelial Barrier and Remodeling of Cell-Cell Junctions during Cytokinesis. *Curr Biol,* 26**,** 1829-42.

HIGASHI, T. & MILLER, A. L. 2017. Tricellular junctions: how to build junctions at the TRICkiest points of epithelial cells. *Mol Biol Cell,* 28**,** 2023-2034.

HIGASHI, T., STEPHENSON, R. E. & MILLER, A. L. 2019. Comprehensive analysis of formin localization in Xenopus epithelial cells. *Mol Biol Cell,* 30**,** 82-95.

JOSHI, S. D. & DAVIDSON, L. A. 2010. Live-cell Imaging and Quantitative Analysis of Embryonic Epithelial Cells in Xenopus laevis. *Journal of Visualized Experiments*, 1-6.

KIM, Y., HAZAR, M., VIJAYRAGHAVAN, D. S., SONG, J., JACKSON, T. R., JOSHI, S. D., MESSNER, W. C., DAVIDSON, L. A. & LEDUC, P. R. 2014. Mechanochemical actuators of embryonic epithelial contractility. *Proceedings of the National Academy of Sciences,* 111**,** 14366-14371.

LAZAR, V. & GARCIA, J. G. 1999. A single human myosin light chain kinase gene (MLCK; MYLK). *Genomics,* 57**,** 256-67.

LEE, J. Y. & HARLAND, R. M. 2010. Endocytosis is required for efficient apical constriction during Xenopus gastrulation. *Curr Biol,* 20**,** 253-8.

LI, J., HOU, B., TUMOVA, S., MURAKI, K., BRUNS, A., LUDLOW, M. J., SEDO, A., HYMAN, A. J., MCKEOWN, L., YOUNG, R. S., YULDASHEVA, N. Y., MAJEED, Y., WILSON, L. A., RODE, B., BAILEY, M. A., KIM, H. R., FU, Z., CARTER, D. A. L., BILTON, J., IMRIE, H., AJUH, P., DEAR, T. N., CUBBON, R. M., KEARNEY, M. T., PRASAD, K. R., EVANS, P. C., AINSCOUGH, J. F. X. & BEECH, D. J. 2014. Piezo1 integration of vascular architecture with physiological force. *Nature,* 515**,** 279-282.

LUO, M., K. Y. HO, K., TONG, Z., DENG, L. & P. LIU, A. 2019. Compressive Stress Enhances Invasive Phenotype of Cancer Cells via Piezo1 Activation. *bioRxiv*, 513218.

MAZO, G. 2020. QuickFigures: a tool to quickly transform microscope images into quality figures. *bioRxiv*, 2020.09.24.311282.

MILLER, A. L. & BEMENT, W. M. 2009. Regulation of cytokinesis by Rho GTPase flux. *Nat Cell Biol,* 11**,** 71-7.

MIROSHNIKOVA, Y. A., MANET, S., LI, X., WICKSTROM, S. A., FAUROBERT, E. & ALBIGES-RIZO, C. 2021. Calcium signaling mediates a biphasic mechanoadaptive response of endothelial cells to cyclic mechanical stretch. *Mol Biol Cell*, mbcE21030106.

MIYAMOTO, T., MOCHIZUKI, T., NAKAGOMI, H., KIRA, S., WATANABE, M., TAKAYAMA, Y., SUZUKI, Y., KOIZUMI, S., TAKEDA, M. & TOMINAGA, M. 2014. Functional role for Piezo1 in stretch-evoked Ca2+ influx and ATP release in Urothelial cell cultures. *Journal of Biological Chemistry,* 289**,** 16565-16575.

NESTOR-BERGMANN, A., STOOKE-VAUGHAN, G. A., GODDARD, G. K., STARBORG, T., JENSEN, O. E. & WOOLNER, S. 2019. Decoupling the Roles of Cell Shape and Mechanical Stress in Orienting and Cueing Epithelial Mitosis. *Cell Rep,* 26**,** 2088-2100 e4.

NOURSE, J. L. & PATHAK, M. M. 2017. How cells channel their stress: Interplay between Piezo1 and the cytoskeleton. *Seminars in Cell and Developmental Biology,* 71**,** 3-12.

PATHAK, M. M., NOURSE, J. L., TRAN, T., HWE, J., ARULMOLI, J., LE, D. T. T., BERNARDIS, E., FLANAGAN, L. A. & TOMBOLA, F. 2014. Stretch-activated ion channel Piezo1 directs lineage choice in human neural stem cells. *Proceedings of the National Academy of Sciences,* 111**,** 16148-16153.

PIDDINI, E. 2017. Epithelial Homeostasis: A Piezo of the Puzzle. *Current Biology,* 27**,** R232-R234.

PRIYA, R., GOMEZ, G. A., BUDNAR, S., VERMA, S., COX, H. L., HAMILTON, N. A. & YAP, A. S. 2015. Feedback regulation through myosin II confers robustness on RhoA signalling at E-cadherin junctions. *Nature Cell Biology,* 17**,** 1282-1293.

PULIMENO, P., BAUER, C., STUTZ, J. & CITI, S. 2010. PLEKHA7 is an adherens junction protein with a tissue distribution and subcellular localization distinct from ZO-1 and E-cadherin. *PLoS One,* 5**,** e12207.

RANADE, S. S., QIU, Z., WOO, S.-H., HUR, S. S., MURTHY, S. E., CAHALAN, S. M., XU, J., MATHUR, J., BANDELL, M., COSTE, B., LI, Y.-S. J., CHIEN, S. & PATAPOUTIAN, A. 2014. Piezo1, a mechanically activated ion channel, is required for vascular development in mice. *Proceedings of the National Academy of Sciences,* 111**,** 10347-10352.

RANADE, S. S., SYEDA, R. & PATAPOUTIAN, A. 2015. Mechanically Activated Ion Channels. *Neuron,* 87**,** 1162-1179.

REYES, C. C., JIN, M., BREZNAU, E. B., ESPINO, R., DELGADO-GONZALO, R., GORYACHEV, A. B. & MILLER, A. L. 2014. Anillin regulates cell-cell junction integrity by organizing junctional accumulation of Rho-GTP and actomyosin. *Current Biology,* 24**,** 1263-1270.

RODE, B., SHI, J., ENDESH, N., DRINKHILL, M. J., WEBSTER, P. J., LOTTEAU, S. J., BAILEY, M. A., YULDASHEVA, N. Y., LUDLOW, M. J., CUBBON, R. M., LI, J., FUTERS, T. S., MORLEY, L., GAUNT, H. J., MARSZALEK, K., VISWAMBHARAN, H., CUTHBERTSON, K., BAXTER, P. D., FOSTER, R., SUKUMAR, P., WEIGHTMAN, A., CALAGHAN, S. C., WHEATCROFT, S. B., KEARNEY, M. T. & BEECH, D. J. 2017. Piezo1 channels sense whole body physical activity to reset cardiovascular homeostasis and enhance performance. *Nature Communications,* 8.

ROSENBLATT, J., RAFF, M. C. & CRAMER, L. P. 2001. An epithelial cell destined for apoptosis signals its neighbors to extrude it by an actin- and myosin-dependent mechanism. *Curr Biol,* 11**,** 1847-57.

SAOTOME, K., MURTHY, S. E., KEFAUVER, J. M., WHITWAM, T., PATAPOUTIAN, A. & WARD, A. B. 2018. Structure of the mechanically activated ion channel Piezo1. *Nature,* 554**,** 481-486.

SESSION, A. M., UNO, Y., KWON, T., CHAPMAN, J. A., TOYODA, A., TAKAHASHI, S., FUKUI, A., HIKOSAKA, A., SUZUKI, A., KONDO, M., VAN HEERINGEN, S. J., QUIGLEY, I., HEINZ, S., OGINO, H., OCHI, H., HELLSTEN, U., LYONS, J. B., SIMAKOV, O., PUTNAM, N., STITES, J., KUROKI, Y., TANAKA, T., MICHIUE, T., WATANABE, M., BOGDANOVIC, O., LISTER, R., GEORGIOU, G., PARANJPE, S. S., VAN KRUIJSBERGEN, I., SHU, S., CARLSON, J., KINOSHITA, T., OHTA, Y., MAWARIBUCHI, S., JENKINS, J., GRIMWOOD, J., SCHMUTZ, J., MITROS, T., MOZAFFARI, S. V., SUZUKI, Y., HARAMOTO, Y., YAMAMOTO, T. S., TAKAGI, C., HEALD, R., MILLER, K., HAUDENSCHILD, C., KITZMAN, J., NAKAYAMA, T., IZUTSU, Y., ROBERT, J., FORTRIEDE, J., BURNS, K., LOTAY, V., KARIMI, K., YASUOKA, Y., DICHMANN, D. S., FLAJNIK, M. F., HOUSTON, D. W., SHENDURE, J., DUPASQUIER, L., VIZE, P. D., ZORN, A. M., ITO, M., MARCOTTE, E. M., WALLINGFORD, J. B., ITO, Y., ASASHIMA, M., UENO, N., MATSUDA, Y., VEENSTRA, G. J. C., FUJIYAMA, A., HARLAND, R. M., TAIRA, M. & ROKHSAR, D. S. 2016. Genome evolution in the allotetraploid frog Xenopus laevis. *Nature,* 538**,** 336-343.

SHEN, L., WEBER, C. R. & TURNER, J. R. 2008. The tight junction protein complex undergoes rapid and continuous molecular remodeling at steady state. *Journal of Cell Biology*.

SHI, Z., GRABER, Z. T., BAUMGART, T., STONE, H. A. & COHEN, A. E. 2018. Cell Membranes Resist Flow. *Cell,* 175**,** 1769-1779 e13.

STEPHENSON, R. E., HIGASHI, T., EROFEEV, I. S., ARNOLD, T. R., LEDA, M., GORYACHEV, A. B. & MILLER, A. L. 2019. Rho Flares Repair Local Tight Junction Leaks. *Dev Cell,* 48**,** 445-459 e5.

STEWART, T. A. & DAVIS, F. M. 2019. Formation and Function of Mammalian Epithelia: Roles for Mechanosensitive PIEZO1 Ion Channels. *Front Cell Dev Biol,* 7**,** 260.

STUART, R. O., SUN, A., PANICHAS, M., HEBERT, S. C., BRENNER, B. M. & NIGAM, S. K. 1994. Critical role for intracellular calcium in tight junction biogenesis. *J Cell Physiol,* 159**,** 423-33.

SYEDA, R., FLORENDO, M. N., COX, C. D., KEFAUVER, J. M., SANTOS, J. S., MARTINAC, B. & PATAPOUTIAN, A. 2016. Piezo1 Channels Are Inherently Mechanosensitive. *Cell Reports,* 17**,** 1739-1746.

TEO, J. L., TOMATIS, V. M., COBURN, L., LAGENDIJK, A. K., SCHOUWENAAR, I. M., BUDNAR, S., HALL, T. E., VERMA, S., MCLACHLAN, R. W., HOGAN, B. M., PARTON,

R. G., YAP, A. S. & GOMEZ, G. A. 2020. Src kinases relax adherens junctions between the neighbors of apoptotic cells to permit apical extrusion. *Mol Biol Cell,* 31**,** 2557-2569.

TRUONG QUANG, B. A., MANI, M., MARKOVA, O., LECUIT, T. & LENNE, P. F. 2013. Principles of E-cadherin supramolecular organization in vivo. *Curr Biol,* 23**,** 2197-2207.

UEHATA, M., ISHIZAKI, T., SATOH, H., ONO, T., KAWAHARA, T., MORISHITA, T., TAMAKAWA, H., YAMAGAMI, K., INUI, J., MAEKAWA, M. & NARUMIYA, S. 1997. Calcium sensitization of smooth muscle mediated by a Rho-associated protein kinase in hypertension. *Nature,* 389**,** 990-4.

VARADARAJAN, S., STEPHENSON, R. E. & MILLER, A. L. 2019. Multiscale dynamics of tight junction remodeling. *J Cell Sci,* 132.

VARADARAJAN, S., STEPHENSON, R. E., MISTEROVICH, E. R., WU, J. L., EROFEEV, I. S., GORYACHEV, A. B. & MILLER, A. L. 2021. Mechanosensitive calcium signaling promotes epithelial tight junction remodeling by activating RhoA. *bioRxiv***,** 2021.05.18.444663.

WANG, Y., CHI, S., GUO, H., LI, G., WANG, L., ZHAO, Q., RAO, Y., ZU, L., HE, W. & XIAO, B. 2018. A lever-like transduction pathway for long-distance chemical- and mechano-gating of the mechanosensitive Piezo1 channel. *Nature Communications,* 9.

WOOLNER, S., MILLER, A. L. & BEMENT, W. M. 2009. Imaging the cytoskeleton in live Xenopus laevis embryos. *Methods Mol Biol,* 586**,** 23-39.

XIAO, R. & XU, X. Z. S. 2010. Mechanosensitive channels: In touch with Piezo. *Current Biology,* 20.

YU, D., MARCHIANDO, A. M., WEBER, C. R., RALEIGH, D. R., WANG, Y., SHEN, L. & TURNER, J. R. 2010. MLCK-dependent exchange and actin binding region-dependent anchoring of ZO-1 regulate tight junction barrier function. *Proc Natl Acad Sci U S A,* 107**,** 8237-41.

ZARYCHANSKI, R., SCHULZ, V. P., HOUSTON, B. L., MAKSIMOVA, Y., HOUSTON, D. S., SMITH, B., RINEHART, J. & GALLAGHER, P. G. 2012. Mutations in the mechanotransduction protein PIEZO1 are associated with hereditary xerocytosis. *Blood,* 120**,** 1908-1915.

ZHAO, Q., WU, K., GENG, J., CHI, S., WANG, Y., ZHI, P., ZHANG, M. & XIAO, B. 2016. Ion Permeation and Mechanotransduction Mechanisms of Mechanosensitive Piezo Channels. *Neuron,* 89**,** 1248-1263.

ZHONG, M., WU, W., KANG, H., HONG, Z., XIONG, S., GAO, X., REHMAN, J., KOMAROVA, Y. A. & MALIK, A. B. 2020. Alveolar Stretch Activation of Endothelial

Piezo1 Protects Adherens Junctions and Lung Vascular Barrier. *Am J Respir Cell Mol Biol,* 62**,** 168-177.

Chapter 4 Conclusion

In this dissertation, I have demonstrated that mechanosensitive calcium signaling is an important feature by which vertebrate epithelial cells sense and respond to mechanical cues to regulate barrier function. In Chapter 2, I found a local calcium increase occurs at the site of barrier leaks in response to elongating cell-cell junctions. Further, I showed that mechanosensitive calcium channel- (MSC-) mediated calcium signaling is required for robust activation of Rho flares to efficiently reinforce tight junctions (TJs) at sites of barrier breaches, thereby maintaining global barrier function. In Chapter 3, I showed that a eukaryotic MSC, Piezo1, localizes to adherens junctions (AJs), and regulates barrier function during cell-generated tensile stress possibly by strengthening cell-cell adhesion. However, many unanswered questions remain about calcium-mediated spatio-temporal regulation of small Rho GTPases, calcium-mediated remodeling of cell-cell junctions, mechanical stimuli that activate MSCs at cell-cell junctions, the role of AJs in regulating barrier function, and the potential for MSC-dependent mechanotransduction during inflammation and wound healing. Throughout this conclusion chapter, I will discuss potential future directions of my findings.

4.1 Calcium-mediated regulation of Rho flares

Prior to my work, studies had correlated intracellular calcium increase and RhoA activation during cell migration in epithelial and endothelial cells (Haws et al., 2016,

Canales Coutino and Mayor, 2021). Often, the techniques used to study this relation were indirect measurements of RhoA activity using formation of actin stress fibers, phosphorylation status of p-MLC, and kinase activity of ROCK, or using a whole cell GST-pull down assay for active RhoA. Though these techniques reveal changes in RhoA activity at a given timepoint and in a global fashion, small transient changes in Rho activity driven by dynamic events are not captured. Given the breadth of calcium-mediated signaling pathways dependent on the amplitude and spread of calcium, it is important to study calcium/RhoA signaling with high spatio-temporal resolution to understand the mechanism.

In Chapter 2, I showed that intracellular calcium increase precedes Rho flares at sites of barrier leaks (Figure 2.2). Further, chelation of intracellular calcium and blocking mechanosensitive calcium significantly reduced the intensity and duration of Rho flare activation, showing that calcium modulates RhoA activity in this process. However, despite the observation that calcium rapidly spreads throughout the cell, Rho flares are spatially confined to the site of paracellular leaks (Figure 2.1 and Figure 2.2). This suggests that calcium may regulate RhoA activity indirectly through modulators of RhoA – Rho GEFs or Rho GAPs – not by direct regulation of RhoA. In this section, I will discuss possible mechanisms by which calcium may regulate activation and dynamics of Rho flares via Rho GEFs, modulating membrane lipid composition, and crosstalk between small GTPases.

4.1.1 Calcium-mediated phosphorylation of RhoGEFs

Interestingly, several members of the regulator of G protein signaling (RGS) family of Rho GEFs that have been implicated in regulation of cell-cell junctions including

p115RhoGEF, LARG, Lbc-RhoGEF, and PDZ-RhoGEF, are regulated by intracellular calcium in endothelial cells stimulated with extracellular signaling ligands (Ryan et al., 2005, Ying et al., 2009, Abiko et al., 2015, Holinstat et al., 2003, Singh et al., 2007). Upon screening these RGS family RhoGEFs, recent data from a fellow graduate student in our lab shows that p115RhoGEF localizes spatio-temporally to Rho flares (Shahana Chumki, unpublished). Evidence from the literature shows that the GEF activity of p115RhoGEF is activated by phosphorylation of p115RhoGEF by the calcium-dependent kinase PKCα (Holinstat et al., 2003) in addition to $G\alpha_{12/13}$-mediated activation via the RGS domain of p115RhoGEF (Kozasa, 1998). Thus, it is of interest to explore if the activity of p115RhoGEF is dependent on calcium signaling during Rho flares by testing the localization of p115RhoGEF to Rho flares in the absence of intracellular calcium. If calcium is indeed involved in the activation of p115RhoGEF in this process, this could explain the low intensity, short-duration Rho flares observed when MSCs are blocked (Figure 2.4) vs. total loss of active Rho flares. To further confirm the parallel activation of p115RhoGEF by calcium and $G\alpha_{12/13}$, it will be necessary to knock down (KD) $G\alpha_{12/13}$ proteins or mutate the RGS domain of p115RhoGEF in combination with intracellular calcium perturbation. Additionally, to expand on this signaling pathway, one could inhibit the activity of PKCα using a conventional PKC inhibitor, Gö6976, to test the role of PKCα in mediating TJ repair via the leak pathway.

4.1.2 Calcium-dependent PIP2 enrichment

The efficiency of RhoA to mediate downstream actomyosin contractility depends on both the amount of RhoA initially activated, and the amount of active RhoA being

retained at the cell cortex to allow enough time for it to interact with downstream effectors to mediate efficient contractility (Budnar et al., 2019, Ratheesh et al., 2012). A recent study showed that the sustained activation of RhoA at cell-cell junctions was regulated by increasing the concentration of PIP2 in the membrane via Anillin binding to PIP2 (Budnar et al., 2019). Further, concentration of PIP2 and thereby stabilization of active Rho in the membrane was dependent on the C2 domain of Anillin (Sun et al., 2015, Budnar et al., 2019). C2 domains are highly conserved regulatory domains, involved in the calcium-dependent membrane binding of proteins that contains C2 domains (Cho and Stahelin, 2006), suggesting that Anillin recruitment to the membrane could be mediated by its C2 domain in the presence of local calcium. However, Sun et al., suggest that recruitment of Anillin to the membrane is not dependent on calcium, although a clearer demonstration of this conclusion is warranted (Sun et al., 2015). Thus, it is possible that Anillin's recruitment to the membrane is mediated by its C2 domain in a calcium-independent manner; however, calcium may mediate PIP2 clustering via Anillin's C2 domain to stabilize active Rho at the junctions. In support of this idea, our lab showed that Anillin KD leads to increased frequency of Rho flares, which are of shorter duration (Reyes et al., 2014), a phenotype similar to blocking MSCs using GsMTx4 (Figure 2.4 and Figure 2.5). Further, calcium has been shown to promote formation of PIP2 clusters in artificial lipid membranes (Wang and Richards, 2012, Sarmento et al., 2014). Together, these results suggest that local calcium increase I observed (Figure 2.1 and Figure S 2.1), might regulate sustained activation of RhoA by locally concentrating PIP2 at the site of TJ leaks.

Future experiments should test this potential mechanism by which calcium regulates the stability of Rho flares by enriching the local concentration of PIP2. For example, one could investigate the localization and dynamics of Anillin and PIP2 (using the Pleckstrin Homology domain of phospholipase C-delta as a probe for PIP2) in control and GsMTx4-treated embryos. If PIP2 clustering and Anillin localization are decreased at sites of barrier leaks in the absence of a calcium increase, this would reveal a mechanism by which calcium regulates the residence time of active RhoA at the junctions, and thereby reduces downstream actomyosin contractility with high spatial specificity.

4.1.3 Calcium-dependent crosstalk between active Cdc42 and active RhoA

Spatial and temporal dynamics of active RhoA are influenced by the crosstalk between active Cdc42 and active RhoA during epithelial wound healing and neuronal dendritic spine enlargement, among other processes (Murakoshi et al., 2011, Benink and Bement, 2005, Abreu-Blanco et al., 2014, Moe et al., 2021). During wound healing, distinct zones of active Cdc42 and active RhoA form around the site of the wound to form a contractile actomyosin array (Benink and Bement, 2005, Clark et al., 2009, Vaughan et al., 2011). Activation of both Cdc42 and RhoA are dependent on intracellular calcium increase mediated by calcium influx via PM damage at the wound site. Chelation of intracellular calcium or wounding in calcium-free media led to a loss of both active Rho and active Cdc42 zones around the wound site (Benink and Bement, 2005, Clark et al., 2009). Further, inhibition of active Cdc42 by expressing a dominant-negative Cdc42 also suppressed the formation of the active Rho zone around the wound site (Benink and Bement, 2005). Together, these results show that while calcium

positively regulates the activity of Cdc42 and RhoA, RhoA activation is also positively regulated by active Cdc42. Thus, it is possible that calcium-mediated activation of Cdc42 modulates the activation of Rho flares via crosstalk at barrier leaks. Indeed, preliminary data from our lab shows that active Cdc42 accumulates at barrier leaks at the same time as active RhoA, although Cdc42 accumulates in a more diffuse pattern compared to Rho (Rachel Stephenson, unpublished). It will be important to characterize the crosstalk between active Cdc42 and active Rho during TJ remodeling, as precise regulation of both is required for maintenance of an intact barrier (Quiros and Nusrat, 2014).

4.2 Calcium-mediated reinforcement of TJ proteins at barrier leaks

Efficient reinforcement of TJ proteins following a barrier leak is dependent on actomyosin-based local contraction of cell-cell junctions (Stephenson et al., 2019). In addition to junction contraction, Stephenson et al. also observed a cortical enrichment of F-actin and cortical flow of NMII towards the junction during Rho flares, which was necessary to recruit ZO-1 from the cytoplasm to the site of the TJ break (Stephenson et al., 2019). These results suggest that 1) cortical flow of actomyosin and 2) local actomyosin-mediated junction contraction could underlie the two phases of TJ repair – reinstatement and reinforcement – respectively. In this section, I will discuss the role of calcium in mediating junction contraction and cortical recruitment of TJ proteins during leak repair.

4.2.1 Calcium-mediated junction contraction during TJ repair

Cytosolic calcium signals play an important role in mediating actomyosin contractility during tissue folding in the *Xenopus laevis* and *Drosophila* epithelium (Balaji et al., 2017, Christodoulou and Skourides, 2015, Hunter et al., 2014). Calcium signals also control cell length during *Zebrafish* brain development (Sahu et al., 2017). In Chapter 2, I showed that during TJ repair, junction contraction initiates during the peak of the intracellular calcium increase, and junction length stabilizes as the calcium level returns to baseline (Figure 2.2). Further, I showed that blocking MSC-mediated calcium increase inhibited junction contraction following barrier leaks (Figure 2.5). These results show that a local intracellular calcium increase is required for actomyosin-mediated junction contraction. In epithelia, apical actomyosin contractility and permeability of TJs is regulated by MLC phosphorylation, which is mediated by Rho/ROCK or MLCK (Clayburgh et al., 2004, Nusrat et al., 1995a). MLCK is a calcium/calmodulin-regulated kinase that activates NMII in the presence of calcium (Lazar and Garcia, 1999). It is not currently clear if the calcium-mediated actomyosin contraction and decreases in cell length during TJ reinforcement are mediated through the RhoA/ROCK or MLCK pathways.

Previous work from our lab has shown that inhibition of ROCK activity had a partial effect on junction contraction and ZO-1 reinstatement (Stephenson et al., 2019), suggesting a possible parallel pathway to Rho/ROCK where calcium activates MLCK. In support of this, my preliminary data shows that MLCK localizes to Rho flares and accumulates at a similar time as active Rho (Figure 4.1).

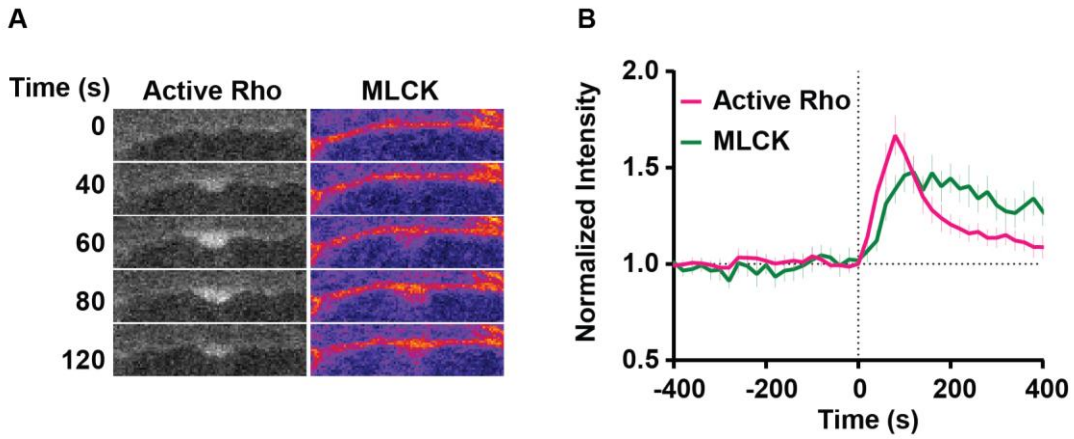

Figure 4.1: MLCK localizes to Rho flares

(A) Montage of active Rho (mCherry-2xrGBD) and mNeon-MLCK in the gastrula-stage *Xenopus* epithelium.
(B) Graph showing MLCK (green) increase follows increase in active RhoA (magenta). Error bars represent mean ± S.E.M. n= 10 flares, 3 experiments.

To expand on this result, one could measure the intensity and timing of MLCK accumulation at Rho flares over time in control and calcium chelated embryos to assess whether MLCK is regulated by the calcium increase at barrier leaks. Further, MLCK localization is enriched at the junction and appears diffuse in the protrusion, compared to active Rho's localization, which is concentrated in the protrusion (Figure 4.1), suggesting that MLCK and Rho/ROCK might be activating different populations of myosin II during TJ repair. Next, to tease apart the contribution of ROCK- and MLCK-mediated myosin II activation during TJ reinforcement, one could block the activity of MLCK using the MLCK inhibitor ML-7 alone, or in conjunction with ROCK inhibitor. If MLCK is indeed involved in regulating local junction contraction and fixing barrier leaks, it would challenge the current view in the field where MLCK activation is often correlated with a leaky barrier during inflammation (Weber et al., 2010, Yu et al., 2010).

4.2.2 Calcium-mediated reinforcement and stabilization of TJ proteins

Previous work from our lab showed a local cortical enrichment of F-actin and cortical

flow of NMII towards the junction around the site of Rho flares and that non-junctional ZO-1 clusters colocalized with cortical F-actin clusters (Stephenson et al., 2019). In addition, we know that the junctional pool of ZO-1 exchanges with the cytoplasmic pool of ZO-1 and does not diffuse along the junction as observed with Occludin (Shen et al., 2008b, Stephenson et al., 2019). Together, this suggests that the majority of ZO-1 recruited to the site of TJ breaks following Rho flares is from the cytoplasmic pool of ZO-1.

In Chapter 2, I observed that bigger ZO-1 breaks were generally correlated with higher intensity calcium increases, and larger size Rho flares. Further, I showed that when the intracellular calcium level is perturbed either by chelation of intracellular calcium (Figure 2.3), or by blocking MSC-mediated calcium influx (Figure 2.4), ZO-1 reinstatement and reinforcement was significantly reduced. Specifically, upon chelation of intracellular calcium, which led to minimal or no Rho flare activation, ZO-1 failed to be reinstated (Figure 2.3). However, upon blocking MSCs, ZO-1 was reinstated but failed to be reinforced to the same extent as controls (Figure 2.4). This indicates that efficient TJ reinforcement is regulated by both the cortical flow of ZO-1 towards the site of the barrier leak and stabilized junction contraction at the site of the barrier leak. An important unanswered question remains: does calcium promote ZO-1 reinforcement independent of junction contraction? I propose that intracellular calcium regulates TJ reinstatement by aiding in phase separation of ZO-1 and cortical flow of non-junctional ZO-1 towards the junction.

ZO-1 is composed of PDZ domains in the N-terminus, PDZ3, SH3, GUK and U6 domains in the central region, and a highly disordered actin binding region (ABR) at the

C-terminus (Figure 4.2) (Citi, 2020, Bazzoni and Dejana, 2004). Two recent studies identified a non-junctional population of ZO-1 that is capable of forming phase separated biomolecular condensates (Beutel et al., 2019, Schwayer et al., 2019). Phase separated ZO-1 condensates recruited other TJ proteins, signaling proteins, and actomyosin to form TJ strand-like structures in the condensates. Further, the condensates are delivered to the junctions by the cortical flow of actomyosin to increase the local concentration of TJ strands at apical cell-cell junctions (Beutel et al., 2019, Schwayer et al., 2019).

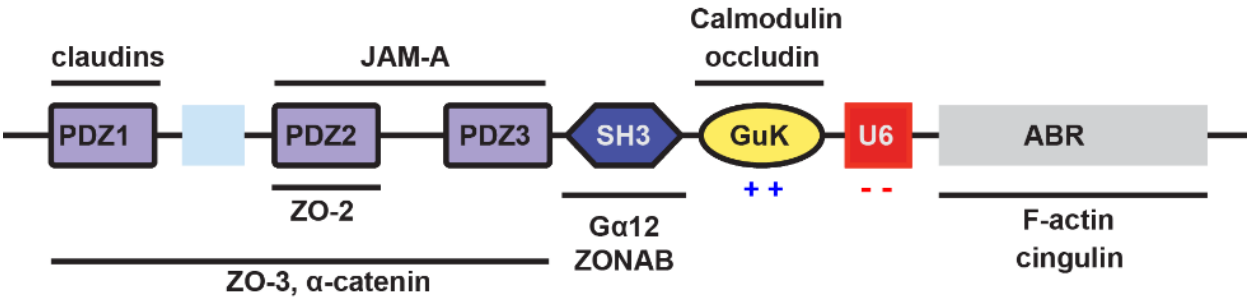

Figure 4.2: Domain diagram of ZO-1 showing the binding regions for other TJ proteins, signaling proteins, and F-actin

The Calmodulin binding region (18 amino acids) with a positively charged amino acid cluster was identified in the ZO-1 GUK domain. Figure modified from (Bazzoni and Dejana, 2004)

Beutel el al. showed that electrostatic interaction between U6 and GUK domains, keeps ZO-1 in a closed conformation thereby preventing ZO-1 from forming phase separated condensates. However, upon release of the interaction between U6 and GUK, ZO-1 is able to form biomolecular condensates via ZO-1 multimerization. Further, they identified that the release of the interaction between U6 and GUK, can be regulated by dephosphorylation of ZO-1 or dimerization of ZO-1 (Beutel et al., 2019). However, it is also possible that in the presence of calcium, calmodulin (CaM) binds to a

calmodulin binding region in the GUK domain of ZO-1 to release the inhibition (Paarmann et al., 2008), allowing biomolecular condensates to form. CaM has been shown to bind the GUK domain of ZO-1 at a higher affinity compared to the U6 domain (Paarmann et al., 2008), indicating that calcium/CaM binding could be a potential mechanism by which ZO-1 undergoes closed→open conformational change – in addition to phosphorylation status or dimerization of ZO-1. This hypothesis is supported by earlier studies showing that chelation of intracellular calcium prevented movement of ZO-1 from the cytoplasm to the junctions, as with calcium chelation, ZO-1 failed to associate with the cytoskeleton during epithelial junction formation (Stuart et al., 1994).

I propose that calcium plays an important role in ZO-1 reinforcement and stabilization by mediating a multi-step process. First, following the local intracellular calcium increase, calmodulin binds to ZO-1 to promote ZO-1 phase separation, and thereby recruitment of TJ components to the biomolecular condensates. Next, the biomolecular condensates are recruited to the site of the TJ break by the cortical flow of actomyosin observed during Rho flares to re-seal the barrier leaks. Finally, the reinforcement of TJ proteins is stabilized by efficient junction contraction at the site of the barrier leaks.

In the future, it would be interesting to test the role of ZO-1's calmodulin-binding region in reinforcement of ZO-1 during Rho flares by mutating the 18 amino acid calmodulin-binding region in the GUK domain, or alternatively by expressing ZO-1 ΔU6 mutant (full length ZO-1 lacking the U6 domain).This would also shed light on the distinct contributions of cortical flow of ZO-1 and actomyosin-mediated junction contraction in re-sealing the barrier leak and strengthening barrier function.

If this hypothesis holds true, it would explain the asymmetric calcium increase observed during Rho flares (Figure 2.1 and Figure 2.2). We predict that during the decrease or loss of ZO-1 preceding Rho flares, ZO-1 is lost in both cells neighboring an elongating junction. It is possible that the amount of ZO-1 lost from each cell is asymmetric, thereby leading to an asymmetric increase in calcium to mediate phase separation and cortical flow of ZO-1 in the respective cells. However, to resolve this question, one would need to express fluorescently tagged-ZO-1 in different colors in cells neighboring the junction with asymmetric calcium increase and use a microscopy technique with higher resolution than conventional confocal microscopy (e.g. Airyscan or super-resolution microscopy). This would allow us to visualize if the ZO-1 loss is symmetrical or asymmetrical in neighboring cells, and if the calcium increase follows a similar trend. Alternatively, one could use laser injury of the cell-cell junction, a technique previously established in our lab to mimic TJ loss and barrier breach (Stephenson et al., 2019), to test the above hypothesis.

4.3 Mechanosensitive calcium channels activated during Rho flares

Based on my results in Chapter 2, I showed that the calcium increase observed during Rho flares originates locally at the site of the TJ break and spreads into the cells (Figure 2.1 and Figure S 2.1). In addition, I demonstrated that the local calcium influx is mediated by MSCs (Figure 2.4). The next logical questions for future studies include: 1) What is the trigger that activates MSCs? and 2) What is/are the mechanosensitive calcium channels involved in this mechanism?

4.3.1 What is the trigger that activates MSCs?

MSCs can be activated by changes in membrane tension generated by mechanical stimuli including compressive stress, tensile stress, or shear stress (Orr et al., 2006, Canales Coutino and Mayor, 2021). Upon activation of PM-localized MSCs, calcium influx via the channel forms a calcium microdomain in the cytoplasm at the mouth of the channel opening. Calcium microdomains mediate local calcium- dependent signaling cascades at the site of MSC activation (Berridge, 2006). Given that the PM is constantly feeling pressure from the external environment of the cell, MSCs are widely studied in the context of externally-applied stress during physiological movements or environmental influences. However, MSCs can also be activated by tension generated inside the cell by the cytoskeleton, and/or change in cortical tension from inside the cell (Nourse and Pathak, 2017, Shi et al., 2018, Heisenberg, 2017, Welf et al., 2020). In living cells, the PM is coupled to the underlying actin cortex. Thus, any change in the connection of the actin cortex to the PM or change in the thickness of the cortex itself can influence membrane tension to modulate the activity of MSCs (Shi et al., 2018, Liu and Montell, 2015, Orr et al., 2006).

Membrane protrusions have been long thought to be areas of increased membrane tension, which was confirmed by a recent study in blebs using a membrane tension probe (Colom et al., 2018). To test if the sites of ZO-1 loss are indeed sites of differential membrane tension, I propose to use the commercially-available membrane tension sensor Flipper-TR (Colom et al., 2018), to measure changes in membrane tension at sites where ZO-1 is reduced and where calcium influx initiates.

Interestingly, Rho flares are associated with apical membrane protrusions (Figure 2.4), displaying a change in membrane curvature and thereby a possible change in

membrane tension (Stephenson et al., 2019). The membrane protrusions observed during Rho flares could be bleb-like protrusions devoid of actin or lamellipodia-like actin-based protrusions. Bleb-like protrusions occur where the connection of the PM to the underlying actin cortex is weakened or lost (Charras, 2008), whereas lamellipodia-like protrusions occur when Arp2/3-mediated branched actin pushes the membrane outward (Taha et al., 2014). Based on preliminary data from our lab, we propose that Rho flares follow a bleb-like model, where the membrane uncouples from the underlying actin cortex due to the loss of ZO-1, and reduction in F-actin that was occasionally detected at sites of ZO-1 loss (Stephenson et al., 2019). The lifecycle of a bleb consists of 3 phases: 1) initiation (detachment of membrane from the cortex), 2) growth (driven by hydrostatic pressure in the cell and devoid of cytoskeletal elements), and 3) retraction (reassembly of the cortex) (Tinevez et al., 2009). While the growth phase of typical blebs is devoid of cytoskeletal elements in the protrusion, the membrane protrusion observed during Rho flares has a homogenous distribution of active Rho (Figure 2.3)., suggesting that Rho flares might follow a combination model, where the initiation phase follows a bleb-like pattern due to the detachment of PM from the cortex, followed by a formin- and Arp2/3-mediated actin-based protrusion model during the growth phase.

To test if there is a loss of membrane-actin coupling at the site of ZO-1 reduction, one could use a membrane-proximal F-actin probe (Bisaria et al., 2020). The enrichment of the membrane-proximal F-actin probe indicated the areas of the junction that are coupled to the underlying actin cortex. Thus, if there is a loss of membrane-actin coupling at the site of ZO-1 decrease prior to the initiation of calcium influx, this would support a bleb-like initiation mechanism where detachment of the membrane

from the underlying cortex activates MSCs due to a change in local membrane tension. This would further explain why MSC-mediated calcium influx is local to the site of TJ loss and not activated along the whole length of the junction that is subjected to elongation (and presumably membrane stretch) preceding local ZO-1 loss. In support, recent evidence points to the importance of linking cortical actin to the membrane as a mechano-protective mechanism by which MSCs are prevented from ectopic activation in intact cells with an underlying actin cortex (Shi et al., 2018).

As noted above, the mechanism of protrusion may not be as simple as bleb-like vs. actin-based protrusions. A recent study showed that both bleb-like protrusions and actin-based protrusions require an initial detachment of PM from the cortex (Welf et al., 2020). This suggests that irrespective of the mode of protrusion growth during Rho flares, initial detachment of the membrane from the cortex could trigger the initiation of calcium influx via MSC activation due to changes in local membrane tension. To further explore this idea, I propose to test the dynamics of local calcium influx and Rho flares following barrier leaks in a system where the membrane-cortex link is stabilized, but still flexible to undergo cell shape changes. A recent study showed that ZO-1 can bind F-actin with a higher affinity by swapping the actin binding site (ABS) of ZO-1 with actin binding domain (ABD) of α-Catenin (Belardi et al., 2020). Further, the same study showed that tight coupling of ZO-1 to F-actin increased macromolecular flux via the leak pathway possibly by breaking of TJ strands (Belardi et al., 2020). Thus, if initial detachment of the PM from cortex is crucial for calcium influx, I predict that in cells expressing ZO-1 where the ABS is swapped with α-catenin's ABD, calcium influx and Rho flare activation will be significantly reduced following a barrier leak.

4.3.2 What is/are the MSCs regulating epithelial barrier function?

I show that the calcium influx following barrier leak is mediated by MSCs; however, the identity of the channel mediating the calcium influx is still an open question. Several of the MSCs that belong to the Piezo and TRP families including Piezo1, TRPC1, TRPC5, TRPC6, TRPV2 and TRPV4 are expressed in epithelial tissues (Coste et al., 2010, Tiruppathi et al., 2006, Akazawa et al., 2013, Miyamoto et al., 2014, Weber and Muller, 2017). My data shows that the local calcium influx is blocked by the MSC blocker, GsMTx4 (Figure 2.4). GsMTx4 is widely used in the mechanosensitive ion channel field to block the activity of Piezo1 (Bae et al., 2011). However, GsMTx4 is a peptide that does not interact directly with Piezo1 channel to alter its function, but rather inserts into the membrane to increase the membrane tension threshold for channel activation (Gnanasambandam et al., 2017). Thus, there is growing evidence that shows that GsMTx4 blocks calcium influx mediated by members of the TRP family, specifically TRPC6 and TRPV4, in addition to Piezo1 (Bae et al., 2011, Spassova et al., 2006, Bowman et al., 2007). Of note, Piezo1, TRPC6, and TRPV4 are known to localize to cell-cell junctions (Gudipaty et al., 2017, Weber et al., 2015, Sokabe et al., 2010), thereby making them strong candidates to regulate local calcium influx during TJ remodeling.

Piezo1:

Given that GsMTx4 strongly inhibits the activity of Piezo1 in many systems, I characterized the role of Piezo1 in regulating barrier function. My data in Chapter 3, shows that Piezo1 KD increased the frequency of barrier leaks (Figure 3.5), similar to GsMTx4-treated embryos (Figure 2.5). However, in Piezo1 KD embryos, despite the

increase in the frequency of barrier leaks, the overall integrity of the barrier was maintained (Figure 3.5), contrary to GsMTx4 treatment (Figure 2.5). This suggested that in Piezo1 KD embryos, the barrier leaks were able to be repaired efficiently in order to maintain the overall barrier integrity. Indeed, activation of Rho flares was not reduced in Piezo1 KD embryos (Figure 3.5), whereas Rho flare activation was reduced with GsMTx4 (Figure 2.4). In fact, the size of protrusions associated with Rho flares were bigger in Piezo1 KD embryos compared to controls, and the cell-cell junctions contracted more (Figure 3.5). Together, my data suggests that Piezo1 might not be the primary channel mediating calcium influx involved in activation of Rho flares. This conclusion is further supported by the localization of Piezo1, as Piezo1 localizes strongly to AJs (Figure 3.2), whereas the membrane protrusion is restricted to the most apical Z-planes by the TJ. However, the loss of Piezo1 leads to increased barrier leaks during cell shape change-mediated junction elongation, thus suggesting that Piezo1 is somehow important in regulating the strength of the barrier function. In the future, it will be interesting to find out if there is a threshold speed of elongation that triggers the TJ break and if that threshold is decreased in Piezo1 KD cells.

It is important to note that with our current Piezo1 KD using Piezo1.S. MO, we could only attain a partial knockdown (~50%) of Piezo1 at cell-cell junctions (Figure 3.1). Thus, it is possible that the remaining Piezo1 compensates for the reduced number of channels at the membrane (e.g. by modulating the activation and inactivation kinetics of the channel to let the same amount of calcium into the cell). Thus, it will be important to knockout Piezo1 using CRISPR/Cas9 to determine the precise role of Piezo1 in regulation of local barrier leaks.

TRPC6 and TRPV4:

My data from Chapter 2 shows that 2-APB treatment in conjunction with calcium chelator significantly decreases the intracellular calcium flash during ZO-1 loss (Figure 3.3). As 2-APB blocks TRP channels in addition to IP_3R-mediated calcium release from the ER, it is possible that the local calcium flashes are mediated by TRPC6 or TRPV4. Additionally, TRPV4 and TRPC6 mediate stress fiber formation by activation of RhoA in migrating cells, suggesting a potential role for these MSCs in regulation of Rho flares during TJ remodeling (Sokabe et al., 2010, Zhang et al., 2017).

Both TRPC6 and TRPV4 can be activated by a change in PM tension; however, they have been studied in the context of different kinds of mechanical stimuli. For example, TRPC6 is activated by changes in membrane tension or curvature of the lipid bilayer, while TRPV4 is activated by osmotic pressure and shear stress (Canales Coutino and Mayor, 2021). In epithelial cells, TRPV4 has been shown to co-localize with ZO-1, and activation of TRPV4 strengthens the barrier by upregulation of TJ proteins (Akazawa et al., 2013, Martínez-Rendón et al., 2017). On the other hand, there is growing evidence showing the role of TRPC6 in regulating RhoA activity and actin reorganization in podocytes to regulate barrier function in the kidney (Weber et al., 2015, Zhang et al., 2017). Interestingly, TRPC6-mediated calcium influx has been shown to activate PKCα in endothelial cells stimulated with thrombin (Singh et al., 2007). However, the same group earlier showed that PKCα activated p115RhoGEF by phosphorylation (Holinstat et al., 2003). Taken together, both TRPV4 and TRPC6 are potential MSC candidates that may regulate local calcium influx during TJ remodeling.

In order to understand the function of TRPC6 and TRPV4 during TJ remodeling, it will be necessary to characterize the localization of the channels in gastrula-stage epithelial cells. If one or both of the channels are localized to TJ and are enriched at the site of Rho flares, it will be important to KD one channel at a time to understand the calcium dynamics, Rho flare activation, TJ reinstatement, and effect on local and global barrier function. Further, to understand the dynamics of calcium influx mediated by TRPV4 and TRPC6, one could inhibit the channel activity using other inhibitors or activate channel using specific agonists.

In the future, it will be important to test the role of MSCs (Piezo1, TRPV4 and TRPC6) in regulating junctional RhoA activity and remodeling of cell-cell junctions in response to global mechanical stimuli, either by mechanical stretching using a tissue stretcher or regional stretching using optogenetic activation of RhoA in the neighboring region.

4.4 Role of AJ-mediated regulation of barrier function

Not every instance of junction elongation causes a barrier leak or is followed by subsequent contraction. Thus, Rho flares may be an emergency repair mechanism that initiates when a TJ is severely damaged in response to a mechanical stimulus. This raises the questions: Why are some parts of the junction more susceptible to a TJ break? and Are sites of TJ break regions of reduced mechanical adhesion at the AJ level?

Previous work from our lab showed that following Rho flares, AJ proteins (E-Cadherin and α-Catenin) are enriched at the site of ZO-1 reinstatement. Interestingly,

the increased amount of α-Catenin was sustained for 600 s after Rho flare initiation, suggesting that the AJs are stabilized following the Rho flares as a mechanism to strengthen the TJ barrier (Stephenson et al., 2019). Additionally, we know that AJ proteins are stabilized, in response to mechanical stimuli – both global and local – in order to maintain effective barrier function (Higashi et al., 2016, Acharya et al., 2018). However, AJ proteins do not appear to be altered prior to Rho flares. Together, previous work leads me to propose that junction elongation-mediated increases in tensile stress lead to barrier leaks at regions of the junction with decreased adhesion strength.

Given that we know that Piezo1 localizes strongly to AJs, though there is also a lesser localization to TJs (Figure 3.2), it is possible that the stability of TJ strands is altered indirectly by modulating the E-Cadherin-based strength of AJs. In line with this, preliminary data from our lab shows that E-Cadherin KD leads to discontinuous localization of ZO-1 at the TJ, suggesting sites of increased barrier leaks (Tomohito Higashi, unpublished). Additionally, it is possible that Piezo1 KD alters the myosin II-mediated tension at cell-cell junctions, which is indicated by the altered localization of P-MLC at cell-cell junctions in Piezo1 KD cells (Figure 3.6 A and Figure 3.6 A'). Thus, it would be interesting to test the effect of Piezo1 KD on the localization and stability of TJ and AJ proteins and perform laser ablation to test the junctional tension. This could reveal a mechanism by which AJs regulates the TJ barrier in a mature epithelium.

4.5 Role of MSCs in physiology and pathophysiology

Mechanosensation, the ability of cells to sense and respond to a mechanical stimulus by converting mechanical force into a biochemical signal, is a field of growing interest in

non-excitable tissues that are subjected to physical forces. Almost all cells in our body are subjected to mechanical force – either from the tissue environment or from within the cells themselves, emphasizing the need to understand the mechanisms by which cells sense and respond to different mechanical forces.

In epithelia, cells experience a range of mechanical forces like fluid flow, tissue distention, and tissue compression and contraction, which occur both during development and normal organ function. For example, as food propels through the intestine, different epithelial cells in the immediate vicinity of the food experience different forces including: cells in front of the food (relaxation), site of the food (expansion), and back of the food (compression) (Beyder, 2018). This suggests that during the physiological function of propelling food through the intestine, distinct mechanosensitive mechanisms might play a role in sensing mechanical forces in their local environment. In support of this, Piezo1 has been shown to be expressed highly and mediate stretch-induced calcium influx in the uroepithelium, another epithelium that is exposed physiological mechanical forces due to fluid flow and distention (Miyamoto et al., 2014, Coste et al., 2010). Additionally, it is important to note that TRPV4 is also expressed in uroepithelial cells and activated in response to mechanical stretch, yet at a different magnitude compared to Piezo1 (Miyamoto et al., 2014). However, the cellular mechanism underlying Piezo1- and TRPV4-mediated calcium signaling is unknown, and is a subject of interest for further investigation. We know that healthy epithelia maintains a robust barrier despite these dynamic physiological forces; thus, it is possible that Piezo1- and TRPV4-mediated calcium influx plays a role in mediating TJ remodeling to maintain barrier function during filling and emptying of the urinary bladder.

It is well known that impaired barrier function due to increased paracellular permeability leads to pathological conditions like inflammatory bowel disease (IBD) (Ivanov et al., 2010b, Choi et al., 2017, Lechuga and Ivanov, 2021) and cancer cell metastasis (Martin, 2014). In addition to mis-regulation of RhoA activation, recent studies point to the overexpression of Piezo1 and TRP channels in the progression of cancer metastasis and inflammation (Canales et al., 2019, Weber and Muller, 2017, Aykut et al., 2020). Specifically, Piezo1 has been found to be overexpressed in intestinal gastric cancer, where it leads to increased cell proliferation and migration (De Felice and Alaimo, 2020). Further, increased activation or expression of several of the TRP channels is related to IBD, Crohn's disease, and colorectal cancer (Alaimo and Rubert, 2019). For instance, TRPV4 is found to be overexpressed in the inflamed gut tissue in patients with Crohn's disease, where TRPV4 is shown to activate the production of pro-inflammatory cytokines (Alaimo and Rubert, 2019). Thus, my data that MSC-mediated calcium influx is required to maintain effective barrier function combined with data from the literature suggests that proper function of MSCs is an essential mechanism for healthy barrier function in epithelial tissues. Future studies are needed to further understand the different mechanism by which MSCs are regulated in response to physiological forces, potential crosstalk between the MSCs in mediating a localized or global calcium influx based on the mechanical stimulus, and finally potential crosstalk between MSCs and other mechanosensitive structures in epithelial cells like TJs, AJs, and the cytoskeleton.

4.6 Significance

In my thesis, I show why simple epithelial tissues become leaky and mechanisms by which the leaks are repaired promptly in healthy tissue. Using *Xenopus laevis* embryos to mimic the simple epithelia in our body, our lab found that transient barrier leaks resulted from the lengthening of cell-cell junctions and were repaired by turning on a protein called RhoA. However, we didn't know how RhoA is turned on at the right time and place in response to leaks. In my thesis, I show calcium is the signal that tells the cell to turn on RhoA and maintain RhoA in an "on" state when it knows there is a leak. Next, I showed that calcium from outside the cell enters the cell through MSCs that open in response to local changes in membrane tension. Calcium entry through MSCs is important to promptly fix the leaks and maintain overall barrier function. Further, I show that Piezo1, a MSC widely expressed in epithelial tissues, regulates barrier function by strengthening cell-cell junctions. Together, my work sheds light on the basic molecular mechanisms that convert a mechanical cue into a local biochemical signal to regulate barrier function in the vertebrate epithelium.

Application of my research will help identify new targets to treat chronic inflammation associated with impaired cell-cell junctions in response to failed mechanosensation. For example, inflammatory bowel disease (IBD), caused by a leaky intestinal epithelium, affects more than twenty five percent of western population (Collaborators, 2020). Thus, treating a Crohn's disease patient with a calcium channel inhibitor using a transient, local delivery to the site of a mucosal wound via nanoparticles or hydrogels, would strengthen the epithelial barrier thereby reducing local inflammation. Also, using a specific calcium channel inhibitor could be a more

targeted therapeutic approach compared to current treatments that uses broad inhibitor for Rho signaling with significant side effects.

4.7 References

SATO, M. & MIZUNO, K. 2015. Rho guanine nucleotide exchange factors involved in cyclic-stretch-induced reorientation of vascular endothelial cells. *Journal of Cell Science,* 128**,** 1683-1695.

ABREU-BLANCO, M. T., VERBOON, J. M. & PARKHURST, S. M. 2014. Coordination of Rho family GTPase activities to orchestrate cytoskeleton responses during cell wound repair. *Current Biology,* 24**,** 144-155.

ACHARYA, B. R., NESTOR-BERGMANN, A., LIANG, X., GUPTA, S., DUSZYC, K., GAUQUELIN, E., GOMEZ, G. A., BUDNAR, S., MARCQ, P., JENSEN, O. E., BRYANT, Z. & YAP, A. S. 2018. A Mechanosensitive RhoA Pathway that Protects Epithelia against Acute Tensile Stress. *Dev Cell,* 47**,** 439-452 e6.

AKAZAWA, Y., YUKI, T., YOSHIDA, H., SUGIYAMA, Y. & INOUE, S. 2013. Activation of TRPV4 strengthens the tight-junction barrier in human epidermal keratinocytes. *Skin Pharmacol Physiol,* 26**,** 15-21.

ALAIMO, A. & RUBERT, J. 2019. The Pivotal Role of TRP Channels in Homeostasis and Diseases throughout the Gastrointestinal Tract. *Int J Mol Sci,* 20.

AYKUT, B., CHEN, R., KIM, J. I., WU, D., SHADALOEY, S. A. A., ABENGOZAR, R., PREISS, P., SAXENA, A., PUSHALKAR, S., LEINWAND, J., DISKIN, B., WANG, W., WERBA, G., BERMAN, M., LEE, S. K. B., KHODADADI-JAMAYRAN, A., SAXENA, D., COETZEE, W. A. & MILLER, G. 2020. Targeting Piezo1 unleashes innate immunity against cancer and infectious disease. *Sci Immunol,* 5.

BAE, C., SACHS, F. & GOTTLIEB, P. A. 2011. The mechanosensitive ion channel Piezo1 is inhibited by the peptide GsMTx4. *Biochemistry,* 50**,** 6295-6300.

BALAJI, R., BIELMEIER, C., HARZ, H., BATES, J., STADLER, C., HILDEBRAND, A. & CLASSEN, A.-K. 2017. Calcium spikes, waves and oscillations in a large, patterned epithelial tissue. *Scientific Reports,* 7**,** 42786.

BAZZONI, G. & DEJANA, E. 2004. Endothelial cell-to-cell junctions: molecular organization and role in vascular homeostasis. *Physiol Rev,* 84**,** 869-901.

BELARDI, B., HAMKINS-INDIK, T., HARRIS, A. R., KIM, J., XU, K. & FLETCHER, D. A. 2020. A Weak Link with Actin Organizes Tight Junctions to Control Epithelial Permeability. *Dev Cell,* 54**,** 792-804 e7.

BENINK, H. A. & BEMENT, W. M. 2005. Concentric zones of active RhoA and Cdc42 around single cell wounds. *Journal of Cell Biology,* 168**,** 429-439.

BERRIDGE, M. J. 2006. Calcium microdomains: organization and function. *Cell Calcium,* 40**,** 405-12.

BEUTEL, O., MARASPINI, R., POMBO-GARCIA, K., MARTIN-LEMAITRE, C. & HONIGMANN, A. 2019. Phase Separation of Zonula Occludens Proteins Drives Formation of Tight Junctions. *Cell,* 179**,** 923-936 e11.

BEYDER, A. 2018. In Pursuit of the Epithelial Mechanosensitivity Mechanisms. *Front Endocrinol (Lausanne),* 9**,** 804.

BISARIA, A., HAYER, A., GARBETT, D., COHEN, D. & MEYER, T. 2020. Membrane-proximal F-actin restricts local membrane protrusions and directs cell migration. *Science,* 368**,** 1205-1210.

BOWMAN, C. L., GOTTLIEB, P. A., SUCHYNA, T. M., MURPHY, Y. K. & SACHS, F. 2007. Mechanosensitive ion channels and the peptide inhibitor GsMTx-4: history, properties, mechanisms and pharmacology. *Toxicon,* 49**,** 249-70.

BUDNAR, S., HUSAIN, K. B., GOMEZ, G. A., NAGHIBOSADAT, M., VARMA, A., VERMA, S., HAMILTON, N. A., MORRIS, R. G. & YAP, A. S. 2019. Anillin Promotes Cell Contractility by Cyclic Resetting of RhoA Residence Kinetics. *Dev Cell,* 49**,** 894-906 e12.

CANALES COUTINO, B. & MAYOR, R. 2021. Mechanosensitive ion channels in cell migration. *Cells Dev,* 166**,** 203683.

CANALES, J., MORALES, D., BLANCO, C., RIVAS, J., DIAZ, N., ANGELOPOULOS, I. & CERDA, O. 2019. A TR(i)P to Cell Migration: New Roles of TRP Channels in Mechanotransduction and Cancer. *Front Physiol,* 10**,** 757.

CHARRAS, G. T. 2008. A short history of blebbing. *Journal of Microscopy,* 231**,** 466-478.

CHO, W. & STAHELIN, R. V. 2006. Membrane binding and subcellular targeting of C2 domains. *Biochimica et Biophysica Acta - Molecular and Cell Biology of Lipids,* 1761**,** 838-849.

CHOI, W., YERUVA, S. & TURNER, J. R. 2017. Contributions of intestinal epithelial barriers to health and disease. *Exp Cell Res,* 358**,** 71-77.

CHRISTODOULOU, N. & SKOURIDES, P. A. 2015. Cell-Autonomous Ca(2+) Flashes Elicit Pulsed Contractions of an Apical Actin Network to Drive Apical Constriction during Neural Tube Closure. *Cell Rep,* 13**,** 2189-202.

CITI, S. 2020. Cell Biology: Tight Junctions as Biomolecular Condensates. *Curr Biol,* 30**,** R83-R86.

CLARK, A. G., MILLER, A. L., VAUGHAN, E., YU, H. Y. E., PENKERT, R. & BEMENT, W. M. 2009. Integration of Single and Multicellular Wound Responses. *Current Biology,* 19**,** 1389-1395.

CLAYBURGH, D. R., ROSEN, S., WITKOWSKI, E. D., WANG, F., BLAIR, S., DUDEK, S., GARCIA, J. G., ALVERDY, J. C. & TURNER, J. R. 2004. A differentiation-dependent splice variant of myosin light chain kinase, MLCK1, regulates epithelial tight junction permeability. *J Biol Chem,* 279**,** 55506-13.

COLLABORATORS, G. B. D. I. B. D. 2020. The global, regional, and national burden of inflammatory bowel disease in 195 countries and territories, 1990-2017: a systematic analysis for the Global Burden of Disease Study 2017. *Lancet Gastroenterol Hepatol,* 5**,** 17-30.

COLOM, A., DERIVERY, E., SOLEIMANPOUR, S., TOMBA, C., MOLIN, M. D., SAKAI, N., GONZALEZ-GAITAN, M., MATILE, S. & ROUX, A. 2018. A fluorescent membrane tension probe. *Nat Chem,* 10**,** 1118-1125.

COSTE, B., MATHUR, J., SCHMIDT, M., EARLEY, T. J., RANADE, S., PETRUS, M. J., DUBIN, A. E. & PATAPOUTIAN, A. 2010. Piezo1 and Piezo2 Are Essential Components of Distinct Mechanically Activated Cation Channels. *Science,* 330**,** 55-60.

DE FELICE, D. & ALAIMO, A. 2020. Mechanosensitive Piezo Channels in Cancer: Focus on altered Calcium Signaling in Cancer Cells and in Tumor Progression. *Cancers (Basel),* 12.

GNANASAMBANDAM, R., GHATAK, C., YASMANN, A., NISHIZAWA, K., SACHS, F., LADOKHIN, A. S., SUKHAREV, S. I. & SUCHYNA, T. M. 2017. GsMTx4: Mechanism of Inhibiting Mechanosensitive Ion Channels. *Biophysical Journal,* 112**,** 31-45.

GUDIPATY, S. A., LINDBLOM, J., LOFTUS, P. D., REDD, M. J., EDES, K., DAVEY, C. F., KRISHNEGOWDA, V. & ROSENBLATT, J. 2017. Mechanical stretch triggers rapid epithelial cell division through Piezo1. *Nature,* 543**,** 118-121.

HAWS, H. J., MCNEIL, M. A. & HANSEN, M. D. 2016. Control of cell mechanics by RhoA and calcium fluxes during epithelial scattering. *Tissue Barriers,* 4**,** e1187326.

HEISENBERG, C.-P. 2017. Cell biology: Stretched divisions. *Nature*.

HIGASHI, T., ARNOLD, T. R., STEPHENSON, R. E., DINSHAW, K. M. & MILLER, A. L. 2016. Maintenance of the Epithelial Barrier and Remodeling of Cell-Cell Junctions during Cytokinesis. *Curr Biol,* 26**,** 1829-42.

HOLINSTAT, M., MEHTA, D., KOZASA, T., MINSHALL, R. D. & MALIK, A. B. 2003. Protein kinase Calpha-induced p115RhoGEF phosphorylation signals endothelial cytoskeletal rearrangement. *J Biol Chem,* 278**,** 28793-8.

HUNTER, G. L., CRAWFORD, J. M., GENKINS, J. Z. & KIEHART, D. P. 2014. Ion channels contribute to the regulation of cell sheet forces during Drosophila dorsal closure. *Development,* 141**,** 325-334.

IVANOV, A. I., PARKOS, C. A. & NUSRAT, A. 2010. Cytoskeletal regulation of epithelial barrier function during inflammation. *Am J Pathol,* 177**,** 512-24.

KOZASA, T. 1998. p115 RhoGEF, a GTPase Activating Protein for G12 and G13. *Science,* 280**,** 2109-2111.

LAZAR, V. & GARCIA, J. G. 1999. A single human myosin light chain kinase gene (MLCK; MYLK). *Genomics,* 57**,** 256-67.

LECHUGA, S. & IVANOV, A. I. 2021. Actin cytoskeleton dynamics during mucosal inflammation: a view from broken epithelial barriers. *Curr Opin Physiol,* 19**,** 10-16.

LIU, C. & MONTELL, C. 2015. Forcing open TRP channels: Mechanical gating as a unifying activation mechanism. *Biochem Biophys Res Commun,* 460**,** 22-5.

MARTIN, T. A. 2014. The role of tight junctions in cancer metastasis. *Semin Cell Dev Biol,* 36**,** 224-31.

MARTÍNEZ-RENDÓN, J., SÁNCHEZ-GUZMÁN, E., RUEDA, A., GONZÁLEZ, J., GULIAS-CAÑIZO, R., AQUINO-JARQUÍN, G., CASTRO-MUÑOZLEDO, F. & GARCÍA-VILLEGAS, R. 2017. TRPV4 Regulates Tight Junctions and Affects Differentiation in a Cell Culture Model of the Corneal Epithelium. *Journal of Cellular Physiology,* 232**,** 1794-1807.

MIYAMOTO, T., MOCHIZUKI, T., NAKAGOMI, H., KIRA, S., WATANABE, M., TAKAYAMA, Y., SUZUKI, Y., KOIZUMI, S., TAKEDA, M. & TOMINAGA, M. 2014. Functional role for Piezo1 in stretch-evoked Ca2+ influx and ATP release in Urothelial cell cultures. *Journal of Biological Chemistry,* 289**,** 16565-16575.

MOE, A., HOLMES, W., GOLDING, A. E., ZOLA, J., SWIDER, Z. T., EDELSTEIN-KESHET, L. & BEMENT, W. 2021. Cross-talk-dependent cortical patterning of Rho GTPases during cell repair. *Mol Biol Cell,* 32**,** 1417-1432.

MURAKOSHI, H., WANG, H. & YASUDA, R. 2011. Local, persistent activation of Rho GTPases during plasticity of single dendritic spines. *Nature,* 472**,** 100-104.

NOURSE, J. L. & PATHAK, M. M. 2017. How cells channel their stress: Interplay between Piezo1 and the cytoskeleton. *Seminars in Cell and Developmental Biology,* 71**,** 3-12.

NUSRAT, A., GIRY, M., TURNER, J. R., COLGAN, S. P., PARKOS, C. A., CARNES, D., LEMICHEZ, E., BOQUET, P. & MADARA, J. L. 1995. Rho protein regulates tight

junctions and perijunctional actin organization in polarized epithelia. *Proc Natl Acad Sci U S A,* 92**,** 10629-33.

ORR, A. W., HELMKE, B. P., BLACKMAN, B. R. & SCHWARTZ, M. A. 2006. Mechanisms of mechanotransduction. *Developmental Cell,* 10**,** 11-20.

PAARMANN, I., LYE, M. F., LAVIE, A. & KONRAD, M. 2008. Structural requirements for calmodulin binding to membrane-associated guanylate kinase homologs. *Protein Sci,* 17**,** 1946-54.

QUIROS, M. & NUSRAT, A. 2014. RhoGTPases, actomyosin signaling and regulation of the Epithelial Apical Junctional Complex. *Seminars in Cell and Developmental Biology,* 36**,** 194-203.

RATHEESH, A., GOMEZ, G. A., PRIYA, R., VERMA, S., KOVACS, E. M., JIANG, K., BROWN, N. H., AKHMANOVA, A., STEHBENS, S. J. & YAP, A. S. 2012. Centralspindlin and alpha-catenin regulate Rho signalling at the epithelial zonula adherens. *Nat Cell Biol,* 14**,** 818-828.

REYES, C. C., JIN, M., BREZNAU, E. B., ESPINO, R., DELGADO-GONZALO, R., GORYACHEV, A. B. & MILLER, A. L. 2014. Anillin regulates cell-cell junction integrity by organizing junctional accumulation of Rho-GTP and actomyosin. *Current Biology,* 24**,** 1263-1270.

RYAN, X. P., ALLDRITT, J., SVENNINGSSON, P., ALLEN, P. B., WU, G. Y., NAIRN, A. C. & GREENGARD, P. 2005. The Rho-specific GEF Lfc interacts with neurabin and spinophilin to regulate dendritic spine morphology. *Neuron,* 47**,** 85-100.

SAHU, S. U., VISETSOUK, M. R., GARDE, R. J., HENNES, L., KWAS, C. & GUTZMAN, J. H. 2017. Calcium signals drive cell shape changes during zebrafish midbrain–hindbrain boundary formation. *Molecular Biology of the Cell,* 28**,** 875-882.

SARMENTO, M. J., COUTINHO, A., FEDOROV, A., PRIETO, M. & FERNANDES, F. 2014. Ca(2+) induces PI(4,5)P2 clusters on lipid bilayers at physiological PI(4,5)P2 and Ca(2+) concentrations. *Biochim Biophys Acta,* 1838**,** 822-30.

SCHWAYER, C., SHAMIPOUR, S., PRANJIC-FERSCHA, K., SCHAUER, A., BALDA, M., TADA, M., MATTER, K. & HEISENBERG, C. P. 2019. Mechanosensation of Tight Junctions Depends on ZO-1 Phase Separation and Flow. *Cell,* 179**,** 937-952 e18.

SHEN, L., WEBER, C. R. & TURNER, J. R. 2008. The tight junction protein complex undergoes rapid and continuous molecular remodeling at steady state. *Journal of Cell Biology*.

SHI, Z., GRABER, Z. T., BAUMGART, T., STONE, H. A. & COHEN, A. E. 2018. Cell Membranes Resist Flow. *Cell,* 175**,** 1769-1779 e13.

SINGH, I., KNEZEVIC, N., AHMMED, G. U., KINI, V., MALIK, A. B. & MEHTA, D. 2007. Galphaq-TRPC6-mediated Ca2+ entry induces RhoA activation and resultant endothelial cell shape change in response to thrombin. *J Biol Chem,* 282**,** 7833-43.

SOKABE, T., FUKUMI-TOMINAGA, T., YONEMURA, S., MIZUNO, A. & TOMINAGA, M. 2010. The TRPV4 channel contributes to intercellular junction formation in keratinocytes. *J Biol Chem,* 285**,** 18749-58.

SPASSOVA, M. A., HEWAVITHARANA, T., XU, W., SOBOLOFF, J. & GILL, D. L. 2006. A common mechanism underlies stretch activation and receptor activation of TRPC6 channels. *Proceedings of the National Academy of Sciences,* 103**,** 16586-16591.

STEPHENSON, R. E., HIGASHI, T., EROFEEV, I. S., ARNOLD, T. R., LEDA, M., GORYACHEV, A. B. & MILLER, A. L. 2019. Rho Flares Repair Local Tight Junction Leaks. *Dev Cell,* 48**,** 445-459 e5.

STUART, R. O., SUN, A., PANICHAS, M., HEBERT, S. C., BRENNER, B. M. & NIGAM, S. K. 1994. Critical role for intracellular calcium in tight junction biogenesis. *J Cell Physiol,* 159**,** 423-33.

SUN, L., GUAN, R., LEE, I. J., LIU, Y., CHEN, M., WANG, J., WU, J. Q. & CHEN, Z. 2015. Mechanistic insights into the anchorage of the contractile ring by anillin and Mid1. *Dev Cell,* 33**,** 413-26.

TAHA, A. A., TAHA, M., SEEBACH, J. & SCHNITTLER, H. J. 2014. ARP2/3-mediated junction-associated lamellipodia control VE-cadherin-based cell junction dynamics and maintain monolayer integrity. *Molecular Biology of the Cell,* 25**,** 245-256.

TINEVEZ, J.-Y., SCHULZE, U., SALBREUX, G., ROENSCH, J., JOANNY, J.-F. & PALUCH, E. 2009. Role of cortical tension in bleb growth. *Proceedings of the National Academy of Sciences,* 106**,** 18581-18586.

TIRUPPATHI, C., AHMMED, G. U., VOGEL, S. M. & MALIK, A. B. 2006. Ca2+ signaling, TRP channels, and endothelial permeability. *Microcirculation,* 13**,** 693-708.

VAUGHAN, E. M., MILLER, A. L., YU, H. Y. & BEMENT, W. M. 2011. Control of local Rho GTPase crosstalk by Abr. *Curr Biol,* 21**,** 270-7.

WANG, J. & RICHARDS, D. A. 2012. Segregation of PIP2 and PIP3 into distinct nanoscale regions within the plasma membrane. *Biol Open,* 1**,** 857-62.

WEBER, C. R., RALEIGH, D. R., SU, L., SHEN, L., SULLIVAN, E. A., WANG, Y. & TURNER, J. R. 2010. Epithelial myosin light chain kinase activation induces mucosal interleukin-13 expression to alter tight junction ion selectivity. *J Biol Chem,* 285**,** 12037-46.

WEBER, E. W., HAN, F., TAUSEEF, M., BIRNBAUMER, L., MEHTA, D. & MULLER, W. A. 2015. TRPC6 is the endothelial calcium channel that regulates leukocyte transendothelial migration during the inflammatory response. *J Exp Med,* 212**,** 1883-99.

WEBER, E. W. & MULLER, W. A. 2017. Roles of transient receptor potential channels in regulation of vascular and epithelial barriers. *Tissue Barriers,* 5**,** e1331722.

WELF, E. S., MILES, C. E., HUH, J., SAPOZNIK, E., CHI, J., DRISCOLL, M. K., ISOGAI, T., NOH, J., WEEMS, A. D., POHLKAMP, T., DEAN, K., FIOLKA, R., MOGILNER, A. & DANUSER, G. 2020. Actin-Membrane Release Initiates Cell Protrusions. *Dev Cell,* 55**,** 723-736 e8.

YING, Z., GIACHINI, F. R. C., TOSTES, R. C. & WEBB, R. C. 2009. PYK2/PDZ-RhoGEF links Ca2+ signaling to RhoA. *Arteriosclerosis, Thrombosis, and Vascular Biology,* 29**,** 1657-1663.

YU, D., MARCHIANDO, A. M., WEBER, C. R., RALEIGH, D. R., WANG, Y., SHEN, L. & TURNER, J. R. 2010. MLCK-dependent exchange and actin binding region-dependent anchoring of ZO-1 regulate tight junction barrier function. *Proc Natl Acad Sci U S A,* 107**,** 8237-41.

ZHANG, L., JI, T., WANG, Q., MENG, K., ZHANG, R., YANG, H., LIAO, C., MA, L. & JIAO, J. 2017. Calcium-Sensing Receptor Stimulation in Cultured Glomerular Podocytes Induces TRPC6-Dependent Calcium Entry and RhoA Activation. *Cell Physiol Biochem,* 43**,** 1777-1789.